Approaches to the Synthesis of Pancratistatin and Pancratistatin Analogues

Stefania Margherita Scalzullo

A dissertation submitted to the Faculty of Science,

University of the Witwatersrand,

Johannesburg

In fulfillment of the requirements for the Degree of Master of Science

May 2009

DECLARATION

I declare that the work presented in this dissertation was carried out exclusively by myself under the supervision of Professor W. A. L. van Otterlo and Professor J. P. Michael. It is being submitted for the degree of Master of Science at the University of the Witwatersrand, Johannesburg. It has not been submitted before for any degree or examination in any other University.

_____

Stefania M. Scalzullo
May 2009

ABSTRACT

Pancratistatin is a naturally occurring Amaryllidaceae alkaloid isolated from the bulbs of *Pancratum littorale*. Pancratistatin has been shown to be capable of inducing apoptosis in several cancer cell lines. Although the biochemical mechanism for the apoptosis is not yet well known, results suggest that pancratistatin could be a very effective non-toxic alternative for anticancer therapy. Nevertheless, further analysis of pancratistatin has been hindered by bioavailability and solubility problems. The aim of this research is to find a viable synthesis of pancratistatin, after which an array of analogues containing a variety of aromatic units can be proposed.

The synthesis of pancratistatin began using carbohydrate chemistry for the initial preparation of the key stereochemical cyclitol ring **C** of pancratistatin. *Chapter 2* of this dissertation describes the syntheses of the suitable glucose derived compounds. Previously established carbohydrate chemistry was used to prepare (3a*R*,5*S*,6*R*,6a*R*)-2,2-dimethyl-6-[(phenylmethyl)oxy]tetrahydrofuro[2,3-*d*][1,3]dioxole-5-carbaldehyde **104.** The aldehyde **104** was used to prepare the nitroalkene **105** and the enoate **106**. The Henry reaction was used to synthesize the nitroalkene (3a*R*,5*R*,6*R*,6a*R*)-2,2-dimethyl-5-[(*E*)-2-nitroethenyl]-6-phenylmethyl)oxy]tetrahydrofuro[2,3-*d*][1,3]dioxole **105**.
Similarly, a Horner-Wadsworth-Emmons reaction was utilized to prepare the enoate methyl (2*E*)-3-{(3a*R*,5*R*,6*R*,6a*R*)-2,2-dimethyl-6-[(phenylmethyl)oxy]tetrahydrofuro[2,3-*d*][1,3]dioxol-5-yl}prop-2-enoate **106**.

In *Chapter 3* of the dissertation, the previously prepared nitroalkene **105** and enoate **106** are used in an array of conjugate addition reactions. The first method utilized organocuprate conjugate addition, while the second method adopted a rhodium(I)-catalyzed conjugate addition. A variety of aromatic substituents were used as the nucleophilic partners namely, phenyl, dioxolylphenyl, benzodioxine, and trimethoxyphenyl.

In *Chapter 4* of the dissertation, using only the phenyl and dioxolylphenyl substituted compounds, deprotection of the acetonide group was attempted. This was followed by several attempts at ring closure and acetylation reactions, unfortunately without success and no further progress concerning this synthetic strategy could be made.

Finally, in *Chapter 5* of the dissertation a summary of the results observed for the research project was made. This was followed by the experimental data for the reactions investigated during the project (*Chapter 6*), and a brief appendix.

This dissertation

is dedicated to

my parents, Rita and Roberto

ACKNOWLEDGEMENTS

I would like to express my gratitude to my supervisor, Professor W.A.L. van Otterlo for all his valuable guidance and encouragement during the course of this project. I am truly grateful for everything that I have learnt.

Thank-you to my co-supervisor, Professor J.P. Michael, for the many valuable discussions and for his continual assistance. I would also like to thank Professor C.B. de Koning for all his valuable input and ideas during the project.

To my family – my parents Roberto and Rita, you are my rock, my constant support and encouragement. A dissertation would not be easily done without my dad's good advice and my mom's shoulder to cry on. My brothers, Pietro and Paolo, you are always a ray of sunshine when I need it most! Love you!

I would like to express my gratitude to Mr. Richard Mampa and Professor L. Carlton for running numerous NMR spectra; Dr A. Dinsmore and Mrs. M. Ferreira for mass spectral analysis; and Dr Manuel Fernandes for the crystallographic analysis. Thank-you for all your help!

To all my colleagues and friends in the chemistry department for sharing just a little bit of their talents with me and for creating such a friendly work environment. Particularly, Garreth for all his assistance and guidance, and my lab partners Chevonne and Tlabo. A special mention to some of my dearest friends, Sameshnee, Jeremy, Chris, Stephen and Manuel, for their sound advice and unwavering sincerity.

Finally, I would like to express my appreciation to the University of the Witwatersrand and the National Research Foundation for their financial assistance.

TABLE OF CONTENTS

CHAPTER 1: INTRODUCTION

1.1. Amaryllidaceae alkaloids

The Amaryllidaceae alkaloids constitute an important class of naturally occurring compounds which have interesting biological and medicinal properties[1] that have dated back to the time of the ancient Greeks. The medicinal value of the extracted oils of the daffodil, *Narciclassus poeticus L.*, in the treatment of illnesses related to cancer was already known to the Greek physician Hippocrates of Cos; however, it was not until 1877 that the first Amaryllidaceae alkaloid, lycorine **1,** was isolated *(Figure 1)*.[2] Today the structurally diverse family compromises more than 100 alkaloids.[3,4]

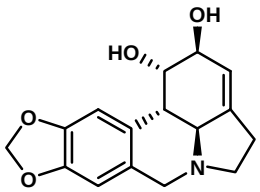

1

Figure 1. The first isolated Amaryllidaceae alkaloid, lycorine **1**.

Structurally, the Amaryllidaceae alkaloids can be sub-divided into three major skeletal arrangements; namely, the lycorane, crinane or the galanthamine cores *(Figure 2)*, although more complex modifications have been noted.[5] However from a biological and thus potentially medicinal perspective, the modified lycorane-type alkaloids with a phenanthridone core *(Figure. 3)*, such as, narciclasine **2**, lycoricidine **3**, pancratistatin **4**, and 7-deoxypancratistatin **5** are up to ten times more active than alkaloids of the remaining two sub-classes, such as galanthamine **6**, ungeremine **7** and hippeastrine **8** as depicted in *Figure 4*. Understandably, the former set of compounds are therefore discussed and studied far more comprehensively in the literature.

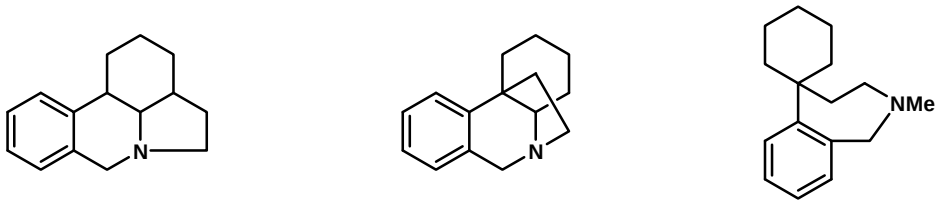

Lycorane-type **Crinane-type** **Galanthamine-type**

Figure 2. Biosynthetic origin of the Amaryllidaceae alkaloids

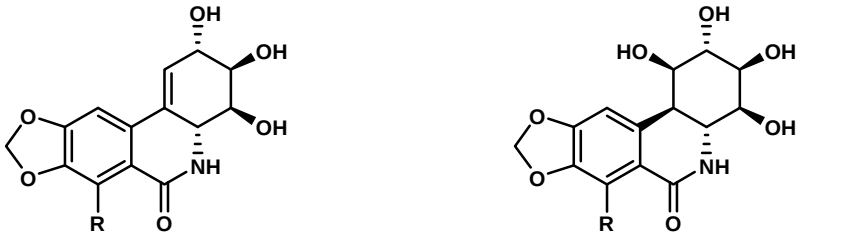

2 narciclasisne, R = OH
3 lycoricidine, R = H

4 pancratistatin, R = OH
5 7-deoxypancratistatin, R = H

Figure 3. Phenanthridone family of alkaloids.

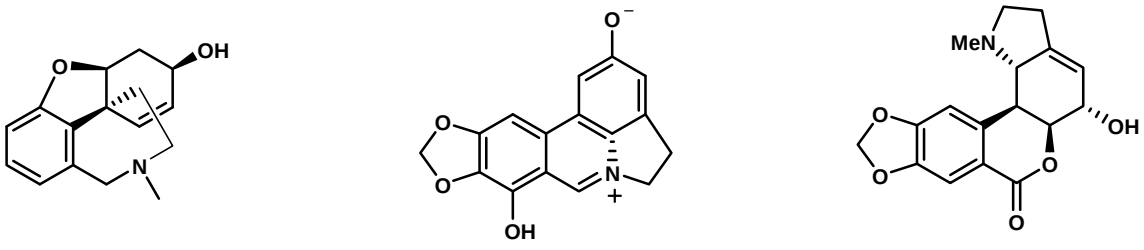

6 galanthamine **7 ungeremine** **8 hippeastrine**

Figure 4. Amaryllidaceae alkaloids showing interesting structural properties.

Narciclasine **2** was first isolated in 1968 from the bulbs of *Lycoris radiate.* The cytotoxic activities of narciclasine **2** was also reported and it was found to inhibit the cytotoxic properties of calproctin, a protein found in neutrophils and in extracellular media during inflammation.[6] These natural products have also been shown to inhibit ribosomal protein biosynthesis and to promote apoptosis and are thus valuable tools and medicinally important leads in the treatment of cancer.[7]

Narciclasine **2** has been found to be highly active against several cancer cell lines, most notably murine P388 lymphocytic leukemia and human cancer cell lines such as pancreas BXPC-3, breast MCF-7, CNS SF-268, lung NCL-H460, colon KM-20L2, and prostate DU-145.[8-11] It is believed that narciclasine **2** inhibits the formation of peptide bonds on eukaryotic ribosomes. The activity of lycoricidine **3** and 7-deoxypancratistatin **5** are some 100-fold lower, and it is thought that the absence of the phenolic hydroxyl group is responsible for the diminished activity.[12] Other medicinally useful physiological effects include antiviral and antimalarial activities,[4] as well as the treatment of neurogenerative diseases such as Alzheimer's[5] and immunostimulatory, acetylcholinesterase inhibition.[4]

The future of the alkaloids as therapeutic agents depends on their availability, because the isolation of large quantities of the alkaloids from the natural source is not practical. Thus there is a strong case for the development of syntheses or semi-syntheses of these alkaloids, their derivatives, and the development of potential prodrugs.[3]

Pancratistatin **4**, shown in *Figure 3*, will be discussed further in the next chapter owing to its direct chemical and biological importance to the proposed project.

1.2. Pancratistatin

Although the mechanism of action of narciclasine has been studied more thoroughly, the most promising activity resides with pancratistatin.[2,13] Pancratistatin was isolated by Pettit and co-workers in 1984 from the bulbs of *Pancratum littorale*.[14] However, clinical development of the natural product has been hampered as a consequence of the minute quantity of material available from its isolation (6.5 g of pancratistatin were extracted from 45 kg of bulbs).[2,15] As a result, it has been an important task to develop an efficient synthesis for the preparation of pancratistatin.

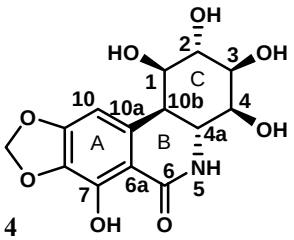

Figure 5. Structure of (+)-pancratistatin

While pancratistatin **4** is not a large molecule, it contains a number of complex structural elements, when combined make it a formidable target molecule to synthesize.[16,17] The overall structure is comprised of six contiguous stereogenic centres in the **C** ring of the phenanthridone skeleton *(Figure 5)*.[17,18] The cyclitol ring also contains further stereochemistry, in addition to the requirement for the stereo-controlled installation of the four surrounding hydroxyl groups. Due to the cyclitol's (**C** ring) interactions with ring **B**, the benzylic stereocentre, **C10b,** which is attached to the pentasubstituted aromatic ring **A**, forms a *trans*-fused **BC** ring system with **C4a**. This has shown to be a particularly difficult synthetic challenge because of the lactam in ring **B** contributing to a highly strained system due to its *trans*-fused relationship with ring **C**. This distorts the planarity created by the four atoms in the sp^2-hybridization state (C10a, C6a, C6 and N5).[4,16,17,19,20] Furthermore, pancratistatin **4** is remarkably insoluble in various organic solvents, as well

as water (53μg/ml),[21] making the search for efficient analogues of pancratistatin **4** necessary.[22,23]

1.3. Biomedicinal aspects of pancratistatin

1.3.1. Structural importance leading to the activity of pancratistatin

The structural skeleton of pancratistatin **4** has revealed an abundance of information about its activity. Through the addition or the removal of certain groups on the pancratistatin **4** backbone, relevant information about the efficiency of the biological and medicinal activity of pancratistatin has been recorded.

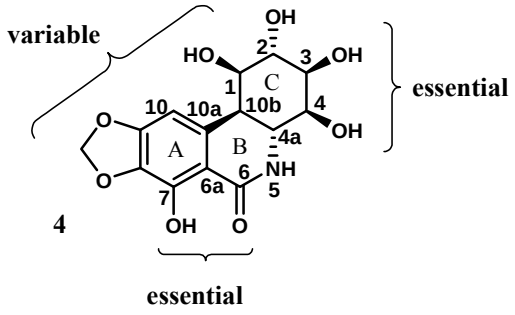

Figure 6. Structural and functional requirements for the minimum pharmacophore of pancratistatin and its congeners.

For instance, the absence of the phenolic hydroxyl at **C7**, as seen in 7-deoxypancratistatin **5**, leads to a 10-fold decrease in activity, so that only moderate cytotoxicity is observed. In addition, the donor-acceptor hydrogen bond pairing of **7-OH** and the carbonyl at **C6** has been found to demonstrate some successful binding to DNA domains.[24-27]

The aminoinositol moiety is probably the structural element responsible for the antiviral activity reported for pancratistatin. The oxygenated phenathridone unit is thought to result in DNA intercalation, which can also be supported by the fact that *cis*-fused

derivatives of pancratistatin are entirely inactive, perhaps due to their three-dimensional structures adopting a more concave appearance. These aminoinositol moieties should thus remain essentially intact, except for minor variations of substituents, functionalities, and configuration at **C1**.[25,26] McNulty *et al.*[25] discovered that the hydroxyl group at **C4** is required in conjunction with either or both of the hydroxyl groups at **C2** and **C3**, thus being important features in the minimum pharmacophore *(Figure 7)*. Similarly, Hakansson[15] and Rinner[28] have tested a series of deoxy analogues of the aminocyclitol part (ring **C**) against a variety of the US National Cancer Institute (NCI) panel of cancer cell lines, showing a highly characteristic cytotoxicity profile of the compounds with a pronounced activity towards the melanoma panel of cell lines, as well as a number of *in vivo* experimental cancer systems. These results have led to the conclusion that at least two hydroxyl groups are necessary for activity on the cyclitol ring, although the activity is usually somewhat reduced from the original pancratistatin model. Conversely, Hudlicky *et al.*[29] established that the minimum requirement for activity of the cyclitol ring requires a 2,3,4-triol pattern that is found in all active constituents *(Figure 8)*.

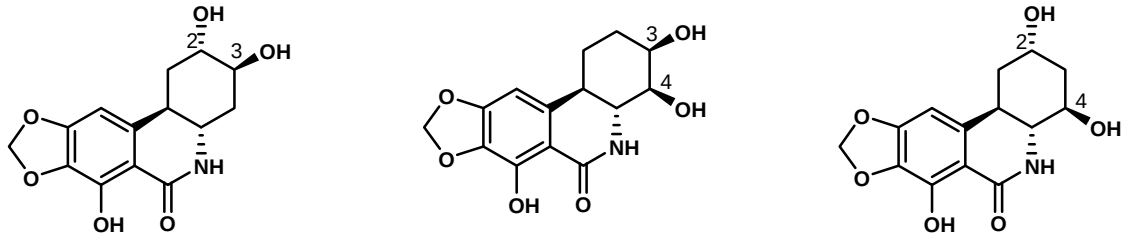

Figure 7. McNulty's systematic refinement of the pancratistatin pharmacophore.[25]

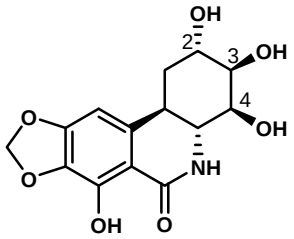

Figure 8. Hudlicky's 2,3,4-triol requirement for activity of pancratistatin analogues.[29]

Another essential feature for the activity of panctratistatin **4**, is the *trans*-fused BC junction formed by the lactam.[15,25,26] The importance of the ring **B** has been addressed, and it has been shown that open ring analogues (i.e. with absent **C10a-C10b** bond) or an ester group as in **9** *(Figure 9) in lieu* of the amide were both devoid of anticancer activity.[30] Recent work has also been accomplished pertaining to the aromatic group of the pancratistatin compound, and some indole mimics of pancratistatin, such as structure **10** in *Figure 9,* have been shown to possess borderline activity against one cancer cell line.[29]

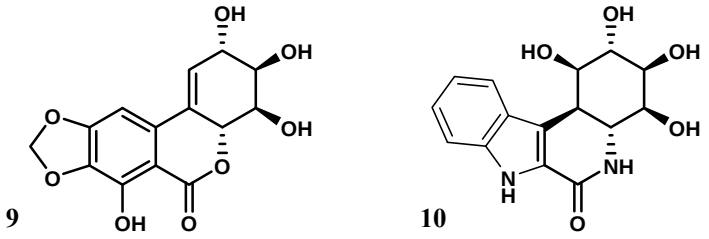

Figure 9. Examples of pancratistatin analogues. Inactive lactone **9** and borderline active indole mimic **10**.

1.3.2. Anticancer biochemical pathway of pancratistatin

Cancer cells are characterized by an accelerated growth and a disrupted apoptotic mechanism.[10] One of the focus points when developing anticancer drugs is to target the biochemical pathway which will induce apoptosis in cancerous cells.[9]

Apoptosis, or programmed cell death, is a physiological process that is essential in normal development and tissue homeostasis as it removes cells that are no longer needed or are potentially harmful. Necrosis is another distinct category of the cell death process and is defined by cell and organelle swelling, leading to the disruption of the cell membrane and cell lysis.[31]

During the process of apoptosis cell shrinkage and nuclear condensation occurs and the eventual non-traumatic removal of the affected cells proceeds via phagocytosis.[9,10] Apoptosis is the counterpart and counterbalance to mitosis in cell population determination. Apoptosis is usually triggered by an apogen, and complex patterns of cell signalling and specific gene expression are involved in the control of a cell's fate. Exposure to an apogen significantly increases apoptotic cell loss during homeostatic processes as well as acute or chronic toxicities.[32] Alternately, disruption of the apoptotic pathway may lead to autoimmunity, neurodegenerative disorders, and acquired immune deficiency syndrome. This could result in pathological accumulation of abnormal cells (tumours), and thus all types of cancer.[10,32]

Mitochondria play a key role in the apoptotic mechanism by releasing caspase-independent death effectors, and causing the loss of essential mitochondrial functions. During apoptosis, the outer mitochondrial membrane becomes permeable, allowing certain proteins such as cytochrome C, Apaf-1 and pro-caspase 9 to activate caspase 9, which will initiate the induction of apoptosis.[9,10,31]

The currently used anticancer treatments, including chemotherapeutics and radiotherapies, are capable of triggering apoptotic cell death in cancer cells by causing DNA damage. Unfortunately there is a degree of risk involved in these treatments, because of the consequence of toxicity to normal cells due to the fact that cancer cells tend to differ from normal cells only in the DNA replication mechanism and rate of proliferation. There are very few anticancer drugs that are capable of targeting receptors or other components of the cell without producing any genotoxic effects. Current therapies thought to be non-genotoxic include paclitaxel and tamoxifen. However, although it was believed that paclitaxel induces non-genotoxic apoptosis by stabilizing tubulin, it has recently been shown to be genotoxic.[9,10]

Pancratistatin **4** has been shown to be capable of effectively inducing apoptosis in several cancer cell lines, including lymphoma cells (Jurkat),[8-11,33] breast cancer cells

(MCF7),[9,10,28] and rat hepatoma cells (5123 tc),[5,9,10,31] within a short period of time at a very low concentration.

Although the biochemical mechanism by which pancratistatin **4** induces apoptosis in cancer cells is still unknown, the involvement of caspase-3 and the plasma membrane proteins (phosphatidyl serine) in the induction phase of apoptosis, indicate that pancratistatin **4** does not cause DNA double-strand breaks or DNA damage prior to the execution phase of apoptosis in cancer cells.[5,9,10]

1.3.3. Antiparasitic biochemical pathway of pancratistatin

The antiparasitic effect of pancratistatin **4** was tested on a mammalian cell line infected with *Encephalitozoon intestinalis*, a microsporidian causing intestinal and systemic infection, such as nephiritis, bronchitis and lytic mandibular lesions in immunocompromised patients. Microsporidia are widespread intracellular parasites, apparently able to invade any cell in animals and humans.[34]

Many parasites share a strategy for transfer between different hosts, whereby an obligatory non-dividing stage precedes the next distinct proliferative phase.[35] The life cycle of *Encephalitozoon intestinalis* consists of two successive developmental sequences, merogony and sporogony, which take place in a parasitophorous vacuole within the host cells. Merogony consists of a proliferation stage, followed by multiple divisions, until sporonts are formed. At this point sporogony occurs, whereby additional division occurs until the final spore is formed. The spores are mononucleated and it has been speculated that the regulation of this development is linked to the control of the cell cycle. These parasitic cell cycles are usually complex and involve a series of specific developmental stages in insect or mammalian hosts.[34]

The antiparasitic effect was evaluated in two ways, firstly, by counting the number of parasitophorous vacuoles detected by immunofluorescence, and secondly, by using a specific group of protein kinases, the cyclin-dependent kinases (CDKs). These enzymes

have been shown to be crucial regulators of the timing and co-ordination of the eukaryotic cell cycle.[35] Their activity is regulated by their phosphorylation status and by the association with negative (cyclin kinase inhibitors) and positive (cyclins) regulators, and by intracellular translocations. Thus, the importance of the CDK enzymes in the multiplication and development of eukaryotes represents an attractive potential target for antiparasitic chemotherapy.[34,35]

The results showed a significant reduction of the microspridian infection. It was found that pancratistatin **4** inhibited the infection without affecting the host cell; furthermore, it was observed that pancratistatin **4** was able to block the development of the sporonts and spores rather than the entry of the parasite into the host cell, suggesting that pancratistatin **4** acted as an inhibitor and was blocking a specific phase of cell division of the parasite.[34]

1.4. A review of previous syntheses of pancratistatin and pancratistatin analogues

The synthetic pathway to the complete synthesis of pancratistatin requires the adaptation of various tactical strategies in order to combat the difficulties with its structural complexity. In order to account for the entire synthesis, certain components need to be considered, namely, the starting material used, the strategy for achieving the asymmetric synthesis if only the (+)-enantiomer of the natural product was prepared, the installation of stereocentres into ring **C**, a strategy for the closure of ring **B** and the regioselective introduction of the substituents in the pentasubstituted aromatic ring **A**.[16] In this section an evaluation of the previous syntheses of pancratistatin **4** will be discussed.

1.4.1. Danishefsky and Lee [19]

Danishefsky and Lee accomplished the first total synthesis of racemic pancratistatin, publishing a full paper in the *Journal of the American Chemical Society* in 1989.[19] The synthesis commenced with the aromatic substituent (ring **A**) from the tri-substituted pyrogallol **11** *(Scheme 1)*. This compound was treated with triethyl orthoformate to give

the orthoester **12**, which protected the diol while the remaining hydroxyl group underwent a carbamoylation to yield compound **13**. The diol was then unmasked to give **14** and the installation of the methylenedioxy moiety could then afford compound **15**. A rearrangement reaction facilitated by a Snieckus directed *ortho*-metalation was then employed to transform the carbamate **15** into the corresponding amide **16**. The tetra-substituted compound **17** then underwent a further metalation and a quench with dimethylformamide (DMF) to provide the required aldehyde **18** in a 70% yield. Thus the components of the aromatic ring (ring **A**) in pancratistatin could be introduced regioselectively.

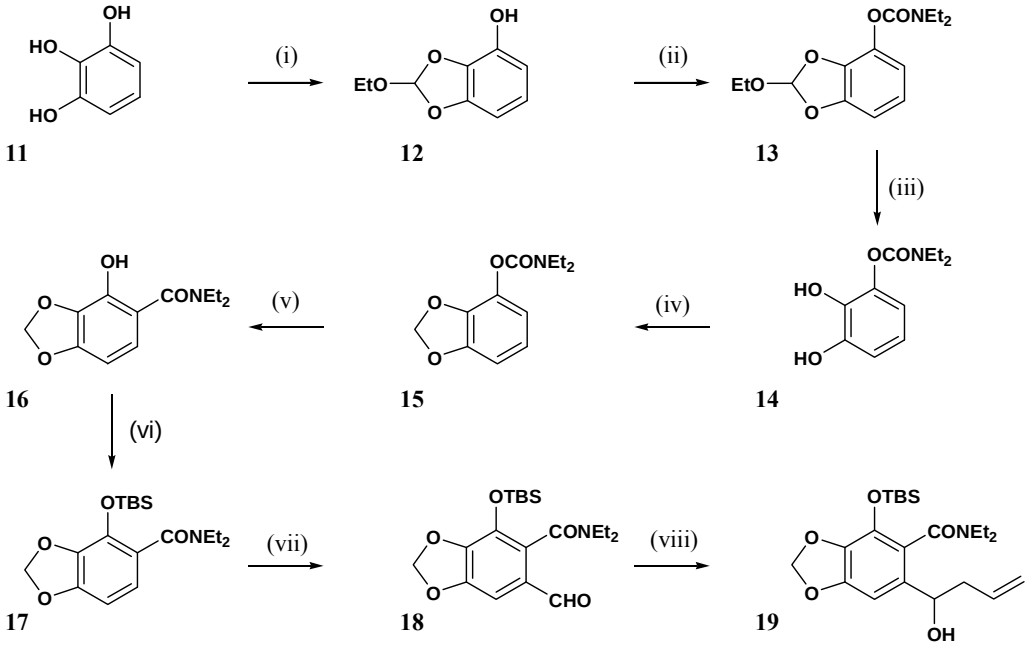

Scheme 1. *(i)* $(OEt)_3CH$, PhH, reflux, Amberlyst-15 (cat), 86%; *(ii)* Et_2NCOCl, NaH, DMAP, THF; *(iii)* *p*-TsOH, MeOH, 86% from **12**; *(iv)* CH_2Br_2, K_2CO_3, CuO, DMF, 70%; *(v)* *s*-BuLi, TMEDA, DMF, THF, 58%; *(vi)* TBSCl, imidazole, CH_2Cl_2, 86%; *(vii)* *s*-BuLi, TMEDA, DMF, THF, 70%; *(viii)* $CH_2{=}CHCH_2MgBr$, Et_2O , 92%.

The formation of ring **C** proceeded from the aldehyde with the addition of an allyl Grignard reagent to **18**, followed by the dehydration of the hydroxyl group from compound **19** to give the diene **20** as shown in *Scheme 2*. The **C** ring could then be formed by the Diels-Alder cycloaddition of the diene with the β-nitrovinyl sulfone **21**, to form the cycloadduct **22** in 96% yield. It was necessary to remove the TBS group (compound **23**) prior to iodolactonization as attempted generation of the halolactone failed with the protecting group because of steric hindrance. The free phenol **24** then reacted to give the iodolactone product **25** in an 80% yield. This transformation initiated the *cis*-**C10b-C1** relationship between ring **A** and ring **C** of pancratistatin. The double bond was then dihydroxylated using catalytic osmium tetroxide (OsO_4) and *N*-methylmorpholine-*N*-oxide (NMO) to give the single stereoisomer **26** in 90% yield.

Before installation of the **C2-C3** functionality it was necessary to prepare for the regiospecific reductive elimination of the **C4a** and **C4** heteroatoms. Thus, compound **26** was reacted with 2-acetoxyisobutyryl bromide, to convert the *cis*-**C4a-C4** diol into *trans*-bromoacetate. This proved somewhat complicated as it afforded the bromoacetate **28** in 63% yield, but also gave rise to a significant amount (25%) of the allylic isomer **27** *(Scheme 3)***.** However the dihydroxylation of the **C2-C3** double bond did indeed occur of the less hindered α-face of the molecule, due to the presence of the **C1-** and **C4-** substituents blocking the β-face, to produce the *cis* diol **29** with 88% yield

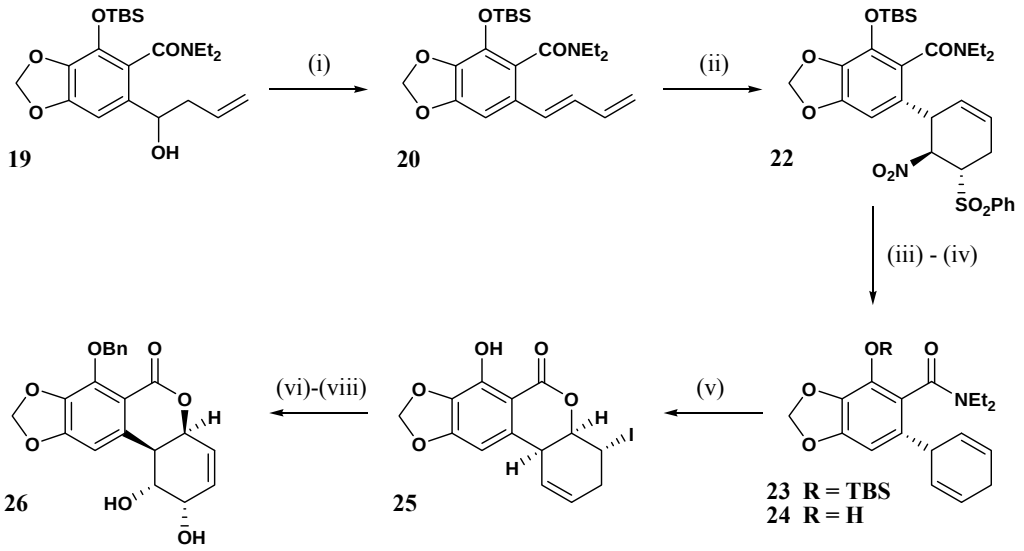

Scheme 2. *(i)* MsCl, Et_3N then DBU, CH_2Cl_2, 54%; *(ii) (E)*-O_2N-CH=CH-SO_2Ph **21**, $CHCl_3$, 96%, *(iii)* Bu_3SnH, AIBN, PhMe, 72%; *(iv)* Bu_4NF, THF, 80%; *(v)* $(Bu_3Sn)_2O$, PhMe, I_2, 67%; *(vi)* BnBr, Ag_2O, DMF, 85%; *(vii)* OsO_4, NMO, THF, H_2O, CH_2Cl_2, 90%; *(viii)* DBU, PhH, 88%.

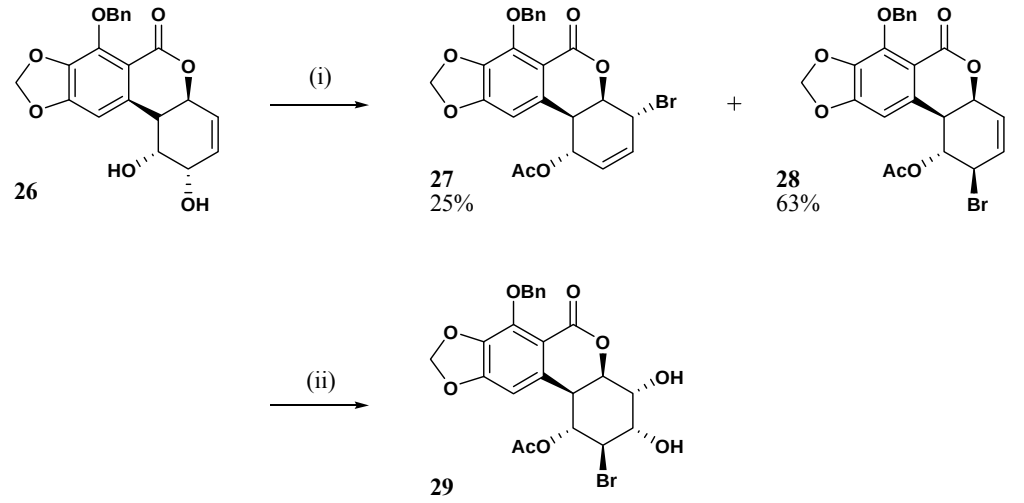

Scheme 3. *(i)* 2-Acetoxyisobutyryl bromide, MeCN, 88%; *(ii)* OsO_4, NMO, THF, 88%.

The *cis*-diol **29** underwent various protections and dehydrations until the reaction with sodium hydride (NaH) and trichloroacetonitrile (CCl_3CN) afforded the sought after imidate **30** in a 74 % yield. The focus now remained on the introduction of the **C4a-** α-amino moiety, which relied upon an Overman imidate-Claisen rearrangement, which took place when the imidate **30** was heated under vacuum, to produce **31** in 56% yield *(Scheme 4)*. With re-exposure to osmium tetroxide (OsO_4) and *N*-methylmorpholine-*N*-oxide (NMO), the remaining olefin was dihydroxylated, and lactone **32**, better known as the "Danishefsky lactone," was formed. This was treated with potassium carbonate in methanol for the removal of the tricholoroacetamide and hydrolysis of the lactone to give the intermediate **33**, which cyclized into the complete phenanthridone ring **34** with the aid of dicyclohexylcarbodiimide (DCC). Finally, hydrogenation of the two benzyl groups provided racemic pancratistatin **4** in a total of 29 steps. Therefore, although the pyrogallol (**11**, *Scheme 1*) provided a reasonably inexpensive starting compound, which already contained three oxygen-bearing groups from ring A of pancratistatin **4**, the synthesis proved to be somewhat lengthy and demanding.

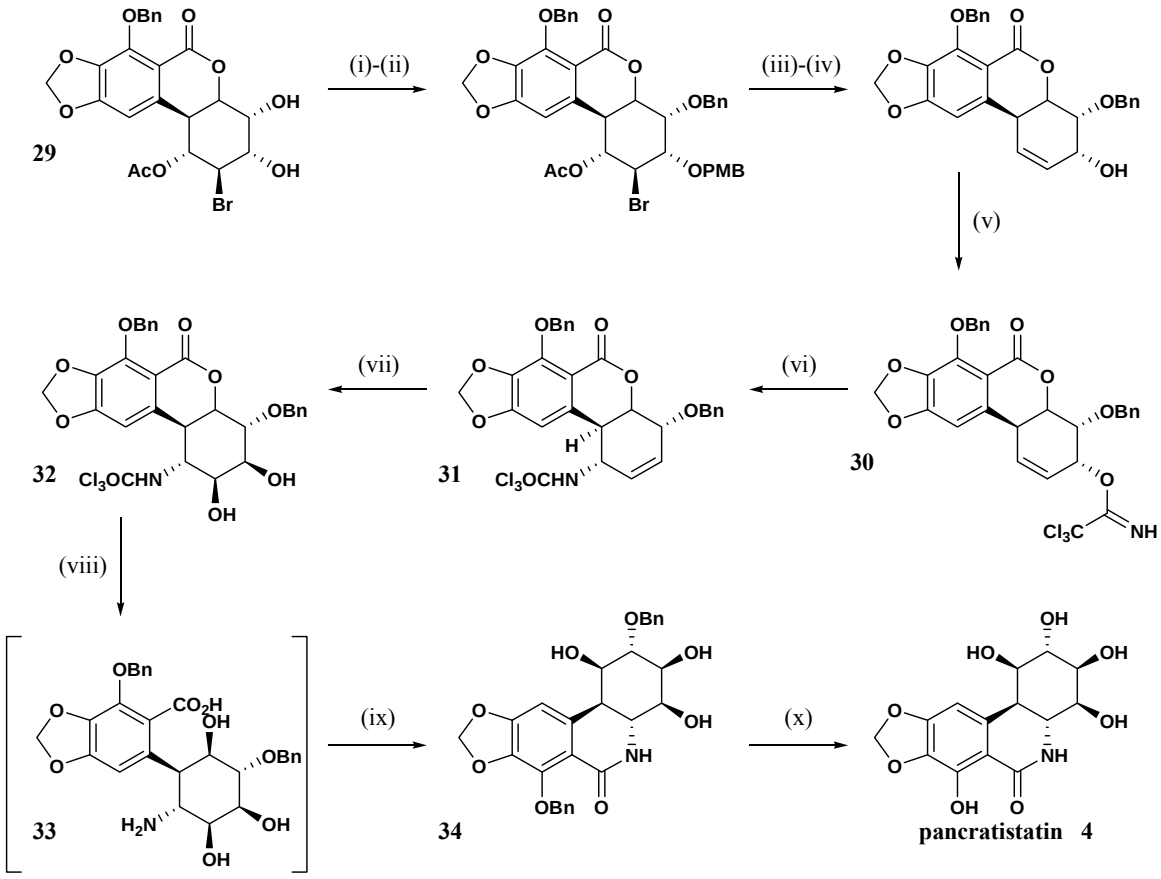

Scheme 4. *(i)* $(Bu_2Sn)_2O$, PMBBr, Bu_4NI, 84%; *(ii)* BnBr, Ag_2O, DMF, 95%; *(iii)* DDQ, H_2O, CH_2Cl_2, 75%; *(iv)* Zn, HOAc, H_2O, 81%; *(v)* NaH, CCl_3CN, THF, 74%; *(vi)* 100°C, high vacuum, 56%; *(vii)* OsO_4, NMO, THF, H_2O, 75%; (viii) K_2CO_3, MeOH, CH_2Cl_2; *(ix)* DCC, CH_2Cl_2, 82% (over two steps); *(x)* H_2, $Pd(OH)_2/C$, EtOAc, 90%.

1.4.2. Hudlicky and co-workers[2,12,36]

In 1995, Hudlicky *et al.* were able to achieve the first asymmetric synthesis of (+)-pancratistatin, with specific rotation $[\alpha]^{26}_D$ of +41.0 (*c* 1.0, *DMSO*). Enatiomerically pure diol **36** were prepared by the oxidation of halobenzene **35** with whole cells of *P. putida* 39/D or recombinant *E. coli* JM109. Hudlicky's group successfully employed a *trans*-aziridine ring opening method in order to set into place the nitrogen component of the pancratistatin **C** ring. Initially, the aziridine **43** was prepared as shown in *Scheme 5*. The two double bonds (in **36**) have different reactivity patterns, making selectivity favourable,

hence the formation of bromohydrin **36**. The azide **39** was then formed, which was subsequently mesylated to afford compound **40**, which was followed by a reduction with lithium aluminium hydride ($LiAlH_4$) to afford the aziridine **41**, which in turn could be tosylated to give compound **42**. It was later found that the synthesis of the aziridine could be reduced to a far more effective approach if the Yamada iodonium ylide *(step ix, Scheme 5)* was employed from compound **37**.[12]

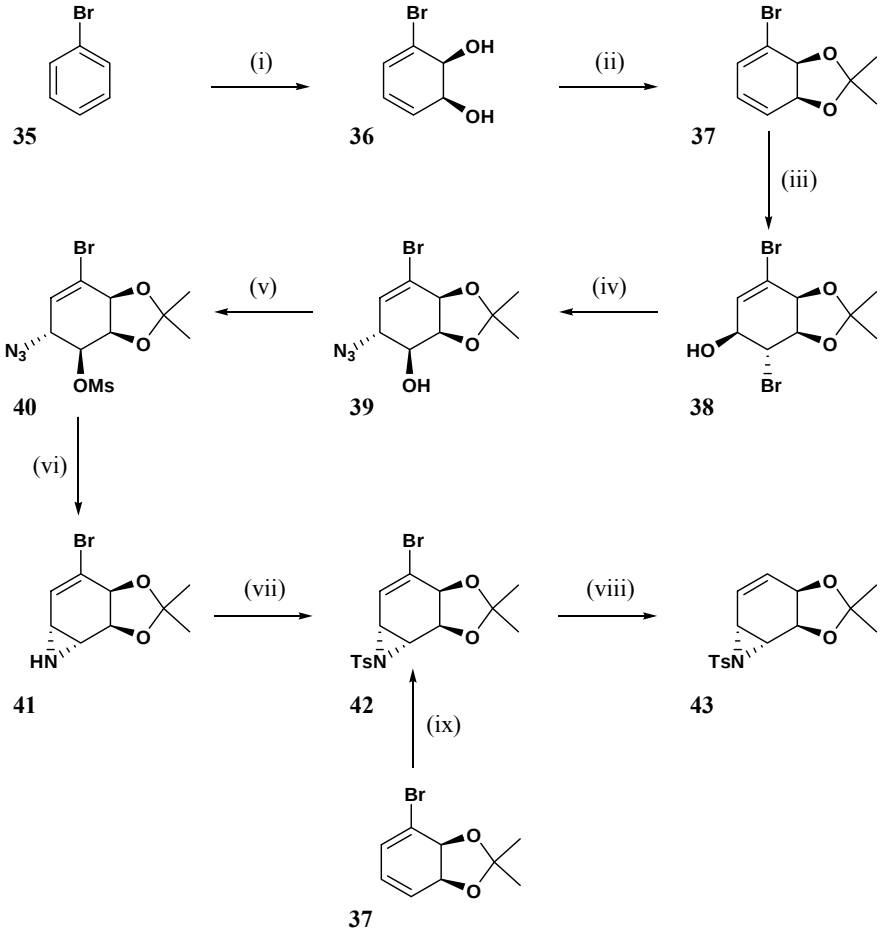

Scheme 5. (i) *P. putida* 39/D; *(ii)* DMP, *p*-TsOH, 85%; *(iii)* NBS, DME, H_2O; *(iv)* NaN_3, DMSO, 87%; *(v)* MsCl, Et_3N, CH_2Cl_2; *(vi)* $LiAlH_4$, THF; *(vii)* TsCl, Et_3N, CH_2Cl_2, 30.7% (from diol **36**); *(viii)* Bu_3SnH, AIBN, PhMe, 78%; *(ix)* PhI=NTs, MeCN, $Cu(acac)_2$, 54%.

The aromatic ring **A** of pancratistatin **4** was then prepared by a directed *ortho*-metalation with the aid of higher order cuprates **47** *(Scheme 6)*. This required the starting material, piperonic acid **44**, to first undergo an amidation to form compound **45** in 71% yield. The **C7** hydroxy group of pancratistatin **4** was then installed by an *ortho*-lithiation with *s*-BuLi/TMEDA, boration with trimethylborate ($B(OMe)_3$) and subsequent oxidation with hydrogen peroxide (H_2O_2) to give compound **46**. An investigation of the higher order cuprates showed that lithium dimethylcyanocuprates gave the *syn*-1,4-addition product, while lithium diphenylcyanocuprates gave the *anti*-1,2-addition product. Therefore, when the nucleophilic S_N2 ring opening of the vinylaziridine **43** was performed, it was found that the use of the higher order cuprate **47** gave the necessary *anti*-1,2-addition product **48** in 75% yield.

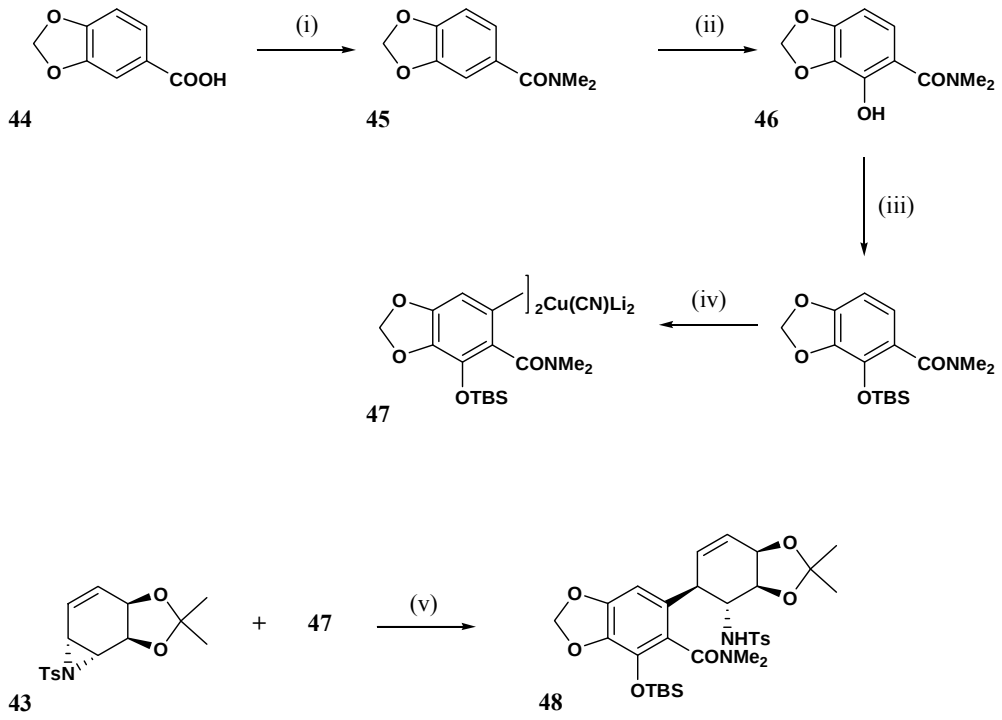

Scheme 6. *(i)* $SOCl_2$, Me_2NH, 71%; *(ii) s*-BuLi, TMEDA, $B(OMe)_3$, H_2O_2, 80%; *(iii)* TBSCl, 95%; *(iv) s*-BuLi, TMEDA, THF, CuCN; *(v)* $BF_3.Et_2O$, 75%.

At this point the synthesis became somewhat complicated, as it was observed that compound **48** existed as α and β atropisomers. Boc protection then formed a mixture of atropisomers **49a** and **49b** in 68% yield *(Scheme 7)*. The mixture of atropisomers was detosylated using Na/anthracene/DME to afford compounds **50** and **51** in a combined yield of 82%. The α-form **51** could be further desilylated to give the β-form **50** in 93% yield. The benzamide **50** was then reduced to the aldehyde **52**, using sodium bis(2-methoxyethoxy)aluminium hydride (SMEAH)/morpholine and the free alcohol was again protected as the benzyl ether **53**. The aldehyde **52** was then oxidized to the acid **54**, followed by methylation using diazomethane which afforded the methyl ester **55**, followed by deprotection of the acetonide **56**, and hydroxyl-directed epoxidation with *tert*-butyl hydroperoxide and vanadyl acetylacetonate (*t*-BuOOH/$VO(acac)_2$) to provide the epoxy diol **57**. Finally, cyclization occurred with refluxing water containing a catalytic amount of sodium benzoate. Under these conditions the Boc amide underwent a retro-ene reaction, thus liberating the amine for cyclization. The benzyl group was finally removed by hydrogenation to give pancratistatin **4**. Overall, the target material was reached in 14 steps and 2% total yield.

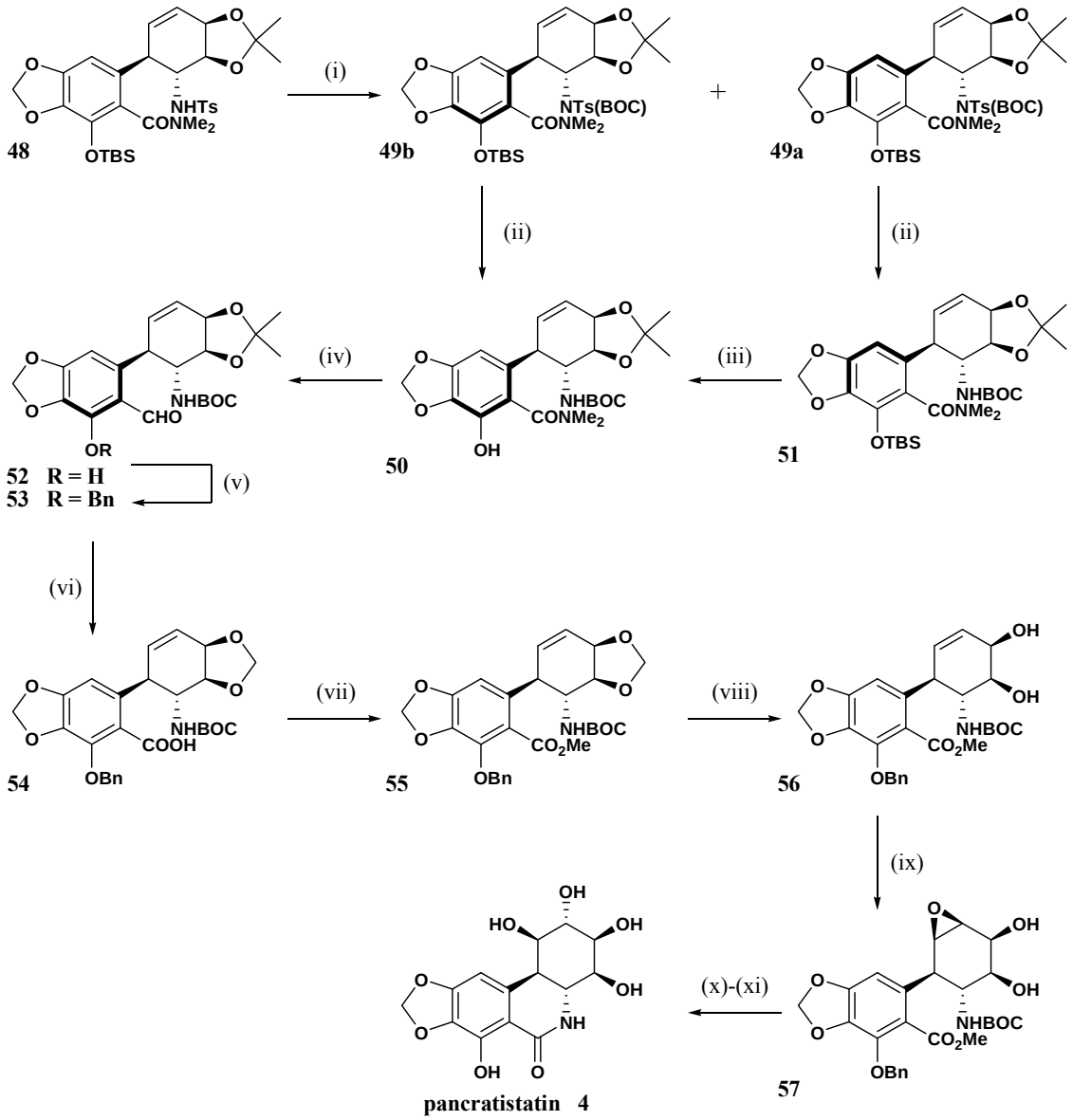

Scheme 7. *(i) s*-BuLi, $(BOC)_2O$, THF, 68%; *(ii)* Na, anthracene, DME, 82% (combined yield from **49** and **50**); *(iii)* TBAF, THF, 93%; *(iv)* SMEAH, morpholine, THF, 72%; *(v)* BnBr, K_2CO_3, DMF, 83%; *(vi)* $NaClO_2$, KH_2PO_4, *t*-BuOH, H_2O, 2-methyl-2-butene, 100%; *(vii)* CH_2N_2, Et_2O; 98%; *(viii)* AcOH, H_2O, 73%; *(ix)* *t*-BuO_2H $VO(acac)_2$, PhH, 53%; *(x)* H_2O, BzONa(cat), 51%; *(xi)* H_2, $Pd(OH)_2/C$, EtOAc.

1.4.3. Paulsen and Stubbe[37,38]

The approach by Paulsen and Stubbe does not directly involve the synthesis of pancratistatin, but rather (+)-lycoricidine **3.** However several key chemistry procedures used in their synthesis have been adapted for the purpose of this MSc project *(see Section 1.5.3)*.

One of the major problems with many approaches to the formation of ring **C** in pancratistatin **4** and other Amaryllidaceae alkaloids that exhibit similar chemical properties and appearance, is the insertion of the oxygen functionalities as well as the tendency of certain adducts toward aromatization. Paulsen solved the problem of oxygenation by starting his synthesis with D-glucose **58** and converting it into the unsaturated nitro olefin **60** to which the aryl fragment **61** could be added (*Scheme 8*). The conjugate addition of the aromatic group **59** to the nitroalkene **60** was not very strongly selective and this provided the two diastereomers **62** and **63** in an overall yield of 77%.

The mixture of diastereomers **62** and **63** *(Scheme 8)* was reacted with acetic acid to expose cyclic hemiacetal intermediates, which were then deprotonated at the α-C to the nitro with the mild base, potassium carbonate. At this point in the synthesis the products could be separated, by forming the "Paulsen-Danishefsky" lactone **64** in a low yield of 34%. The lactone **64** was then hydrogenated with H_2/Pd to give amino alcohol **65**, and reacted with potassium carbonate to induce the formation of the lactam ring and thus by default (+)-7-deoxypancratistatin **5**. However, Paulsen's aim was to synthesize (+)-lycoricidine **3**, so the **C1** hydroxyl group was dehydrated, which in turn caused the **C10b** centre to lose its stereochemistry. Thus when Paulsen published his asymmetric synthesis of (+)-lycoricidine **3** from D-glucose in 1983, it was effectively also the first synthesis of (+)-7-deoxypancratistatin **5**, even though this compound would only be recognized as a natural product in 1984.

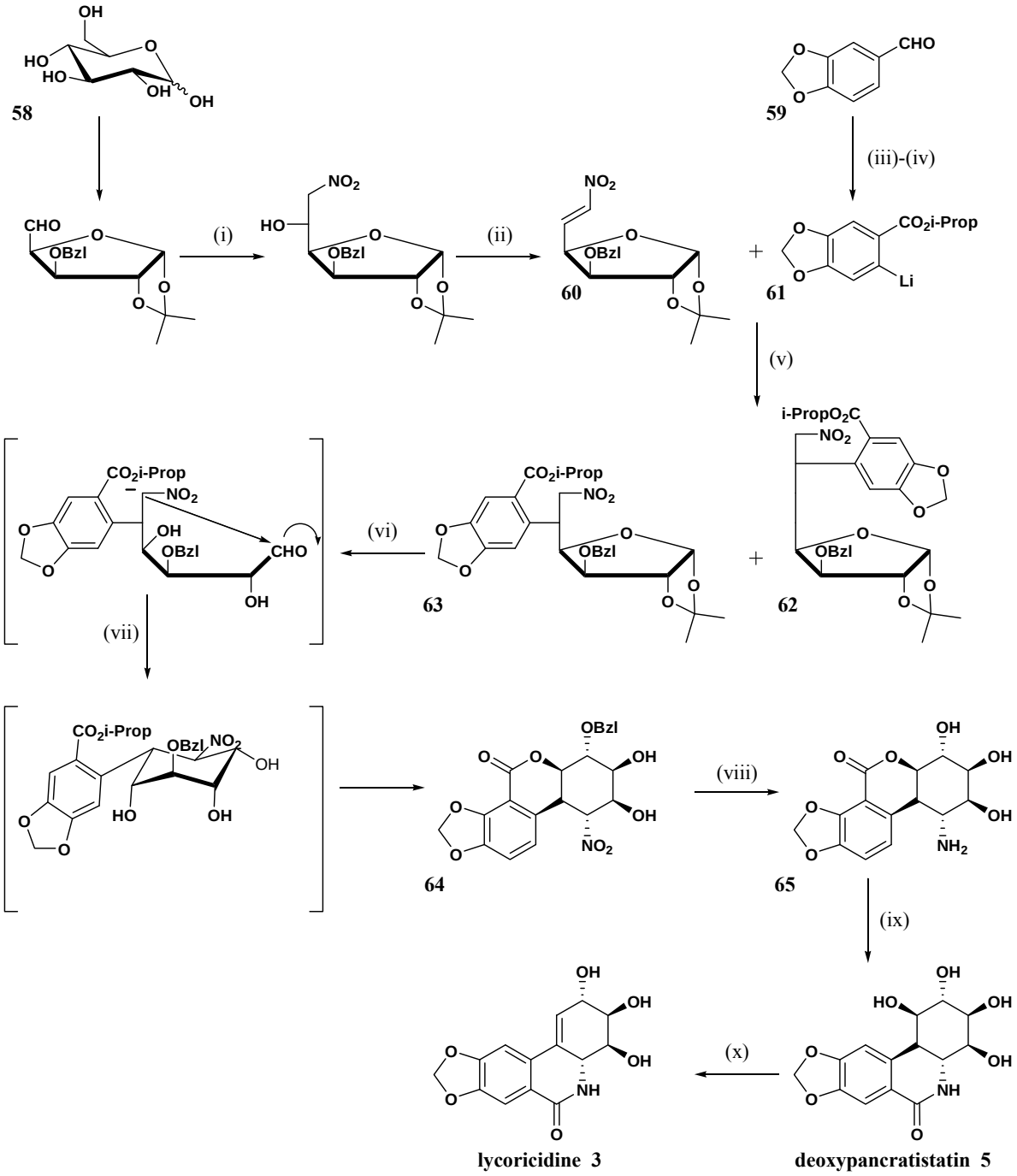

Scheme 8. *(i)* CH_3NO_2, Et_3N, Et_2O, 88% (mixture of epimers); *(ii)* $MeSO_2Cl$, Et_3N, Et_2O, 76%; *(iii)* Br_2; *(iv)* *i*-PrOH, conc. H_2SO_4, 56%; *(v)* CH_2Cl_2, 77% combined; *(vi)* AcOH, $PhCH_3$; *(vii)* K_2CO_3, MeOH, 34% (over two steps); *(viii)* H_2/Pd, MeOH; *(ix)* K_2CO_3, MeOH, 72%; *(x)* $SOCl_2$/Pyridine, 88%.

Scheme 8 shows the synthetic route when using diastereomer **63** only, as it is the apparent compound for accomplishing the synthesis of (+)-lycoricidine **3**. However, the products of diastereomer **62** have been shown in *Scheme 9*. Once the L-*ido*-compound **62** was reacted with acetic acid and potassium carbonate, and cyclized into the acetylated form of the lactam, the two inositol-type products, in the *scyllo* **66** and *myo* **67** conformations were produced. This occurred due to the change in conformation of the **C4** hydroxyl group from equatorial to axial. The overall change to the product, which is itself an adduct of 7-deoxypancratistatin **5**, showed changes in stereochemistry, compared to its parent structure at the **C10b** stereocentre and the **C4** stereocentre.

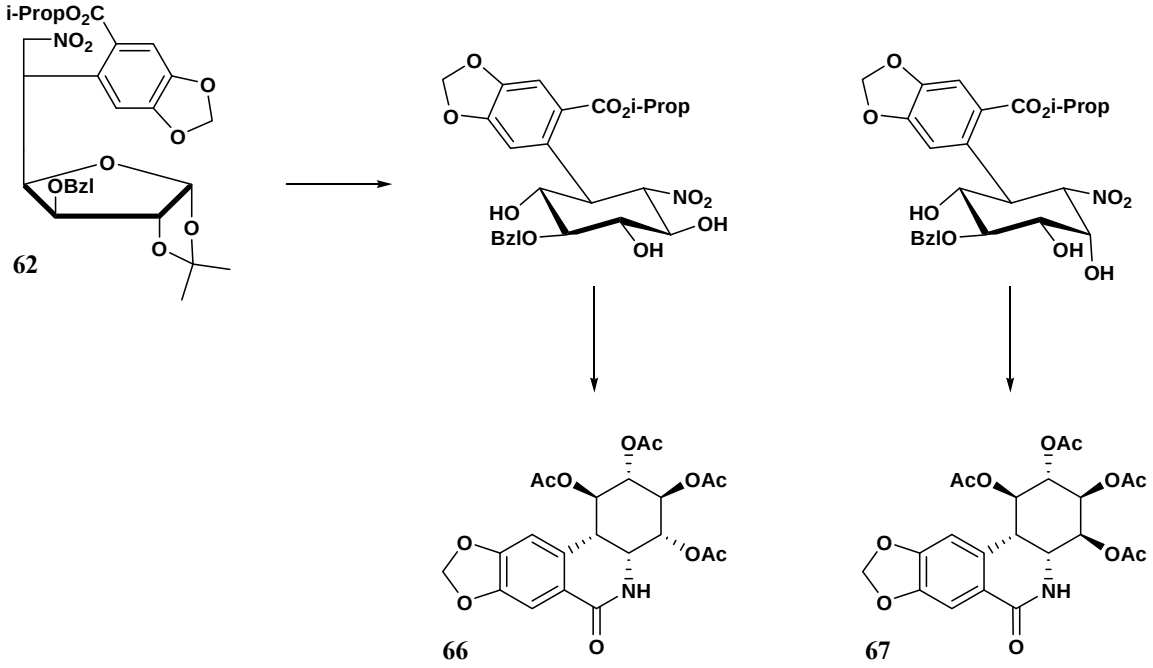

Scheme 9. Key stereochemical changes in diastereomer **62**.

1.4.4. Trost and co-workers[12,39]

In 1995 Trost *et al.* achieved the second asymmetric synthesis of pancratistatin **4** by using the method of palladium-catalyzed desymmetrization. Benzoquinone was converted into a key conduritol derivative, which was treated with *n*-BuLi and methylchloroformate to form the symmetric dicarbonate **68** shown in *Scheme 10.* The *meso* conduritol **68** was then subjected to the key desymmetrization process in the presence of the azide nucleophile, trimethylsilyl azide, the palladium complex, and a C_2-symmetric catalyst **A**, to give the homochiral carbonate **69**. The aryl group was then introduced by a regio- and diastereo-controlled S_N2 cuprate-controlled Grignard addition to give compound **70**.

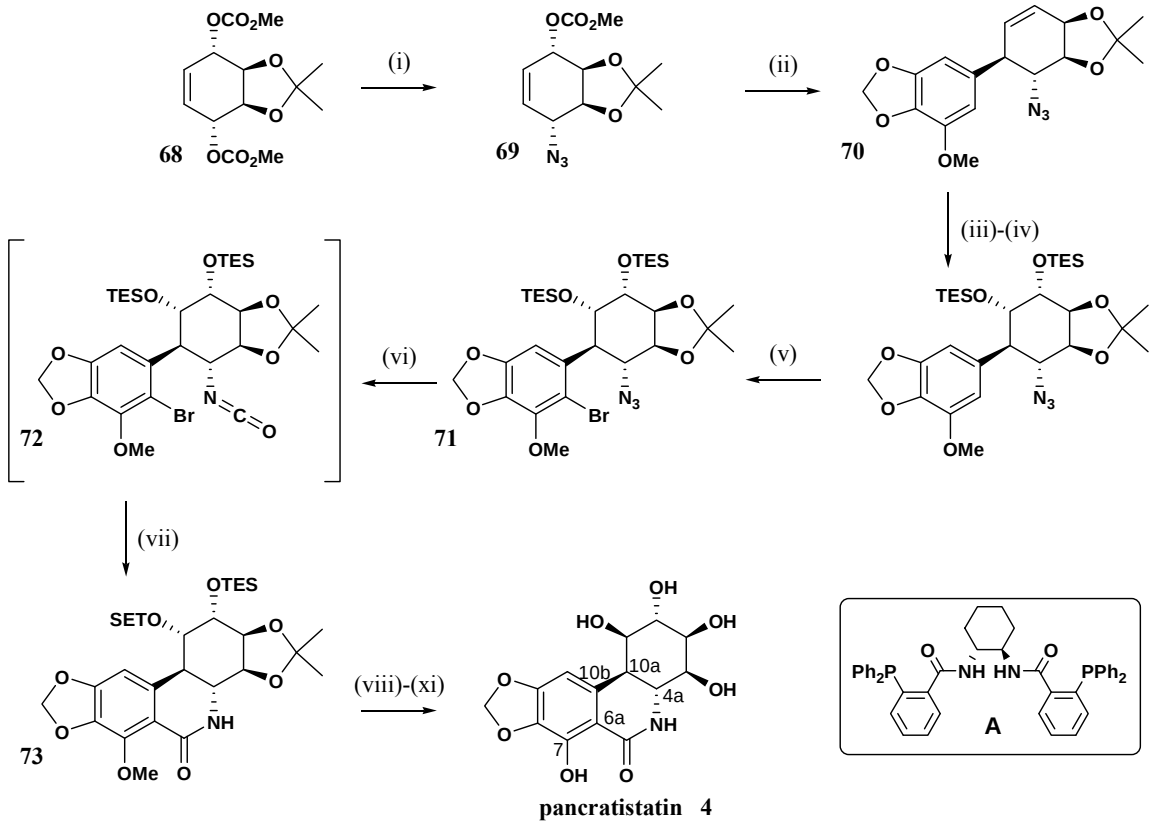

Scheme 10. *(i)* 0.5% (p-$C_3H_7PdCl)_2$, 0.75% **A**, $TMSN_3$, 82%; *(ii)* ArMgBr, CuCN; *(iii)* cat. OsO_4, $NMO.H_2O$, 62% from **69**; *(iv)* $TESOSO_2CF_3$, 2,6-lutidine, 100%; *(v)* NBS, 75%; *(vi)* $(CH_3)_3P$, H_2O, $COCl_2$; *(vii)* *t*-BuLi, 65% from **70**; *(viii)* TBAF; *(ix)* $SOCl_2$, pyridine, cat. $RuCl_3.H_2O$, $NaIO_4$, 72% from **72**; *(x)* $PhCO_2Cs$, H_2O, cat. H_2SO_4, 85%; *(xi)* MeOH, K_2CO_3, LiI, 85%.

At this point in the synthesis both the **A** and **C** rings are in place, and some of the most necessary components, such as the nitrogen substituent and three hydroxyl groups are present. The remainder of the synthesis required a regioselective bromination of the group *ortho* to the methoxy **C6a** using *N*-bromosuccinimide (NBS) to afford compound **71**, followed by the formation of the isocyanate intermediate **72** from a trimethylphosphine [$(CH_3)_3P$] and phosgene ($COCl_2$) reaction. This compound could then be cyclized to form the lactam **73**, which underwent various protections and deprotections to achieve the correct stereochemical inversions of the hydroxyl groups to

finally achieve the synthesis of pancratistatin **4.** The synthesis was accomplished in 19 steps with an overall yield of 8% from benzoquinone.

1.4.5. Haseltine and co-workers[40]

Haseltine and co-workers reported a total synthesis of (+)-pancratistatin **4** in 1997. As with the synthesis reported by Trost and co-workers[39] their approach utilized benzoquinone as a starting material, which eventually underwent a retro Diels-Alder to afford a protected conduritol, similar to the intermediates utilized by Trost's group for their synthesis. An enzymatic acetylation using P30 lipase led to desymmetrization of the conduritol to form the enantiopure acetate, which was exchanged with *tert*-butyldimethylsilyl (TBS) to give product **75** as shown in *Scheme 11*. The aromatic substrate **74** was prepared from piperonal and contained the methylenedioxy moiety and the **C6a** bond. The construction of the C10b-C10a bond was accomplished using the aromatic group **74** with the *meso* conduritol **75** by an intramolecular elecrophilic aromatic S_N2 substitution to give the coupled product **76**. Introduction of the **C7** hydroxyl into ring **A**, and the stereoselective cylization of the **C10a-C10b** bond created some setbacks in the synthesis; however the Danishefsky-type lactone, intermediate **77** *(Section 1.4.1, scheme 4)* was synthesized, which led to convergence for the remainder of the synthesis. This includes the installation of the stereocentres by a *syn*-specific Overman rearrangement that resulted in the introduction of the **C4a** nitrogen.

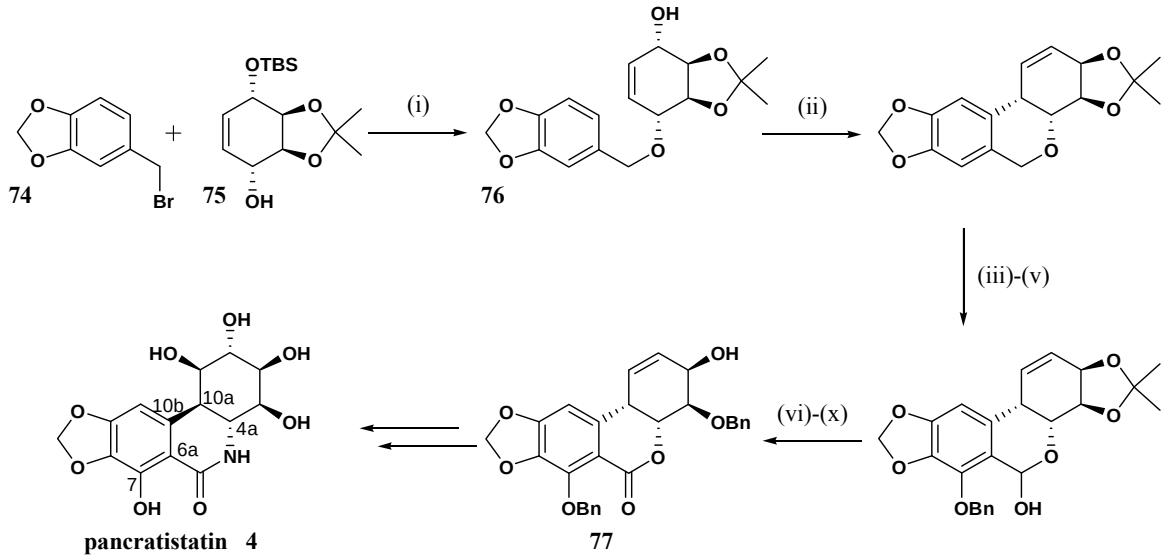

Scheme 11. *(i)* NaH, Bu_4NI, TBAF, 83%; *(ii)* Tf_2O, 2,6-lutidine or 2,6-di-*t*-Bu-pyridine, 73%; *(iii)* $HOCH_2CH_2OMe$, DDQ, 62%; *(iv)* *t*-BuLi, $B(OMe)_3$, H_2O_2; *(v)* NaH, BnBr, CSA, 71%; *(vi)* TPAP, NMO, 91%; *(vii)* aq. HCl, 97%; *(viii)* MEMCl, *i*-Pr_2NEt, 65%; *(ix)* Ag_2O, BnBr, 65%; *(x)* TsOH, MeOH, 67%.

1.4.6. Magnus and co-workers[41,42]

Magnus *et al.* employed a β-azidonation to introduce the **C4a** stereocentre containing the nitrogen substituent into the silyl enol ether product **81**. The synthesis began with the methylenation and bromination of *o*-vanillin to yield to aryl bromide **78** in 65% yield *(Scheme 12)*. Lithiation of the aryl bromide, followed by the addition to ketone **79** gave the tertiary alcohol, which was then dehydrated to produce a double bond that was then hydrogenated, affording the desired ketone **80** in good yield. The ketone was then protected in its enol form thus exposing the double bond nature of compound **81**. The double bond later underwent a shift with the addition of meta-chloroperoxybenzoic acid (*m*-CPBA), to give **82.** This compound was then reacted with $EtOH/H_3O^+$ to return the structure to its ketone form because the incorrect stereochemistry was obtained as **C4**. Various other attempts at elimination were carried out and finally a successful epoxidation from the α-face, to give **83** was confirmed. By selective reduction of the ketone from the α-face followed by trans diaxial S_N2 ring opening of the epoxide with

benzoate ion at **C1**, all the hydroxyl groups of the pancratistatin **4** ring **C** were stereoselectively installed. Modified Bischler-Napieralski conditions were then used to induce the formation of the lactam, along with its regioisomer in a ratio of 1:7 in favour of the desired product. The regioisomers were isolated in 60% yield, as an inseparable mixture. Once deprotection occurred, the synthesis of pancratistatin **4** was completed in an overall yield of 1.2% over the 22 step synthesis.

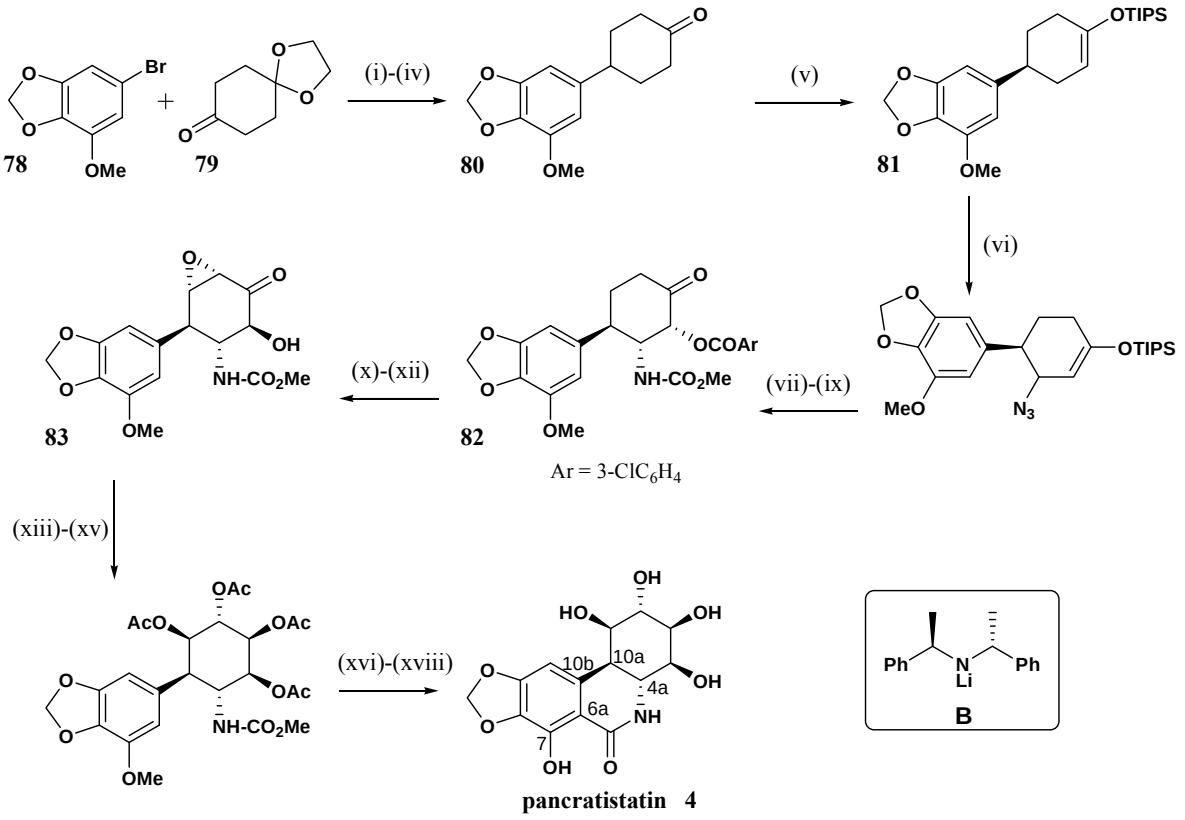

Scheme 12. *(i) n*-BuLi, THF, 85%; *(ii)* $POCl_3$, DBU, pyridine, 97%; *(iii)* H_2, Pd/C, 87%; *(iv)* Dioxane, H_3O^+, 89%; *(v)* **B**, LiCl, TIPSOTf, 95%, ≥85% ee; *(vi)* PhIO, $TMSN_3$, 95%; *(vii)* $LiAlH_4$, MeCOCl, pyridine, 56%; *(viii) m*-CPBA, 83%; *(ix)* $EtOH/H_3O^+$, 88%; *(x) t*-BuOK, HMPA, 91%; *(xi)* TMSOTf, Et_3N, $PhSeOCOCF_3$, H_2O_2, pyridine, 64%; *(xii)* H_2O_2, $NaHCO_3$, 75%; *(xiii) L*-selectride, 63%; *(xiv)* Ac_2O, Et_3N, 71%; *(xv)* $PhCO_2Na$, Ac_2O, pyridine, 60%; *(xvi)* Tf_2O, DMAP, 60%; *(xvii)* BBr_3, 70%; *(xviii)* NaOMe, MeOH, 87%.

1.4.7. Rigby and co-workers[43]

In 2000, Rigby and co-workers reported the syntheses of (+)-pancratistatin **4** and (+)-narciclasine **2.** The key transformation in their syntheses ensued from the hydrogen bond controlled enamide photocylization, which in the case of pancratistatin **4**, resulted in the desired *trans*-fused precursor **85** as seen in *Scheme 13*.

The isocyanate **84** contained three of the necessary stereocentres at the start of the synthesis, although **C1** had an inverted stereochemistry. Irradiation of **85** gave phenanthridone **86**. The remaining hydroxyl groups were later introduced by conversion of the epoxide **86** into the olefin **87**. This compound could then be oxidized with osmium tetroxide to install the **C3** and **C4** hydroxyl groups at the β-face of ring **C** to finally reach the target molecule, pancratistatin **4**. The final product was achieved in an overall yield of 0.35% in 23 steps.

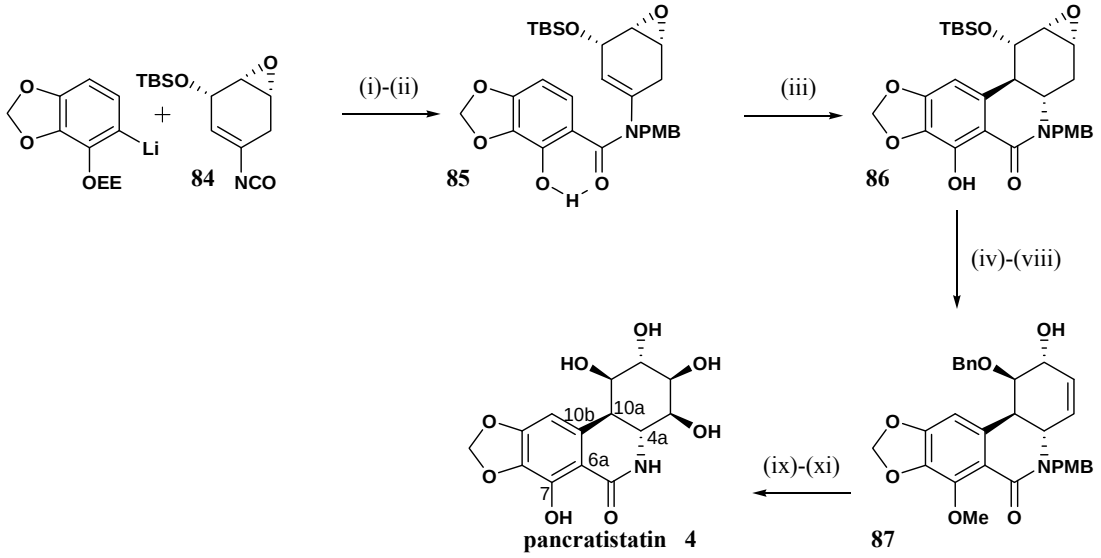

Scheme 13. *(i)* –70°C, 52%; *(ii)* NaH, PMBBr, PPTS, 73%; *(iii)* hν, PhH, 30%; *(iv)* NaH, MeI, 98%; *(v)* TBAF, 85%; *(vi)* Dess-Martin, $NaBH_4$, –20°C; *(vii)* NaH, BnBr, 73%; *(viii)* $(PhSe)_2$, $NaBH_4$, H_2O_2, 84%; *(ix)* OsO_4, 89%; *(x)* $Pd(OH)_2/H_2$, 87%; *(xi)* LiCl, DMF, 78%.

1.4.8. Kim and co-workers[18,44]

Kim *et al.* utilized the Claisen rearrangement as a key step in their 2002 synthesis, by transforming the *E*-alkene **90**, into the aldehyde **91** *(Scheme 14)*. Initially, a Horner-Wadsworth-Emmons reaction was employed with the prepared phosphonate **88** and the aldehyde **89**, in order to obtain the *E*-olefin **90** exclusively. The **C1** hydroxyl was then introduced by iodolactonization as shown by the intermediate **92**. Dihydroxylations and cyclic sulfate elimination reactions introduced the **C2, C3** and **C4** hydroxyl groups. Compound **93** was treated with osmium tetroxide (OsO_4) on the α-face to produce a diol. The regioselective elimination of the C-3 hydroxyl group to generate the unsaturation was achieved by employing a cyclic sulfate elimination reaction; the cyclic sulfate was then treated with DBU in refluxing toluene to form the desired allylic alcohol **94**. The nitrogen was installed into the compound earlier in the reaction by the Curtius rearrangement with diphenylphophonic azide (DPPA), but lactamization was only accomplished by the Bischler-Napieralski cyclization to form the desired compound **95**, along with a minor amount of regioisomer **96** in 78% combined yield and 7:1 regioselectivity, later in the synthesis.

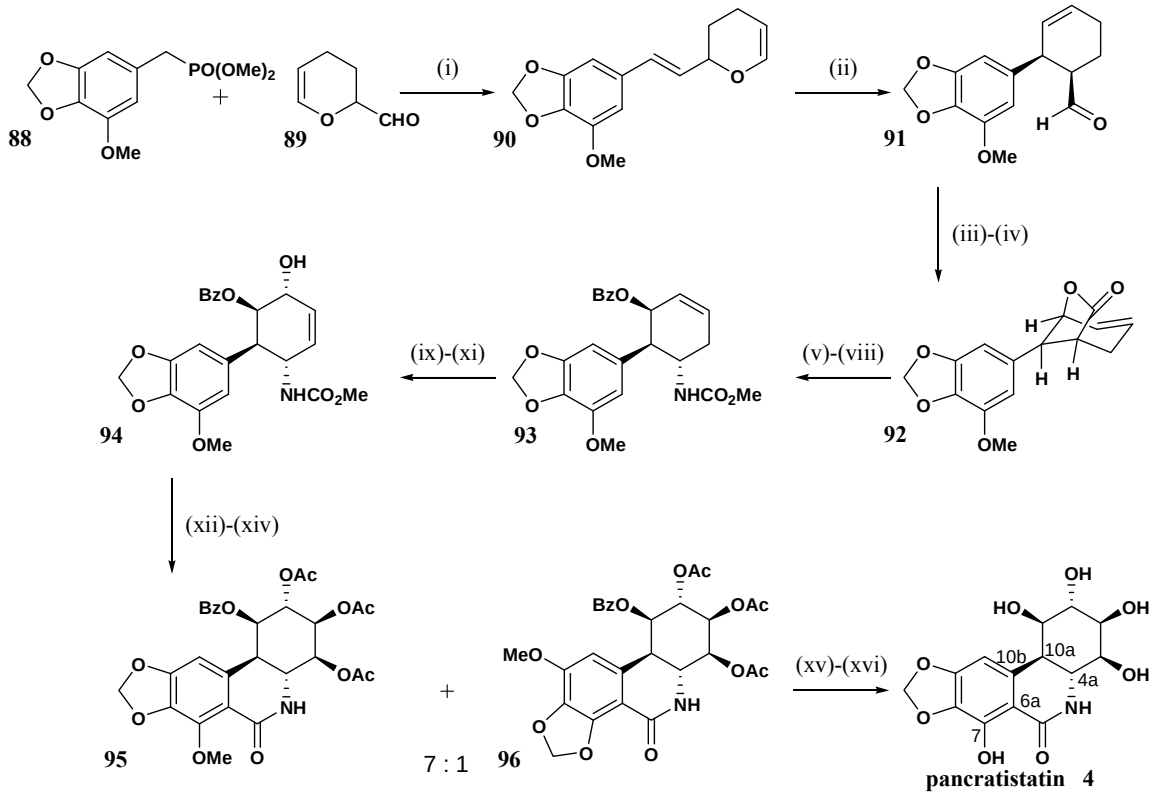

Scheme 14. *(i)* LHMDS, 60%; *(ii)* PhMe, sealed tube, 78%; *(iii)* $NaClO_2$, $NaH_2PO_4.2H_2O$, 90%; *(iv)* KI_3, DBU, 78%; *(v)* NaOMe, 93%; *(vi)* LiOH, 99%; *(vii)* DDPA, Et_3N, NaOMe, 82%; *(viii)* BzCl, Et_3N, 99%; *(ix)* OsO_4, NMO, 96%; *(x)* $SOCl_2$, Oxone, $RuCl_3.3H_2O$, 67%; *(xi)* DBU, H_2O, THF, 67%; *(xii)* OsO_4, NMO, 88%; *(xiii)* Ac_2O, 77%; *(xiv)* Tf_2O, DMAP, 78%; *(xv)* BBr_3, 65%; *(xvi)* NaOMe, 83%.

1.4.9. Li and co-workers[20]

Li and co-workers have thus far been able to develop the shortest synthesis of (+)-pancratistatin **4** in only 12 steps *(Scheme 15)*. The starting material used for the synthesis was pinitol **97**, which is a somewhat expensive material because of its precise absolute stereochemistry. It contains five of the necessary carbon stereocentres found in the cyclitol ring of the pancratistatin **4**.

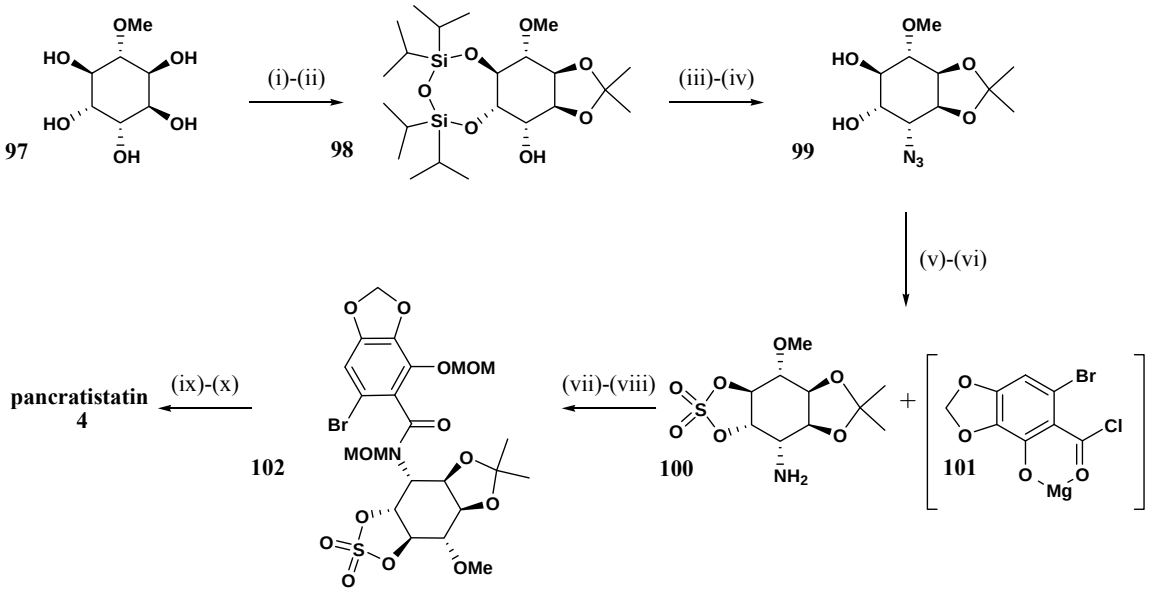

Scheme 15. *(i)* *i*-Pr_2SiCl_2, imidazole, DMAP, 94%; *(ii)* $(MeO)_2C(CH_3)_2$, *p*-TsOH, 81%; *(iii)* PPh_3, DEAD, CH_3SO_3H, NaN_3, 72%; *(iv)* TBAF, 100%; *(v)* $SOCl_2$, Et_3N, $NaIO_4$, $RuCl_3$, 87%; *(vi)* PPh_3, H_2O, 94%; *(vii)* $MgBr_2.OEt_2$, $COCl_2$, 64% *(viii)* K_2CO_3, MOMCl, 84%; *(ix)* *t*-BuLi, $CeCl_3$, ultrasound, 72%; *(x)* BBr_3, MeOH, 52%.

The synthesis required the differential protection of the *trans* and *cis* hydroxyl groups with the bulky 1,1,3,3-tetraisopropyldisiloxane (TIPDS) group and an acetonide to provide product **98**. The configuration of the only remaining hydroxyl could then be inverted using the Mitsunobu reaction with methanesulfonic acid (CH_2SO_3H); this was followed by the insertion of the **C4a** nitrogen centre by azide substitution with a second inversion to get compound **99**. The Staudinger reduction then afforded the amine **100.** The aryl substituent **101**, which had been previously prepared, was reacted under the conditions shown in *Scheme 15* to give the MOM protected amide **102**. The key transformation however, was the $CeCl_3$-catalyzed intramolecular opening of the cyclic sulfate **102.** The organocerium, a softer nucleophile, was used as a halogen metal exchange, which led to nucleophilic ring opening of the cyclic sulfate closing the B ring of the pancratistatin precursor. Thus the **C10b** centre was formed and the synthesis of pancratistatin **4** was completed in an overall yield of 9%.

1.5. Origins and background to the present project

In the description of the main aim of the project, it will be necessary to discuss certain aspects pertaining to the project that may be of interest and could add some clarity to the topic.

The Paulsen and Stubbe[37,38] synthesis discussed previously *(Section 1.4.3.)* lends two very important synthetic protocols to our synthesis, the first being the use of D-(+)-glucose **58** as a starting material, and the second is the use of conjugate addition as a key step for the introduction of the aryl substituent of pancratistatin. A detailed study of these aspects will be discussed in sections 1.5.1 and 1.5.2 below.

1.5.1. Glucose and aspects of carbohydrates

Carbohydrates have been extensively used as starting materials in enantioselective syntheses because they are a relatively inexpensive natural source of chiral compounds.[45] Glucose is normally represented in a chair conformation to best represent its five stereogenic centres. Most carbohydrate building blocks are capable of existing in more than one form (pyranose and furanose forms), and glucose is no exception. This is owing to the stereogenic centre closest to the oxygen in the tetrahydopyran ring (represented as an undefined hydroxyl group, whereas the other stereogenic centre consists of CH_2OH), which exists as a hemiacetal and therefore the molecule is in equilibrium with the open-chain aldehyde form (*Figure 10)*.[46] It is therefore important to control which forms glucose exists in, because of the added complexity pertaining to the glucose with its five stereogenic centres and the fact that it can exist as an open-chain system, and a 5-membered or 6-membered ring systems. The incorporation of protecting groups into the carbohydrate can therefore be pursued to ensure that only the hydroxyl groups required for certain reactions are available.[47]

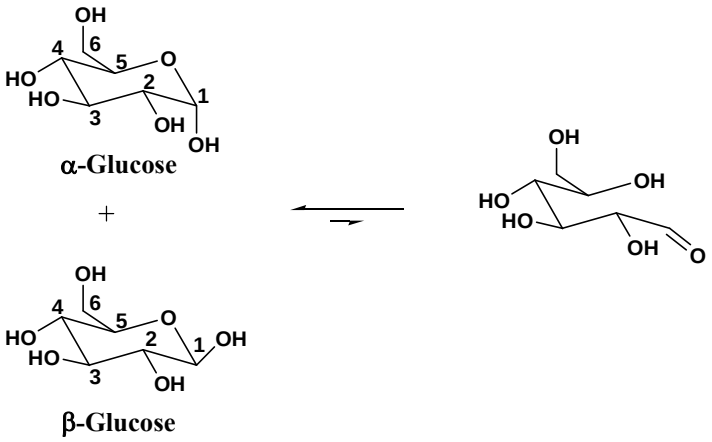

Figure 10. α- and β-glucose forms showing hemiacetal formation.

Glucose has four chiral centres and exists in two groups of stereoisomers, L and D. In addition to this when glucose cyclizes two anomers are formed owing to the asymmetric centre or anomeric carbon, **C1.** These anomers differ structurally by the relative configurations of the position of the **C1** hydroxyl group. α-D-glucose contains a hydroxyl group in the axial position (or *trans* to **C6**, below the plane of the ring), while β-D-glucose contains an hydroxyl group in the equatorial position (or *cis* to **C6**, above the plane of the ring).[48]

1.5.2. Cuprate and rhodium catalysed conjugate addition

The stereoselective insertion of the aryl substituent (ring **A)** of pancratistatin **4** onto the **C10b** site of the ring **C** fragment is an essential aspect to our synthesis of pancratistatin **4**. The previous investigation into the synthesis by Paulsen and Stubbe[37,38] showed that selectivity during the conjugate addition with the use of lithiated cuprates (i.e. compound **65**) was very poor and in fact an almost racemic mixture of diastereomers (compounds **66** and **67**) was achieved (*Scheme 16*). Thus in our proposed synthesis, a further investigation into cuprate conjugate additions will be conducted, as well as some research into other possibilities for an approach to the selective addition of the aromatic moieties into the pancratistatin core.

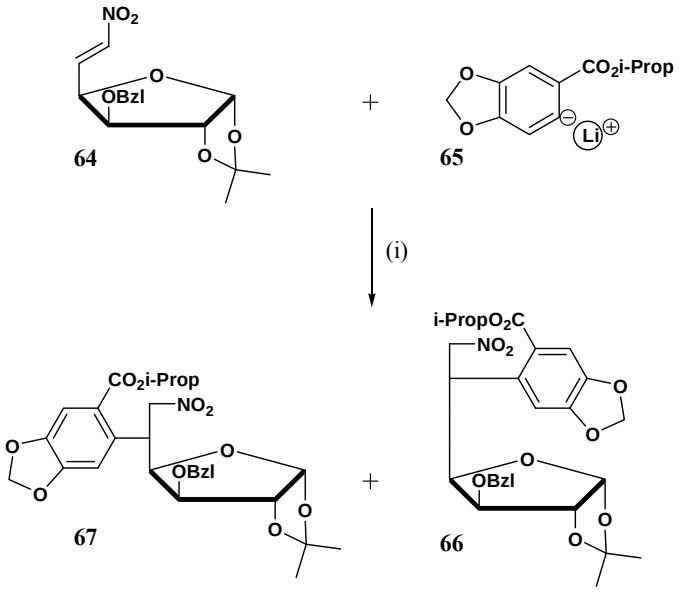

Scheme 16. *(i)* CH_2Cl_2, 77% combined.

In the case of our model synthesis and the proposed precursor required for many Amaryllidaceae compounds, including pancratistatin **4**, the reaction of the aryl cuprate with the α,β-unsaturated compound should afford exclusively *anti*-selective product (for example compound **67**, *Scheme 16*), although this is seldom the case. There are many factors that have an effect on the outcome of the selectivity, such as the effect of solvents[49] and additives,[50] whether or not the cuprate being added is a higher or a lower order cuprate,[50,51] and the electronic and steric properties of the alkene substrate.[51] The investingation of these properties has continued intensively due to the mechanistic details of the cuprate reactions remaining elusive and under constant debate.

The mechanism of the 1,4-conjugate addition reaction has been extensively studied both experimentally and theoretically. There have been many proposed transition state models involving significant complexation between the metal centres and the substrate, which have accounted for the anti-selective additions.[52] Early investigations proposed "Cu^{III} intermediates" as the key transformation to the C–C bond by a reductive elimination of the β-carbon, where both square planar and T-shaped complexes have been proposed.[53-55] However, recent mechanistic investigations favour a "modified Felkin-Anh"

interpretation, in which an allylic 1,3-strain greatly destabilizes a transition state, owing to the acute angle of attack in the copper-π-complex, that leads to a *syn*-product.[4] It has nonetheless been suggested that because of the complex and diverse nature of organocopper reagents, no single mechanistic model generally explains or predicts the outcome of these reactions.[4]

It is for this reason, amongst others that will become apparent during the discussion of the synthesis, that an additional methodology was proposed to achieve the required 1,4-*anti* addition. The Hayashi-Miyaura reaction of arylboronic acids under rhodium catalysis, had accomplished a high degree of versatility in that the reactions can be carried out with electron-deficient alkenes that are highly functional-group tolerant.[56] Most importantly the reaction is water-tolerant, unlike the highly moisture-sensitive Grignard reactions, which are also conducted on a stoichiometric scale in terms of copper, whereas the rhodium compounds can be used sparingly in catalytic amounts. The Rh-catalysed conjugate addition has also been shown to be highly *anti*-selective, irrespective of the double bond geometry. This can be understood by transition state models in which steric destabilization is more energetically favourable thus leading to the formation of the desired *anti* product. The nucleophile thus enters antiperiplanar to the lowest-lying σ* orbital γ-C-X groups (X = H, OR, CH_2OR).[56]

1.5.3. Aim and strategy of the project

The aim of this project is to synthesize (+)-pancratistatin stereoselectively, using D-(+)-glucose, and by using a similar strategy employed by Paulsen and Stubbe in 1983 who utilized a nitroalkene and inserted the aryl substituent by conjugate addition (see *Scheme 17*).[37,38] An additional adaption to the above project will attempt the formation and hence the use of an enoate in the place of the nitro group, which will undergo a similar 1,4-addition for the introduction of the aryl group. Finally, a variety of aromatic anologues will be produced to create a library of compounds that could be potentially analyzed for biological activity against a variety of cell lines as well as to compare the biological activity with pancratistatin **4**.

Scheme 17 details the proposed steps for the formation of the nitroalkene **105** and the enoate **106**, which are known building blocks in carbohydrate chemistry and have been used considerably in natural product synthesis. The commercially available sugar is trapped into its furanose form under acetalisation conditions *(step i),* the remaining hydroxyl can then be protected as a benzyl ether **103** *(step ii)*, which can then undergo selective deprotection of one acetonide *(step iii)*, followed by an oxidation to produce the aldehyde **104** *(step iv)*. The synthesis would diverge at this point into the nitroalkene **105**, prepared by a Henry reaction *(step v),* and into the enoate **106** prepared by a Horner-Wadsworth-Emmons reaction *(step vi)*.

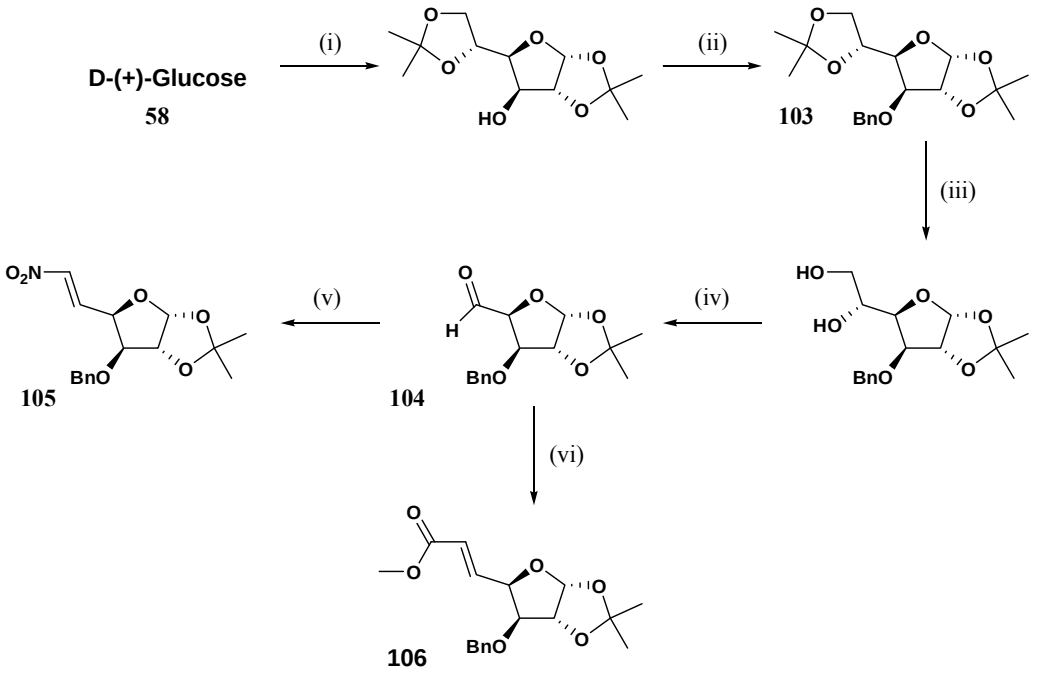

Scheme 17. Proposed synthetic route for the preparation of α,β-unsaturated compounds.

Scheme 18 and *19* show the possible approaches to the formation of the ring **C** and finally the ring **B** of pancratistatin **4**. The routes would progress in a similar fashion, with the described conjugate addition *(Section 1.5.2)* occurring, followed by the deprotection of the acetonide *(step iii)* to expose the hemiacetal in the furanose sugar moiety. We envisage that if the carbon α to the nitro group in **107** is treated with a mild base as

previously seen in the Paulsen and Stubbe synthesis,[37,38] that this will induce ring closure and thus set into place the **C** ring of pancratistatin with all its stereogenic centres intact and the functionality necessary to create the lactam and thus final ring **A**.

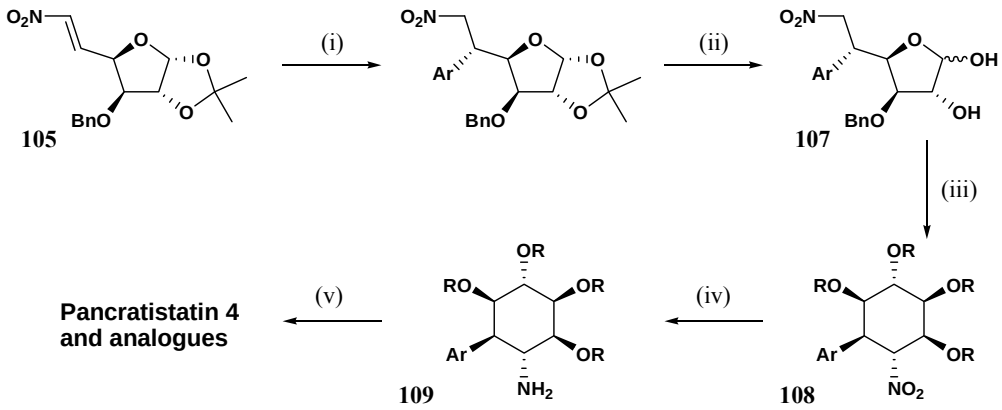

Scheme 18. Proposed synthetic route for pancratistatin and its analogues from nitroalkene **105**.

The nitrogen is already in place in *Scheme 18* and thus once ring closure has occurred all that is expected is for nitro **108** to be reduced into the amine **109**. This compound should then be transformed into an isocyanate and undergo the Bischler-Napieralski reaction *(step v)* to form the natural product **4**. Similarly, in *Scheme 19*, once ring **C** has formed, the amide **111** can be produced from a Curtius-type reaction *(step iv)* on the ester functionality **110** (via a conversion to the carboxylic acid), which can then undergo the Bischler-Napieralski reaction as in *Scheme 17* to produce pancratistatin **4**. The same methodology can then be employed to prepare analogues with varying aromatic substituents.

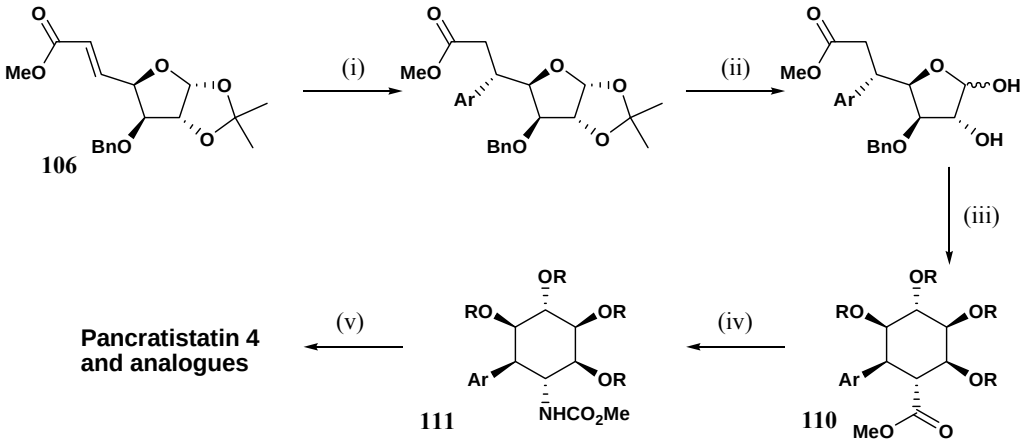

Scheme 19. Proposed synthetic route toward the synthesis of pancratistatin and its analogues with enoate **106**.

CHAPTER 2: RESULTS AND DISCUSSION

THE SYNTHESIS OF THE KEY ENOATE AND NITROALKENE

2.1. Toward the aldehyde precursor 104

The methodology for the formation of the sugar derivatives shown in *Scheme 20* has been well documented and several isomers are commercially available. D-(+)-Glucose **58** was used as the starting material for the synthesis because of its commercial availability and in view of the fact that it contained the stereochemical information required for the synthesis of the cyclitol **C** ring of pancratistatin **4**. The envisaged synthetic route for this section of the project are shown in *Scheme 20*.

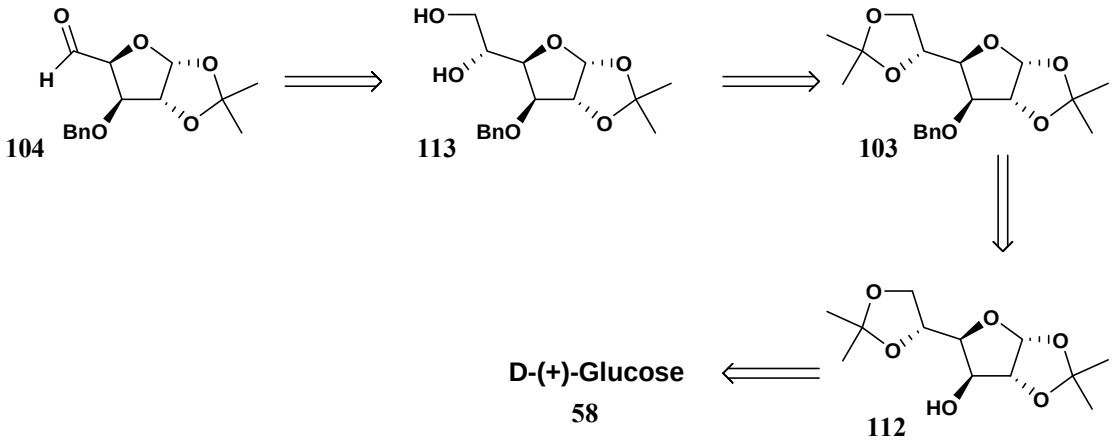

Scheme 20. Retrosynthetic route to aldehyde precursor **104.**

This specific form of D-(+)-glucose **58** was chosen as the chiral material necessary to produce the sought after product. Optical rotation of the material gave an indication of the purity of the material. The reported literature value of the α-D-glucose anomer was $[\alpha]_D$ = +109.0 (*c* 4.0, H_2O, 20 °C)[57] and the value attained from our optical analysis showed that the specific rotation was +91.3 (*c* 2.0, H_2O, 22 °C), therefore confirming that

our purchased glucose was the correct anomer. The specific rotation of the β-D-glucose anomer is reported as +20.1 (*c* 2.0, H_2O, 25 °C).[57]

2.1.1. Synthesis of the 5-membered furanose 112

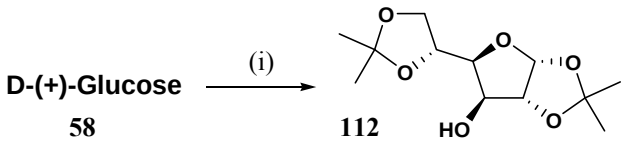

Scheme 21. *(i)* CH_3COCH_3, I_2, r.t., 20 h, 58%.

D-(+)-Glucose **58** was treated with acetone in the presence of iodine to form the protected furanose diacetonide derivative of glucose **112** *(Scheme 21)*.[47] The reaction was found to be highly selective for the formation of the 5- rather than the 6-membered ring, because the 6-membered pyranose ring has been shown to adopt a stable chair conformation more readily on reacting with acetone. In this case, the more likely arrangement of the newly formed compound would distinguish one of the methyl groups of the acetone as axial and there would therefore be a direct interaction between the methyl group and the axial hydrogen, which would be sterically and energetically unfavourable. Conversely, the furanose form has a larger probability of undergoing the protection due to the proximity of the 1,2-diols in the structure, which will thus demonstrate a greater selectivity toward the acetal fusion, which the pyranose glucose does not adhere to because of its complex conformational structure.[46,57]

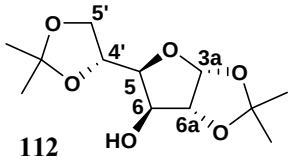

112

In the ^{1}H NMR spectrum of bisacetal **112** four prominent methyl singlet peaks at 1.50, 1.45, 1.37, and 1.32 ppm were the foremost features observed. This gave a clear indication that the glucose had been protected as the acetonide at both of the required sites on the starting material. When comparing the spectrum to that of glucose, it became clear that the material had undergone the transformation from the 6-membered to the 5-

membered ring, based on the complex hydrogen couplings. The doublet furthest downfield (δ = 5.94 ppm) was assigned to the H-3a with J = 3.6 Hz. The 3a-H hydrogen could be regarded as acetal hydrogen due to the acetonide protection and for this reason and because of the close proximity of the polar oxygen groups, the signal was observed remarkably downfield. A CH correlated spectrum (HSQC) was used to assign all the carbon signals to their respective hydrogen signals and to clarify some of the complexity in the spectrum. For instance, the CH_2 protons could be easily deduced from the spectrum, as they showed nonequivalence. Each of the corresponding ^{1}H NMR signals separated into doublet of doublet signals at 4.17 and 4.00 ppm. The H-4' signal was complex due to the overlap with the H-6 signal. It would be expected that the H-4' proton would split into a doublet of doublet of doublets due to the two nonequivalent CH_2's and H-5. Coupling appeared to have occurred between the OH proton and the proton of H-6 as evident from the doublet at 2.76 ppm. No coupling between H-6 and H-6a was apparent with H-6a producing only a doublet due to coupling H-3a. The possible outcome of the H-6 signal could then be understood to be a doublet of doublets. The IR spectrum of the acetonide protected compound **112** clearly showed the appearance of the acetonide CH_3 peaks in the 2984 and 1458 cm^{-1} region.

2.1.2. Benzylation of the remaining hydroxyl to synthesize 103[58,59]

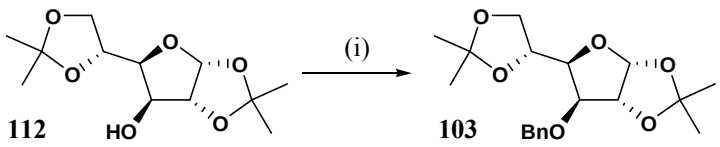

Scheme 22. *(i)* NaH (65% in oil), Bu_4NI, BnBr, THF, r.t., 22 h, 72%.

The protection of the remaining unprotected hydroxyl group was carried out with benzyl bromide and a base (*Scheme 22*). This was necessary for the subsequent acetonide deprotection to occur successfully and because of the benzyl group's stability toward most organic and inorganic reagents (requires hydrogenation over Pd/C for deprotection).

Furthermore, it was necessary for the remaining hydroxyl to be protected, owing to the nucleophilicty of the oxygen posing a potential problem as well as the potential for the polar hydroxyl to generate a more insoluble compound (insoluble in organic solvents). The salt tetrabutylammonium iodide (Bu_4NI) was used as a phase transfer catalyst to ensure optimal results during the benzylation process (*Scheme 22*).

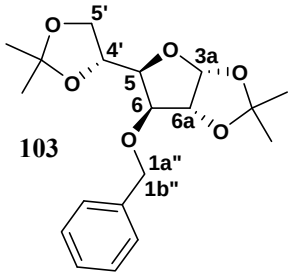

103

The most notable feature in the ^1H NMR spectrum of compound **103** was the appearance of the aromatic multiplet in the region of 7.36-7.30 ppm, which integrated for exactly five protons. Another obvious feature was the disappearance of the OH signal at 2.76 ppm. This together with the benzyl ether caused the H-6 proton signal to be unambiguously assigned which was not observed previously with compound **112**. Accordingly, H-3a and H-6a were observed to couple only to each other and H-6a did not couple to H-6. This was probably due to the dihedral angle between and H-6a being approximately 90°, causing coupling to be very weak. The CH_2 from the benzyl could also be accounted for, although the H-1a" and H-1b" protons were observed as nonequivalent and the signals were embedded in the H-5' and H-5 signals, making full interpretation of coupling problematic. In the ^{13}C NMR spectrum, the aromatic region unmistakably accounted for the benzyl group at 129.5, 129.0 and 128.6 ppm. Lastly, the IR spectrum clearly showed the loss of the OH peak in the region of 3424 cm^{-1}. An $[\alpha]_D$ was obtained for the benzylated product **103** of –22.5, which was found to be in good agreement to the reported literature value of –21.6.[58]

2.1.3. Selective isopropylidene deprotection to synthesize 1,2-diol 113

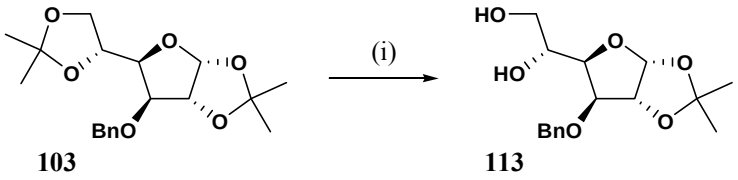

103 **113**

Scheme 23. *(i)* 50% acetic acid/H_2O, r.t., 48 h, 76% or conc. HCl, MeOH, r.t., 96 h, 78%.

Selective deprotection transpires quite readily on acetonide groups that are not fused to the 5-membered ring. This occurs not only because of the increased steric hindrance of the ring system but also because of the ether oxygen adjacent to the C-5' methylene group, which will react readily under the mildly acidic conditions, leaving the remaining isopropylidene unaffected. The selective deprotection of the acetonide was initiated using a 50% aqueous mixture of acetic acid and the reaction was allowed to take place over several days *(Scheme 23)*.[60] A TLC analysis showed that the reaction had failed to go to completion; however, despite this the yields were reasonably high at 76%. Another method[59,61] was later utilized which used a solution of water, methanol and concentrated hydrochloric acid to promote the deprotection *(Scheme 23)*. The TLC analysis of this method also showed that the reaction did not fully go to completion. Nonetheless, product **113**, a highly viscous yellow oil was obtained in 78% yield.

The upfield region of the ^1H NMR spectrum clearly showed the loss of two CH_3 singlets. Interestingly, the OH protons all coupled to the adjacent protons on the carbon, thus making the central region of the spectrum highly complex. For instance, the OH signal adjacent to the H-5' CH_2 gave a triplet signal, whereas the OH adjacent to H-4' gave a doublet. Similarly, the H-5' and H-4' signals became more complicated due to their added coupling to OH over and above their other couplings. Thus in the NMR spectrum these signals appeared as broad multiplets, however, in actuality the nonequivalent H-5' protons should appear as a doublets of doublets of doublets and the H-4' proton should be

a doublet of doublet of doublet of doublets (dddd). The spectrum did however clearly show the benzyl CH_2's H-1a" and H-1b", the nonequivalent protons were observed at 4.71 and 4.56 ppm on the spectrum and each signal split into a doublet, which gave geminal coupling of 11.8 Hz. As seen previously with IR spectroscopic analysis, the OH signal reappeared in the region of 3423 cm^{-1} as expected.

2.1.4. Synthesis of aldehyde 104[59,61]

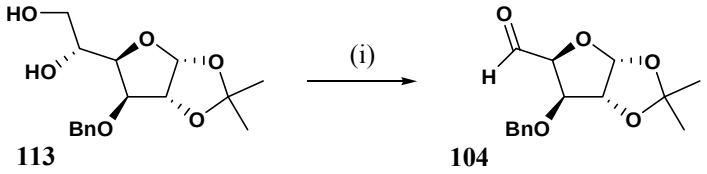

113 **104**

Scheme 24 *(i)* $NaIO_4$, MeOH, H_2O, 0 °C–r.t., 96% crude yield.

Under the influence of an aqueous solution of sodium periodate ($NaIO_4$), at low temperatures, the exposed diol **113** was readily cleaved into the aldehyde **104** as depicted in *Scheme 24*. The reaction formed a white emulsion which after an aqueous work-up afforded the desired product **104** as a clear colourless oil.

The TLC of this reaction mixture showed a distinct difference in R_f (0.41 to 0.75) indicating the formation of a less polar entity, with no indication that any starting material remained. *Figure 11* illustrates the possible mechanism for the formation of the aldehyde with the oxidant $NaIO_4$. The aldehyde **104** was assumed to be unstable and therefore as a precaution was not purified further but carried directly through to the next reaction step *(Section 2.2 & 2.3)*.

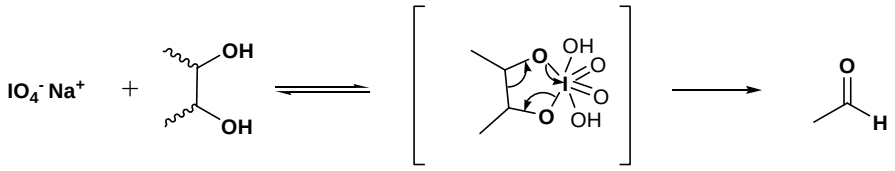

Figure 11. Proposed mechanism for the cleavage of diols by sodium periodate.[57]

The ^{1}H NMR and IR spectra for the crude aldehyde **104** both indicated the presence of the aldehyde through a distinct aldehyde peak. An aldehyde proton singlet was observed at 9.67 ppm in the ^{1}H NMR spectrum and significant peaks at 2936 cm^{-1} (C-H stretch) and 1738 cm^{-1}(C=O stretch), as well as the loss of the broad OH peak, undoubtedly signified the presence of the aldehyde in the IR spectrum.

2.2. Horner-Wadsworth-Emmons reaction to synthesize compound 106

Having prepared the aldehyde **104**, a carbonyl extention reaction was required, namely the Horner-Wadsworth-Emmons reaction. It was anticipated that the reaction would produce the required *E*-alkenoate ester. Stereoselectivity in Wittig reactions depends on the nature of the substituent on the carbon of the ylid. Stabilized ylids contain anion-stabilizing substituents or are in conjugation with adjacent substituents and therefore are able to balance the charge from the phosphorus cation. *E*-selectivity is therefore more likely to occur in the Horner-Wadsworth-Emmons reaction because of the reaction with phosphonate esters and their ability to form good stabilized ylids. The preference toward *E*-selectivity of the stabilized ylids is thought to be due to thermodynamic control taking preference over kinetic control, and therefore the intermediate oxaphosphetane formation being more stable in the *anti* arrangement, resulting in the major product being the *E*-alkene.[46]

The phosphonate ester, trimethyl phosphonoacetate, was thus treated with NaH (60% in paraffin oil) in THF at –60 °C. The reaction mixture was then left to warm to room temperature so that deprotonation could occur. The reaction vessel was again cooled to –60 °C and the aldehyde **104** was added to the reaction mixture *(Scheme 25)*. The reaction was then left to stir for 20 hours. The total consumption of starting material was observed by TLC. However, purification needed to be performed by flash column chromatography for ideal separation and good purity. Nevertheless, the procedure proved to be quite successful and afforded the desired *E*-alkene **106**, in a yield of 78% based on diol **113**.

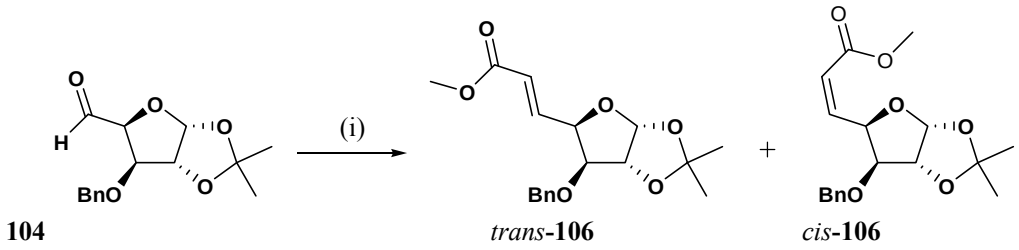

104 *trans*-**106** *cis*-**106**

Scheme 25. *(i)* Trimethyl phosphonoacetate, NaH (60%), THF, 78% – *trans*-**106**, 2% – *cis*-**106**.

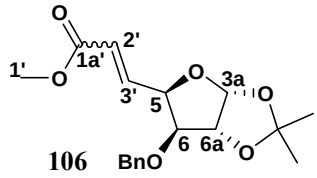

106

In the ^{1}H NMR spectrum, the loss of the aldehyde peak at 9.67 ppm suggested that the reaction had been successful. The appearance of a new singlet at 3.66 ppm indicated that the methyl protons H-1' were present and that the methyl propenoate had indeed formed. Protons H-2' and H-3' were significantly deshielded due to the presence of the alkene system conjugated to the carbonyl ester. The two doublet of doublet signals of H-2' and H-3' gave the vicinal coupling constants of 15.8 Hz, maintaining that the *E*-isomer (***trans*-106)** was in fact the major isomer isolated. On occasion, very small quantities of the *Z*-isomer **(*cis*-106)** could be isolated (1:25 ratio compared to *E*-alkene). The ^{3}J coupling for the minor Z-isomer was found to be 11.7 Hz.

Several other interactions of interest giving some insight into the arrangement of the compound were ascertained from the NOESY spectrum. For instance, the interaction of H-3a and H-6a with only one methyl group from the adjacent acetonide protecting group gave a clear indication as to how the methyl groups are arranged. The remaining methyl group on the acetonide was seen to interact only with the H-5 proton, thus indicating that the proton was on the opposite face to H-3a and H-6a, as expected.

2.3. Henry reaction to synthesize the nitroalkene 105

The formation of a second alkene compound **105**, containing a nitro functionality instead of the ester observed above (*Section 2.2*), was attempted through the application of the Henry reaction. The already prepared aldehyde **104** was utilized for the preparation of the nitroalkene **105**. The Henry reaction or nitroaldol reaction occurs between an aldehyde **104** and nitromethane. Nitromethane has a pKa of 10.2 and therefore deprotonation at the position adjacent to the nitro group may be achieved with a number of mild bases. The nucleophilic addition will therefore occur readily with the aldehyde, followed by an elimination to attain the nitroalkene **105** (*Scheme 26*).[46,62,63]

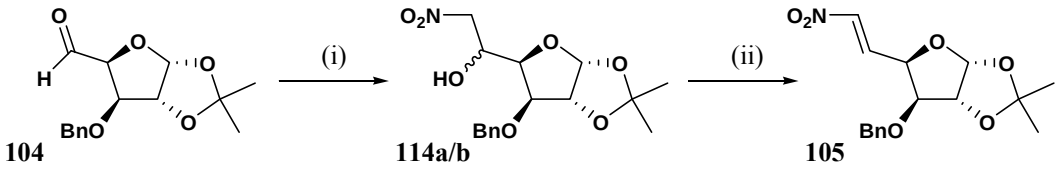

Scheme 26. *(i)* CH_3NO_2, Et_3N, Et_2O, 95% mixture of diasterioisomers (7:1 ratio);
(ii) $MeSO_2Cl$, Et_3N, Et_2O, 84%.

2.3.1. Preparation of epimeric nitroalcohols 114a and 114b[62,64-66]

The nitroalcohols were prepared by a reaction of the previously prepared aldehyde **104** with nitromethane *(Scheme 26)*. The base used to deprotonate the nitromethane and induce the aldol-type reaction was triethylamine (Et_3N). The reaction mixture was purified by column chromatography by increasing the polarity from 5 to 20% AcOEt/hexane. The major isomer **114a**, which existed in the α-D-*gluco*-configuration and the minor isomer **114b**, in the β-L-*ido*-configuration were isolated in a 7:1 ratio. The establishment of the relative configuration will be explained below.

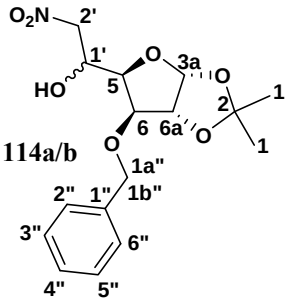

The ^{1}H NMR spectral analysis was very similar for both isomers. There was no evidence for the presence of the aldehyde **104** and hydroxyl peaks could be clearly distinguished. Only very subtle shifts in the spectrum were indicative of the difference in the spectra of the isomers. The β-L-*ido*-nitroalcohol was observed to have a slight downfield shift in the distinctive 3a-H doublet at 6.00 ppm, the shift of the OH peak was also slightly affected to 3.34 ppm. The major α-D-*gluco*-epimer contained an additional spectral feature, in that the signal for the OH was not a broad singlet as seen with its isomeric counterpart; instead, it was found to couple to generate a doublet. It was suspected that the OH may have coupled with the H-1' proton adjacent to the hydroxyl group, however as a result of overlapping peaks and the H-1' signal appearing as a broad multiplet, closer inspection of the COSY spectrum indicated that no coupling occurred. Intramolecular hydrogen bonding between either the benzyl ether oxygen or the nitro oxygens and the hydrogen of the hydroxyl on C-1'was possible when considering the distortion of the compound based on ring strain. Nonetheless, the most plausible reasoning was that intermolecular hydrogen bonding could have occurred with water that was present in the sample. In addition, a NOESY spectrum of the product suggested interactions with water. It was therefore necessary to add D_2O to a sample of the major α-D-*gluco*-epimer **114a** to analyze the change in coupling relative to the hydroxyl to the doublet at 2.64 ppm. The loss of the hydroxyl doublets showed no effect on the remaining spectrum and thus led to the conclusion that the compound was indeed interacting with water. The configuration of the isomers **114a/b** was assigned based on a comparisons made from characterizations previously encountered.[62,64-66]

The IR spectra of the isomers **114a/b** gave a clear indication that the reaction had proceeded, due to the disappearance of the peaks coinciding with an aldehyde in the region of 1720 cm^{-1} and the appearance of the distinctive alcohol peaks (OH stretch) at 3448 cm^{-1}. The presence of the NO_2 was also observed by a significant peak at 1550 cm^{-1}. The specific rotation for the major isomer **114a** was $[\alpha]_D = -37$, which was in satisfactory

agreement to the literature value of –40[67]. The optical rotation of the minor isomer **114b** confirmed that the isomer was actually an epimeric mixture since the $[\alpha]^{25}{}_{D}{}^{64} = -107$ in the literature coincided with the obtained value of –110.5. This was also corroborated by the fact that the isomer did not form a white solid as expected. It could not be purified further; however, the results were substantial on the basis of comparison.

2.3.2. Dehydration to synthesize nitroalkene 105

The dehydration in *Scheme 26* was performed with both the pure α-D-*gluco*-epimer and with the mixture of both epimers. Methanesulfonyl chloride ($MeSO_2Cl$) was slowly added to the reaction mixture containing the pure nitroalcohol **114a** in diethyl ether (Et_2O) and triethylamine (Et_3N); on addition of the $MeSO_2Cl$ a haze of gas was emitted and a yellow glutinous substance precipitated in the flask. The mixture was then left to stir overnight, after which it was neutralized with acid, extracted and purified (column chromatography) to afford nitroalkene **105** as a yellow oil. When comparing the outcome of the product to when the mixture of epimers was used and when the starting compound contained only the major isomer, the dehydration occurred without any major differences in the outcomes, as expected.[64,65,68]

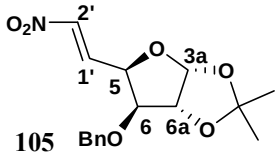

105

In the ^{1}H NMR spectrum of compound **105**, intricate coupling occurred due to the formation of the alkene, which made for an almost completely transformed spectrum (in regard to the central region of the spectrum when compared to its nitroalcohol adducts **114**). Proton H-3a was unchanged and only coupled to H-6a to give a doublet. Proton H-6a was embedded within the CH_2 signal of the benzyl region at 4.67 ppm. The ^{13}C NMR spectroscopy signals for C-6a and C-6 were closely related to one another giving values of 82.4 and 82.3 ppm, respectively. In addition, the nonequivalent protons in the benzyl CH_2 gave two expected doublets at 4.66 and 4.56 ppm with a coupling constant of approximately 12.0 Hz. Finally, the presence of the alkene led to the H-5 proton becoming considerably more complex due to coupling with both of the alkene hydrogens as well as H-6, thus

becoming a doublet of doublet of doublets, although it appeared as a doublet of triplets on the spectrum due to similarities in two of the three coupling constants.

The nitro group is electron-deficient; therefore the electron density in the alkene is expected to be distorted toward the nitro site. The β-proton would thus be expected to be deshielded as confirmed by the chemical shift at about 7.31 ppm which is rather downfield due to these interactions.[46] It was therefore expected for our alkene protons to be as far downfield as our aromatic protons at 7.39–7.20 ppm. It was also thought that both alkene signals would produce a doublet of doublets due to their interaction with each other and H-6, nonetheless, only one doublet of doublet signal could be clearly observed and analysed within the aromatic region at 7.16 ppm, with coupling constants of 13.3 and 3.5 Hz.

In the next chapter, the prepared unsaturated alkenes **105** and **106** will be used in an array of conjugate addition reactions, in an attempt to insert the aromatic **A** ring into the pancratistatin precursor. The conjugate addition procedures and the aromatic derivatives used will be described accordingly.

CHAPTER 3: RESULTS AND DISCUSSION

CONJUGATE ADDITION

In this chapter, the stereoselective addition of aromatic derivatives by conjugate addition to the systems described in the previous chapter will be discussed. The chapter will begin by describing in *Section 3.1* and *3.2* the most appropriate method for achieving this stereoselectivity, so as to attain the necessary pancratistatin precursor. The result obtained in this project will then be described.

3.1. The use of cuprates in conjugate addition: The work of Paulsen and Stubbe[37,38]

Initially, the organocuprate method for conjugate addition was adapted to insert the aromatic ring substituent into our developing synthetic system (described previously in *Chapter 2*) with the expectation of achieving the stereoselectivity necessary to eventually introduce the troublesome *trans* fused ring system, one of the major synthetic challenges in making pancratistatin **4** (*Scheme 27*). A modified Felkin-Anh model was proposed suggesting that the nucleophilic organocuprate would react on the opposite face to the alkoxy group as seen in *Scheme 27*.[69]

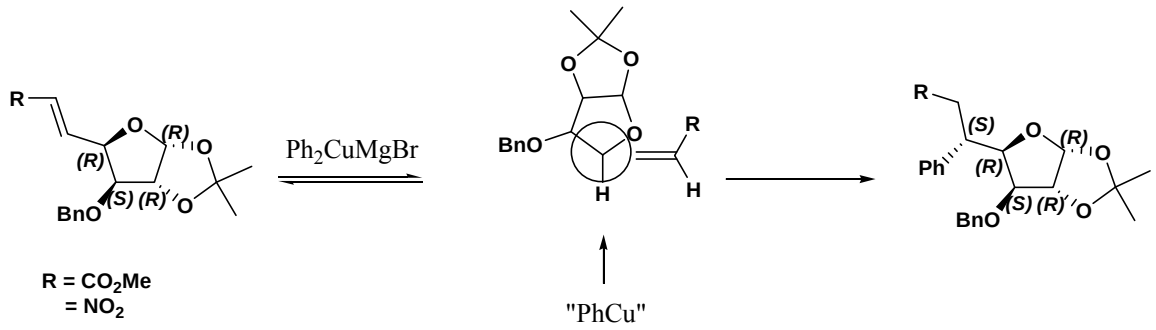

Scheme 27: Proposed *anti* configuration based on the modified Felkin-Anh model.

In a previous attempt to perform the conjugate addition, Paulsen and Stubbe[37,38] employed lithiated cuprates in an effort to achieve the synthesis of sufficient L-*allo*-product **63** (*Scheme 28*), unfortunately, with only modest success. After a comprehensive literature survey[30,67,69-71] was carried out, an adaption to the methodology was initiated with stereoselectivity in mind. This will be presented in detail in *Section 3.3.1*.

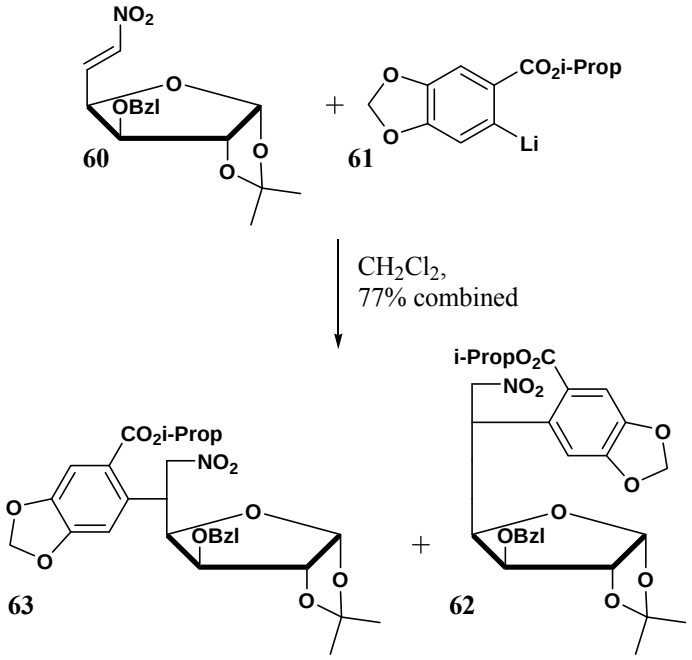

Scheme 28. Previous conjugate addition by Paulsen and Stubbe.[37,38]

3.2. Conjugate addition with arylboronic acids under rhodium(I) catalysis

A brief survey of the literature, led to a paper by Segura and Csaky,[56] in which the Hayashi-Miyaura reaction[72] was applied to conjugate esters. They showed that a stereoselective synthesis could be achieved through the application of rhodium complexes, and they proposed a mechanism for the transformation.

The Hayashi-Miyaura reaction involves the reaction of unsaturated esters with organoboronic acids using cyclooctadiene rhodium chloride dimer {$[(cod)RhCl]_2$} as the catalyst, in a dioxane-water (10:1) solution in the presence of a base. It has recently been proposed that the catalytic cycle of the rhodium conjugate addition mechanism, illustrated in *Scheme 29,* contributes greatly to the understanding of the diastereoselectivity of the newly formed carbon-carbon adducts.[73] The cycle proceeds with three intermediates, the first being the arylrhodium **A** which binds to the alkene making it more electrophilic. Alkene coordination is followed by diastereoselective insertion of the alkene into the rhodium-carbon bond followed by isomerisation to form the thermodynamically stable oxa-π-allylrhodium **B**. This complex then forms the hydroxorhodium complex **C** on addition of water, thus liberating the final arylated product.

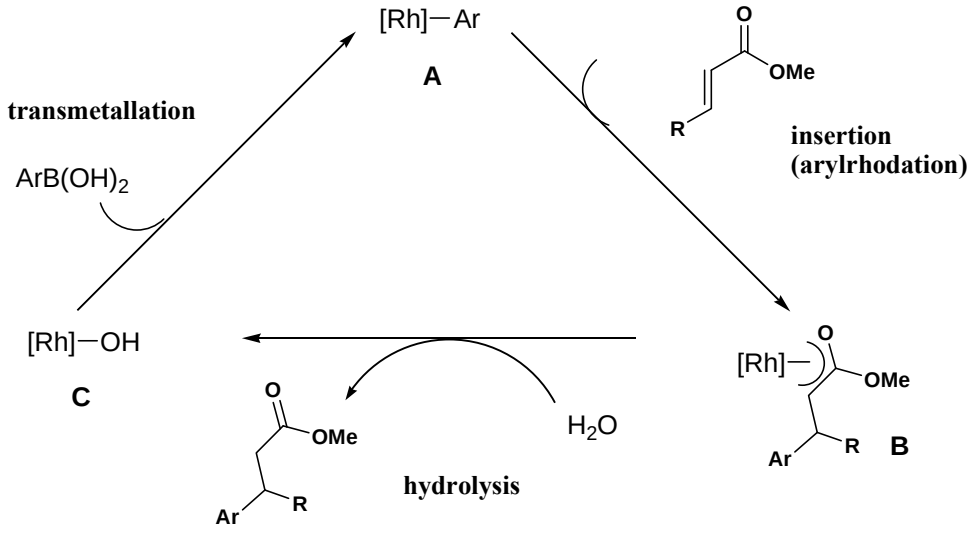

Scheme 29. Proposed catalytic cycle for rhodium(I) catalysts

The mildness of the reaction conditions circumvents aldol condensations of the substrates and products which could be problematic in a basic environment. However, under these conditions, hydrolytic deboronation of the arylboronic acid can be a competing side reaction, which can be overcome by adding an excess of boronic acid. Moreover, in nearly all of the rhodium-catalyzed conjugate addition reactions a side reaction occurs due to catalytic demetalation of the organometallic component. This occurs because the aryl-rhodium bond is more sensitive to protonolysis than the original organometallic compound from which it was derived.

The stereochemical outcomes of the conjugate addition reactions have been rationalized by Segura and Csaky through transition state models that minimize steric interactions. A nonchelation-controlled model was thus used to better understand the means by which the compound would undergo conjugate addition in a stereoselective manner.[56] It has been suggested that the formation of the oxo-π-allyl-Rh[1] intermediate **B** *(Scheme 29)* could possibly be the rate-limiting step in the catalytic cycle and thus the assumption could be made that diastereoselection could take place at this point.

In *Figure 12*, two possible models are proposed, which describe the stereochemical outcome of the conjugate addition reactions. Model **I** *(Figure 12)* predominates as it leads to the desired *anti* adducts. The *syn* adducts of model **II** are destabilized by steric congestion between the phenyl and benzyloxy substituents; as indicated.

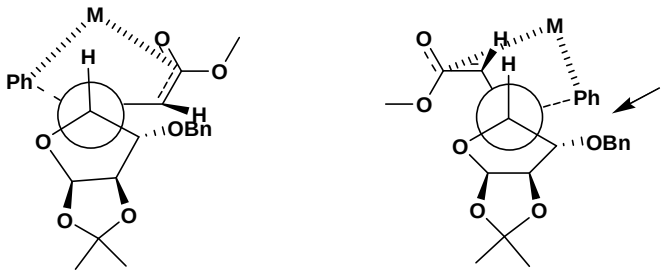

Model I **Model II**

Figure 12. Proposed stereochemical outcome for aromatic additions.

The numerous attempts at conjugate addition using a variety of aromatic adducts will be describe below in *Section 3.3*, in relation to the previously prepared α,β-unsaturated ester **106** and in *Section 3.4*, in relation to the nitroalkene **105**.

3.3. Conjugate addition of aryl groups to α,β-unsaturated esters

3.3.1. Conjugate addition of phenyl group to ester 106

As part of the initial model investigation of the synthesis of pancratistatin, it was advantageous to attempt the conjugate addition using a simple, more cost-efficient aryl system for insertion into the enoate adduct **106**, for both synthetic and economical purposes.

The cuprate reagent for our proposed synthesis was prepared from a transmetallation reaction with the corresponding aryl Grignard. Therefore, it was necessary to first synthesize the Grignard reagent under dry conditions due to its hygroscopic nature. The Grignard reagent was thus prepared using magnesium turnings which underwent an exothermic reaction with bromobenzene in THF. The Grignard reagent was then transferred by cannula into a cooled suspension of cuprous iodide (CuI) in THF. During the reaction the suspension changed in appearance from an opaque white to a dark yellow colour. The alkene **106** was then dissolved in THF along with the trimethylsilyl chloride (TMSCl) which was also cannulated into the organocuprate reagent.

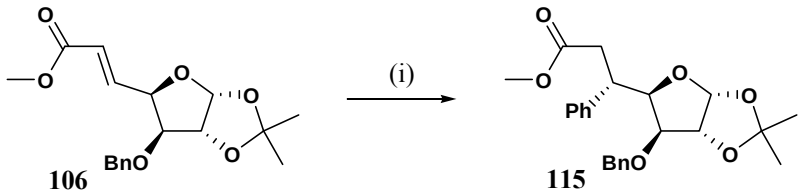

106 **115**

Scheme 30. *(i)* PhBr, Mg, CuI, Me_3SiCl, THF, –78 °C–r.t., 55% or
$PhB(OH)_2$, $[(cod)RhCl]_2$, Et_3N, dioxane/water (10:1), r.t., 94%.

Purification of the product was fortunately possible, despite the TLC (10 and 20% ethyl acetate in hexane) depicting a range of spots. With the use of column chromatography (10% ethyl acetate in hexane) the highest yield achieved for the conjugate addition to afford compound **115** was 55% *(Scheme 30)*. However on average yields of only 40% were isolated for both the nitro and ester adducts when bromobenzene was added. This yield was improved slightly with the nitro adduct as it was found that the use of TMSCl was not important and could be omitted *(see Section 3.4)*.

In an attempt to investigate the problems relating to the moderately low yields the Grignard reagent was added in an excess of 20 equivalents, relative to the starting material **106**, in an attempt to increase the yield of the final product **115**, as it was suspected that the preparation and transfer of the Grignard reagent at an earlier stage of the reaction was causing the low yields. It was established that the complication in the preparation of the Grignard reagent was due to the reaction not going to completion, even if the reaction mixture was heated. This was thought to arise from the grade and surface exposure of the magnesium turnings and the possible rapid degradation of the Grignard reagent itself.

The rhodium method for conjugate addition of phenylboronic acid to enoate **106** was far more efficient; the reaction was persistently higher yielding and afforded almost exclusively the (3'*S*)-diastereomer. Initially, a mixture of diastereomers was achieved once purification by standard silica gel column chromatography was performed; however, later it was discovered that the diastereomers (**115-3'*S*** and **115-3'*R***) could be separated using flash chromatography. Consistently, the ratio of diastereomers was found to be approximately 12:1.

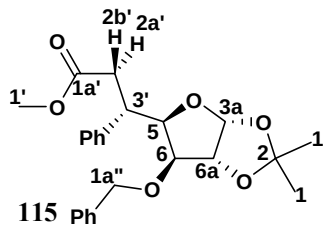

The ^{1}H NMR spectrum of the isolated major diastereomer **115**, was especially encouraging with numerous interesting novel couplings as well as some anticipated peaks. As expected, the alkene peaks previously reported with chemical shifts in the region of 6.40-5.65 ppm, had disappeared. From

the C-H correlated spectrum (HSQC) both CH_2 groups could be assigned. It was previously observed that the benzylic protons showed nonequivalence, and this was also expected with the protons at C-2' because of the formation of the new chiral centre adjacent to it. The two C-2' protons gave rise to the peaks most upfield at 3.89 and 3.68 ppm, both giving doublets of doublets, with the geminal coupling of 15.6 Hz. Furthermore, the positions of the individual hydrogens in the structure could be estimated from the coupling interactions between the hydrogens. A ^3J value of 10.5 Hz was observed for H-2'–H-3'which suggested a dihedral angle of approximately 180°, based on the Karplus equation.[74] This projection led to the deduction that the added phenyl adduct had stereochemistry that was overall *anti* (C-3' and C-5) because of the position of H-5 in relation to H-3'. The stereochemistry at C-5 was already known and therefore the stereochemistry of H-3' could be confirmed. It could also be assumed by analogy, based on the X-ray crystal structure of **117** (*Section 3.4*) that the similarities in the aromatic groups would lead to similar overall (3'*S*)-stereochemical arrangement for compound **115**.

The H-3a signal was generally used as a "reference point" for the analysis of most of the compounds prepared, because of the signal's distinguishable position in the spectrum. For instance, in the ^{1}H NMR spectrum of the minor diastereomer a slight upfield shift in the peaks of the doublet in the region of 5.95-6.00 ppm could be seen, corresponding to the H-3a proton. Accordingly, when analyzing the spectrum of the diastereomer for the conjugate addition product various other shifts were also discerned, especially where signals of H-2' and H-3' were concerned.

At this point a debenzylation was attempted under hydrogenation conditions using 10% palladium on carbon in methanol at a pressure of 7 bar, the reaction was left at room temperature for 72 hours. It was expected that lactone formation would occur with the exposed hydroxyl and the ester *(Figure 13)*. It was assumed a lactone would more readily form a solid and thus potentially crystals. From the crystal a more accurate depiction of the stereochemistry could be obtained by the use of X-ray diffraction analysis. The rigidity of the lactone would hopefully also improve NMR analysis and

allow stereochemical assignments by the use of coupling constants. However the debenzylation did not occur, most probably as a result of the conditions being too mild and therefore the reaction was abandoned.

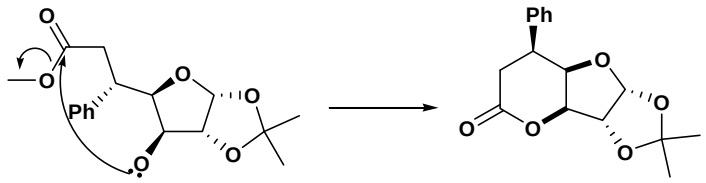

Figure 13. Attempted debenzylation and lactonization of ester **115**.

3.3.2. Synthesis of conjugate addition compound 116

Conjugate addition using cuprate methodology was not attempted using the dioxolylphenyl substrates because the rhodium-catalyzed approach was found to have improved results. The addition of commercially available 3,4-dioxolylphenylboronic acid to the enoate adduct **106** *(Scheme 31)* proceeded by a procedure equivalent to that described previously *(Section 3.2)*. However, the reaction required longer reaction times and only produced the major product in a yield of 26%, with the diastereomers produced in a 7:1 ratio. The reaction conditions were not optimized due to the abandonment of the ester approach of the project (See *Chapter 4* for discussion).

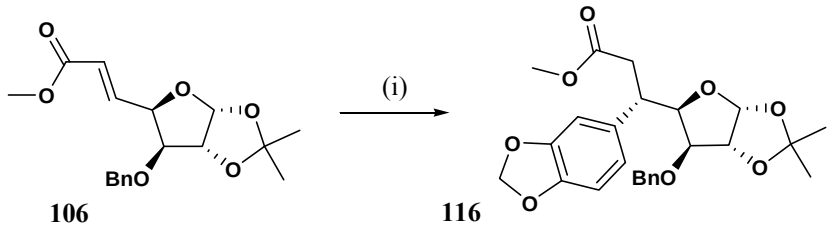

106 **116**

Scheme 31. *(i)* 3,4-$(OCH_2O)C_6H_3B(OH)_2$, $[(cod)RhCl]_2$, Et_3N, dioxane/water (10:1), r.t., 26%

When comparing the ^{1}H NMR spectrum of the newly formed aryl addition product **116** to the phenyl compound **115**, a prominent difference was the aromatic region which showed three distinct multiplets at 7.38-7.24 ppm (five benzyl protons), 6.74-6.67 ppm (three dioxolyl protons), and 5.98-5.87 ppm (dioxolyl CH_2 and H-3a signal). The central region of the spectrum was in agreement with that observed for the spectra of adduct **115**. Analysis of **116** by high resolution mass spectrometry afforded a mass of 456.1762 amu, in good agreement with the expected value of 456.1784 amu. The stereochemistry for the addition was assumed based on the same arguments postulated in the previous system described in *Section 3.3.1.*.

3.4. Conjugate addition to nitroalkenes

Investigation of conjugate addition using both the organocuprate and the rhodium-catalyzed method on the nitro olefin was an important component of this research in order to replicate the Paulsen and Stubbe-type[37,38] chemistry established in 1982. However, it was anticipated that the novelty in the conjugate addition methodology would lead to an improved stereochemical ratio as compared to that achieved by Paulsen and Stubbe reported previously.

It was decided that a variety of aromatic adducts would be investigated *(Table 3.1)*, in order to better understand the underlying principles of conjugate addition with our system and for the investigation of the synthesis of potential pancratistatin analogue precursors. The aromatic substituents were chosen because of their oxygen donating groups, which could possibly mimic the biological and medicinal potential of analogues of pancratistatin **4**. All of the arylboronic acids used were commercially available and used as supplied.

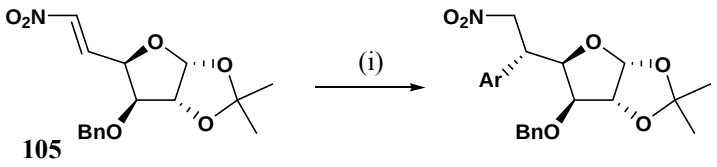

Scheme 32. *(i)* PhBr, Mg, CuI, Me_3SiCl, THF, –78°C–r.t., 55% or $ArB(OH)_2$, $[(cod)RhCl]_2$, Et_3N, dioxane/water (10:1), r.t., 30–84%.

Table 3.1. Aromatic groups and yields for conjugate addition reaction.

Compound	Ar	Scale (mmol)	$[\alpha]^{22}_D$	Yield (%)
117	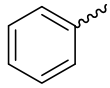	6.10	-28.6	(55)* 68 de = (6:1)*14:1
118	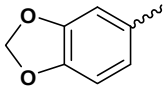	6.75	-37.0	84
119	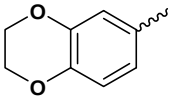	1.15	-36.5	48
120	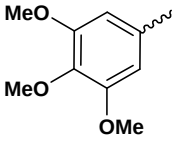	1.12	-36.2	38

*Yield and diastereomeric excess (de) corresponds to the cuprate conjugate addition experiment.

Diastereomeric excess for **118**, **119** and **120** were not attainable.

Initially (3a*R*,5*R*,6*R*,6a*R*)-2,2-dimethyl-5-[(1*R*)-2-nitro-1-phenylethyl]-6-[(phenylmethyl) oxy]tetrahydrofuro[2,3-*d*][1,3]dioxole **117** was synthesized by utilization of the cuprate methodology. This was prepared using bromobenzene as discussed in *Section 3.1* with the highest yield obtained being 36% *(Scheme 32)*. In previous investigations, the use of trimethylsilyl chloride (TMSCl) had resulted in an increase in the yields of the product obtained. This has been explained by the silicon-containing reagent undergoing additional interactions with the enolates at the carbonyl oxygen because of the silicon's affinity for oxygen. This increases the nucleophilicity of the oxygen site and thus improves the electrophilic site for conjugate addition.[50] The same interaction does not obtain with nitro compounds and therefore when TMSCl was omitted the yield obtained increased slightly to 55%. Nonetheless, the organocuprate approach was thus abandoned due to low yields and the promising potential of the rhodium-catalysis method was pursued instead.

When the rhodium-catalysis method for conjugate addition was employed the yield of compound **117** was increased to 68% and a ratio of 1:10 was attained for the minor diastereomer (*syn*-addition of phenyl) to that of the major diastereomer (*anti*-addition of the phenyl). Flash column chromatography was necessary to ensure that the diastereomers were separated. Furthermore, the desired product became crystalline and a recrystalization was performed with diethyl ether for additional purification to afford clear rhombus-like crystals.

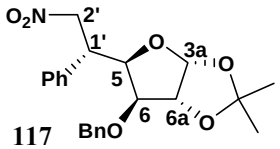

117

In the ^{1}H NMR spectrum of compound **117**, the aromatic region was immediately observed to integrate for ten protons, suggesting that the addition of the phenyl substituent had been successful. The doublet peak at 5.92 ppm corresponding to the proton signal of H-3a was observed to be an excellent indicator for the presence of the diastereomer in mixed samples. The presence of the diastereomer would show a second doublet appearing slightly upfield in the NMR spectrum. The central region of the spectrum was unambiguously distinguishable, indicating clear coupling pertaining to the two H-2' protons at 5.00 and 4.72 ppm, both giving doublets of doublets with ^{2}J of 12.8 Hz. These in turn both

coupled to H-1' which instead of the expected doublet of doublet of doublets, gave a doublet of triplets as a result of similar coupling constants between one of the H-2' protons and the H-5–H-1' coupling constants. The two benzyl CH_2 doublets were readily discernible and displayed geminal coupling to one another of 11.7 Hz. When comparing the ^{13}C NMR spectrum of compound **117** to that of the nitroalkene **105** *(Chapter 2, section 2.3.2)* the signal at 43.1 ppm (for C-1') is a distinct confirmation of the presence of the phenyl adduct, in addition to the number of additional quaternary carbon and aromatic CH carbon signals.

A crystal structure was obtained, by X-ray diffraction (XRD) analysis, confirming that the *(R)*-product **117** had indeed been synthesized *(Figure 14)*. The crystallographic analysis of this structure afforded a satisfactory "goodness of fit" of 1.062 and an R factor of 3.3% for the orthorhombic crystal system in the $P2_12_12_1$ space group. Interesting features, such as the alignment of the bulky aromatic benzyl and phenyl groups to one another and other substituents in the structure could be observed. Furthermore, the ring strain on the 5-membered furanose and its fused acetonide was noted. The consequence on the geometry of substituents as a result of the ring strain was apparent and can be seen in *Figure 14*.

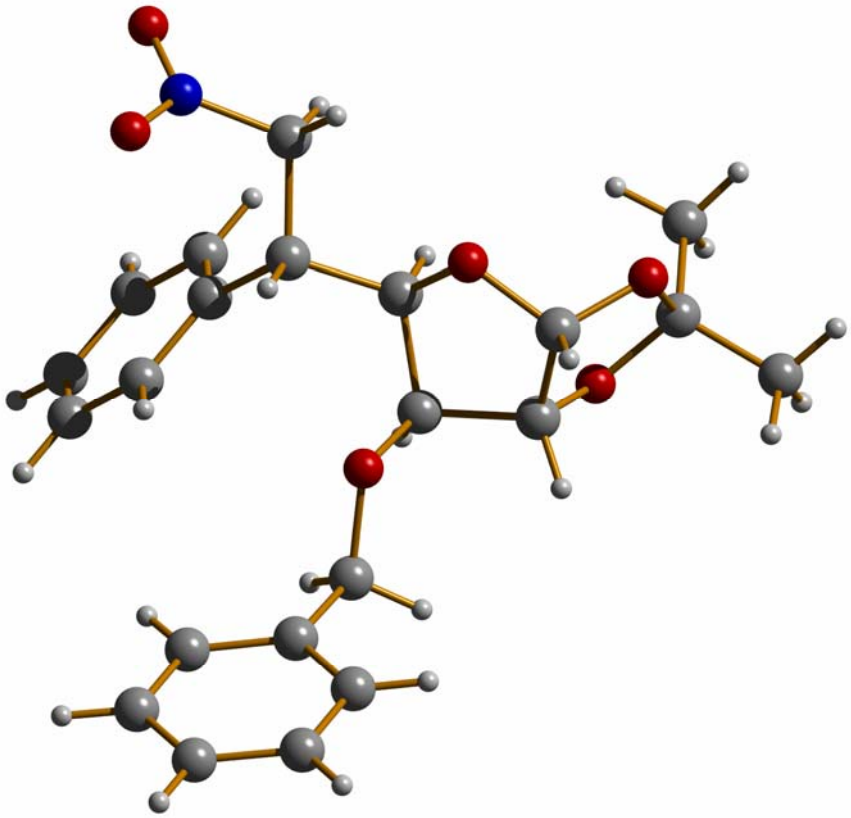

Figure 14. Molecular structure of **117** according to a single crystal X-ray analysis.

Having attained positive results for the phenyl aryl substituent **117**, it was now necessary to attempt the conjugate addition using an aryl derivative that could better lead to the synthesis of pancratistatin **4**. Thus 3,4-dioxolylphenylboronic acid was used to synthesize compound **118**, a glassy yellow pseudo-solid that when under the slightest influence of heat (≥ 35 °C) would melt into an oil (*Scheme 32)*. The TLC analysis of the reaction suggested that more than one product was being formed; however, a closer inspection of the spectra, obtained for the other isolated spots, suggested that the material was not a diastereomer, but rather some by-products.

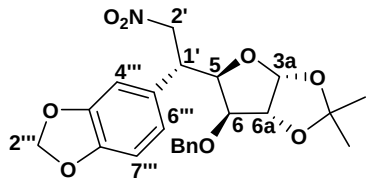

118

The ^{1}H NMR spectrum obtained for compound **118**, clearly indicated three downfield signals indicative of the dioxolylphenyl group. The multiplet furthest downfield at 7.38–7.23 ppm integrated for five aromatic hydrogens correlating to the benzyl ether protons as expected. The second multiplet at 6.73–6.63 ppm integrated for three protons and correlated to the dioxolylphenyl aromatic protons H-4’’’, H-6’’’ and H-7’’’. Finally, the signals at 5.92 and 5.94 ppm were slightly overlapping and consisted of the H-2’’’ signal, which appeared to be two doublets, and then the expected H-3a signal with ^{3}J coupling of 3.8 Hz, which coincided with the expected doublet at 4.55 ppm for H-6a. Similar couplings and chemical shifts to compound **117** were observed for the bulk of the spectrum. The NOESY spectrum revealed an interaction between the H-5 proton and the aromatic hydrogens on the dioxolylphenyl substituent **118**, which suggested that the aromatic group was indeed in the *anti*-conformation as anticipated in view of the fact that the stereochemistry of the H-5 proton had already been established previously. Several ^{13}C NMR spectrum signals attested to the presence of the addition product. The aromatic CH carbon signals for the dioxolylphenyl ring were found at 121.6, 108.2, 108.1 and 106.6 ppm. The IR spectrum also showed the presence of new peaks at 1445 (CH bend) and 1375 cm^{-1} (CO stretch), which indicated the presence of the oxygen substituents on the aromatic phenyl group. The mass spectrum showed a molecular ion at m/z 443.1559 amu consistent with the formula $C_{23}H_{28}O_8N$ (calculated 443.1580 amu) further confirming the formation of the dioxolylphenyl conjugated **118**.

The commercially available benzodioxineboronic acid was chosen for the synthesis of compound **119** because of its chemical similarity to the dioxolylphenyl aromatic substituent **118.** It was thus anticipated that it would react in a similar manner. Although the reaction did occur the yield was unfortunately low when compared to compound **118** (48% versus 84%).

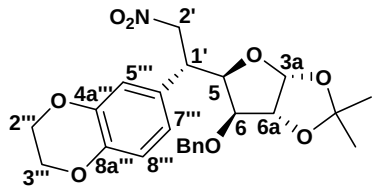

119

In the ^{1}H NMR spectrum for 6-((1*R*)-1-{(3a*R*,5*R*,6*R*,6a*R*)-2,2-dimethyl-6-[(phenylmethyl)oxy]tetrahydrofuro[2,3-*d*][1,3]dioxol-5-yl}-2-nitroethyl)-2,3-dihydro-1,4-benzodioxine **119**, the aromatic region accounted for an additional three protons at 6.78–6.74, corresponding to H-5''' and H-8''', and 6.70–6.64 ppm, corresponding to H-7''' of the compound. When comparing the H-7''' signal to its counterpart in the somewhat similar dioxolylphenyl substituent **118**, there has been a definite downfield shift, thus exposing the H-3a signal at 5.93 ppm. The only other feature which was immediately obvious in the spectrum was the appearance of a singlet which integrated for four protons at 4.19 ppm, corresponding to the equivalent CH_2 groups on the benzodioxine structure. Besides those two adequately corroboratory signals the remainder of the spectrum bore a remarkable resemblance to that seen previously with compound **118**. In the ^{13}C NMR spectrum, the carbon signal corresponding to the CH_2's of the benzodioxine was clearly observed at 64.1 ppm. The quaternary carbons making up the benzodioxine structure were also evident at 143.4 and 143.4 ppm, as seen previously with the adduct **118**. Similarly, the IR spectrum reproduced many of the same peaks observed in **118**, as expected due to their structural resemblance. Nevertheless, evidence of new peaks at 1287 and 1207 cm^{-1} occurred, coinciding with the peaks associated with the aromatic ether. High resolution mass spectrometry of the benzodioxine **119** ($C_{24}H_{27}O_8N$) afforded a mass of 457.1715 amu, in good agreement with the expected value of 457.1737 amu.

Finally, in this section the 3,4,5-trimethoxyphenylboronic acid was used to synthesize compound **120**. The aryl substituent was envisaged as a precursor to a pancratistatin analogue because it contained similar functionality but posed interesting steric and structural diversity. However, the results were also poor (38%).

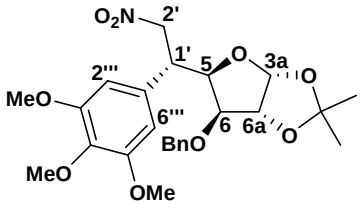

120

(3a*R*,5*R*,6*R*,6a*R*)-2,2–Dimethyl-5-{(1*R*)-2-nitro-1-[3,4,5-tris(methyloxy)phenyl]ethyl}-6-[(phenylmethyl) oxy]tetrahydrofuro[2,3-*d*][1,3]dioxole **120**, was characterized in the associated ^{1}H NMR spectrum by the appearance of three signals having been added to the spectrum, similar to that observed previously with the phenyl substituent **117**. The aromatic adduct possessed an axis of symmetry, and thus the aromatic hydrogens H-2''' and H-6''' were seen as equivalent and were therefore identified as a singlet at 6.41 ppm. The OMe aromatic substituents also gave singlets, one integrating for three protons, corresponding to the OMe (on C-4''') and one integrating for six protons, corresponding to the symmetrically equivalent, remaining OMe groups. These signals occurred at 3.82 and 3.69 ppm on the spectrum, respectively. The remainder of the spectrum correlated to what was seen previously with the compound **117** and **118**, with chemical shifts and coupling constants remaining relatively unchanged, despite the electronic influence of the aromatic adduct. The ^{13}C NMR spectrum clearly showed the quaternary carbons for C-3''' and C-5''' at 153.3 ppm, where C-4''' gave a signal at 137.1 ppm. The OMe signals also gave noteworthy signals further upfield in the spectrum at 60.8 and 56.1 ppm, which coincided with the signals at 3.82 and 3.69 ppm of ^{1}H NMR spectrum; this was assigned using the CH correlated spectrum (HSQC). When comparing the IR spectrum for compound **120** to that of the nitroalkene **105**, the spectrum undoubtedly indicated the appearance of two sharp peaks at 1243 and 1072 cm^{-1}. These peaks are in the region of aromatic ethers and are thus rather specific to this group. The results of the high resolution mass spectrometry (HRMS) showed a molecular ion at 489.1985 amu, which was in close agreement with the expected molecular formula ($C_{25}H_{31}O_9N$ requires 489.1999).

Despite several attempts the yields for addition products **119** and **120** could not be improved further. It is unclear why the yields are low; it may be due to the different electronic effects of the substituents or even steric effects. As a result the reactions were carried out for longer periods of time, ranging from three to six days, and in some cases heating of the system was attempted, ranging from room temperature to 80°C. However, the results showed no significant effect on the yields of the final products.

In conclusion, it was observed that the two approaches used for the conjugate addition of the aryl substituents were successful. Owing to poor yields using the organocuprate method, only the phenyl adducts **115** and **117** were prepared using this approach. It was shown that a variety of aromatic derivatives could be used for conjugate addition using the rhodium(I)-catalyzed approach due to the versatility of the methodology. However, the yields achieved for these products ranged from 94 to 38%. The major diastereomer was the sought after *anti* product. In the next chapter, an examination of different methods used for the ring closure of the cyclitol (ring **C**) will be done, while maintaining all the stereochemical structure already put into place.

CHAPTER 4: RESULTS AND DISCUSSION

ATTEMPTED RING CLOSURE

As described in the previous chapter, the aromatic ring **A** was successfully introduced into the system by conjugate addition. Accordingly, it was necessary to introduce the important contiguous stereocentres of the cyclitol ring of the pancratistatin ring **C**. As described previously (*Chapter 1, Section 1.4.3*) Paulsen and Stubbe[37,38] successfully obtained a deprotection of the acetal with the use of Dowex H^+ resin in the presence of methanol, followed by the ring closure with sodium or potassium carbonate. However, in the Paulsen and Stubbe synthesis additional rigidity was observed through lactone formation to give compound **64**, from the ester substituent on the aromatic group *(Scheme 33)*. Nonetheless, when considering our compounds the same chemical strategy was applied.

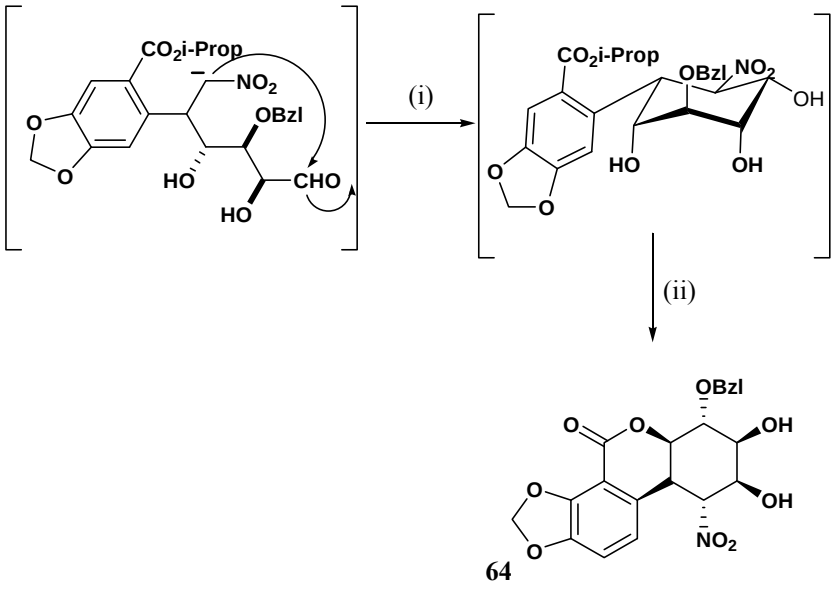

Scheme 33. *(i)* K_2CO_3, MeOH, 34% over two steps.

4.1. Attempted ring closure using ester compound 115

4.1.1. Attempted acetonide deprotection of the ester adduct 115

The deprotection of the acetonide in compound **115** was performed under mildly acidic conditions as seen previously (Section 2.1.3); however, the Dowex H^+ resin was used as a form of mild acid because it could easily be removed by filtration once the reaction was complete, resulting in a more efficient process. It was surmised that the deprotection would expose the hemiacetal, and that equilibrium would be established between the diol **121** and the aldehyde **122** of the deprotected open-chain tautomer (*Scheme 34)*. The deprotection was attempted on the phenyl adduct **115** only, due to the effort necessary for its preparation.

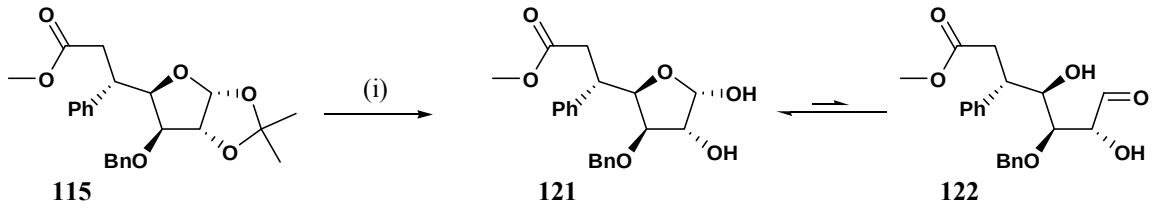

Scheme 34. *(i)* Dowex H^+ resin, MeOH, reflux–r.t.

Initially, when the reaction was attempted, small amounts of starting material **115** remained. It was thus necessary to stir the reaction mixture under reflux until the reaction was complete, or the addition of more resin was required (3 times mass of starting material **115** versus 1.1 times used initially) in order to increase the acidity of the system. The reaction was therefore monitored by TLC to check for a change in polarity. The R_f changed from 0.86 for the starting material **115**, to 0.61 and 0.53 for the two spots of the presumed hemiacetal.

A ^{1}H NMR spectrum of the crude product was obtained in order to assess whether the hemiacetal had indeed formed. Despite the central region of the spectrum showing vast complexity due to a mixture of products (starting material, diol and aldehyde), an

aldehyde singlet at 9.87 ppm appeared, in a very small ratio (~1:5) compared to the hemiacetal **121** (as expected because the equilibrium lies significantly toward the hemiacetal). Another significant feature pertaining to the ^{1}H NMR spectrum related to the H-3a proton signal at 5.95 ppm, which suggests the presence of the anomeric carbon C-3a of the hemiacetal. However, because of the presence of the starting material in the compound causing ambiguity in the remaining peaks, no other defining conclusions could be drawn. Unfortunately, all attempts at further purification of the product resulted in its complete decomposition. It was therefore decided that the ring closure would be attempted on the crude product in an effort to gain the ring-closed product.

4.1.2. Attempted cyclization of ring *C* using compound 122

The ester approach toward the synthesis of pancratistatin produced very promising results up until the point of ring closure. The proton α to the carbonyl (pKa ≈ 24.5) is far less acidic than that α to the nitro group (pKa ≈ 10). A diversity of bases was thus attempted for the ring closure (*Table 4.1*); however, decomposition of the starting material did pose a problem, as observed previously when purification was attempted. A diversity of reagents was also tested in an effort to improve the chances of cyclization *(Scheme 35)*.

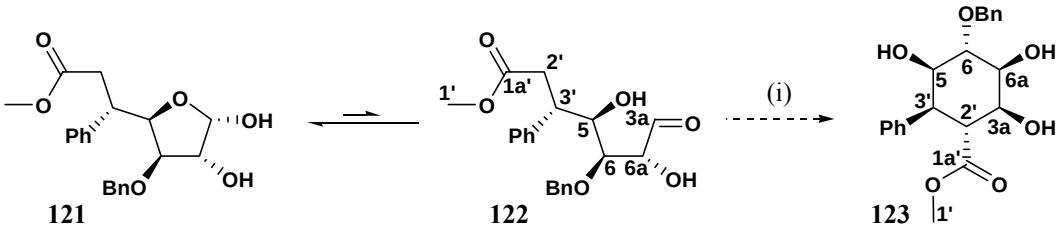

Scheme 35. *(i)* See *Table 4.1.* for reagents and conditions.

Table 4.1. Bases used for the attempted ring closure of ester **122**.

Reaction	Reagents	Conditions	pKa of conjugate acid[46]
1	K_2CO_3	MeOH, r.t., 48 h	10.2
2	Et_3N	CH_2Cl_2, r.t., 72 h	10.7
3	*t*-BuOK	DMF, r.t., 48 h	18.0
4	DBU	CH_3CN, r.t., 60 h	12.5

Unfortunately, none of the attempts at cyclization into compound **123** afforded any substantial results and the spectra of the crude products were complex. None of the final spectra for the above attempts coincided, suggesting that in some cases decomposition was highly likely; nonetheless in all the spectra the aromatic signal persisted as well as some other distinctly coupling peaks. In spite of this, no conclusion could be drawn about what had formed in the product; it was felt that the complexity of the compound could be due to a mixture of diastereomers formed during the ring closure. Therefore, it was decided that an acetyl protection of the putative cyclic product **123** could be undertaken in order to improve the spectral information and draw a clearer conclusion.

4.1.3. Acetyl protection of the presumed cyclized ester product 123

Approximately one equivalent of acetic anhydride and one equivalent of pyridine were added for every presumed hydroxyl group formed and the reaction mixture was left to stir at room temperature while being monitored by TLC *(Scheme 36)*. The TLC analysis proved rather promising as it demonstrated that one of the spots of high polarity (low R_f) had disappeared and a relatively prominent spot with a lower polarity began to feature strongly.

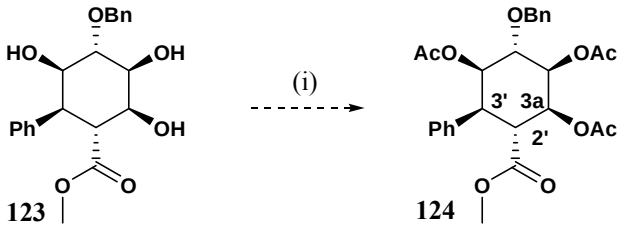

Scheme 36. *(i)* Ac_2O, pyridine, r.t., 48 h.

The crude ^1H NMR spectrum of proposed compound **124** suggested that three acetyl CH_3 singlets were present at 2.07, 2.06 and 2.04 ppm. However, the bulk of the spectrum remained ambiguous and no further conclusions could be drawn. Only slight changes in some of the chemical shifts of the more apparent signals such as H-3a seemed to appear at 6.44 ppm. Also, a new singlet appeared at 6.14 ppm, which could not be accounted for. This suggested that perhaps there could have been additional hydroxyl groups present but not as part of the sought after ring **C**. All efforts at further purification resulted in decomposition or complete loss of the product. The ester route was therefore discontinued and it was decided that all efforts would be concentrated on the nitro cyclization due to the close association with the Paulsen and Stubbe methodology.[37,38]

4.2. Attempted ring closure using nitro compounds

4.2.1. Attempted acetonide deprotection of nitro compounds

The phenyl **122** and dioxolylphenyl **123** substrates prepared previously (*Chapter 3*), were used for the acetonide deprotection reactions. Initially, the acetonide deprotection was thought to have occurred under the Dowex H^+ resin conditions described previously (See *page 73*, *Scheme 37*). However, from analysis of the ^1H NMR spectrum, it was apparent that the two CH_3 signals previously seen in the region of 1.50 and 1.40 ppm for the acetonide were no longer present. However, after numerous repetitions of the experiment a pattern in the ^1H NMR spectra became apparent, whereby a singlet at 3.44 ppm

appeared. This indicated that the hemiacetal that was forming was reacting with the solvent, methanol, which was reacting at C-1 to form the new acetal **125** (*Scheme 37*). The signal for H-1 (δ = 5.04 ppm) gave a doublet which coupled to the adjacent H-2 at 4.36 ppm. The coupling constant of 4.4 Hz was suggestive of a *cis* relationship between H-1 and H-2. Similarly, in the methyl-α-glucofuranoside anomer (or the *cis* isomer) reported in literature,[75] a chemical shift value was observed at 4.52 ppm (in DMSO) which gave a coupling constant of 3.6 Hz. Conversely, the methyl-β-glucofuranoside anomer (or *trans* isomer) at 4.38 ppm gave *J* value of 8.0 Hz. This suggests that the anomer that was isolated was the methyl-α-glucofuranoside or the *cis* anomer. Only one diastereomer was isolated

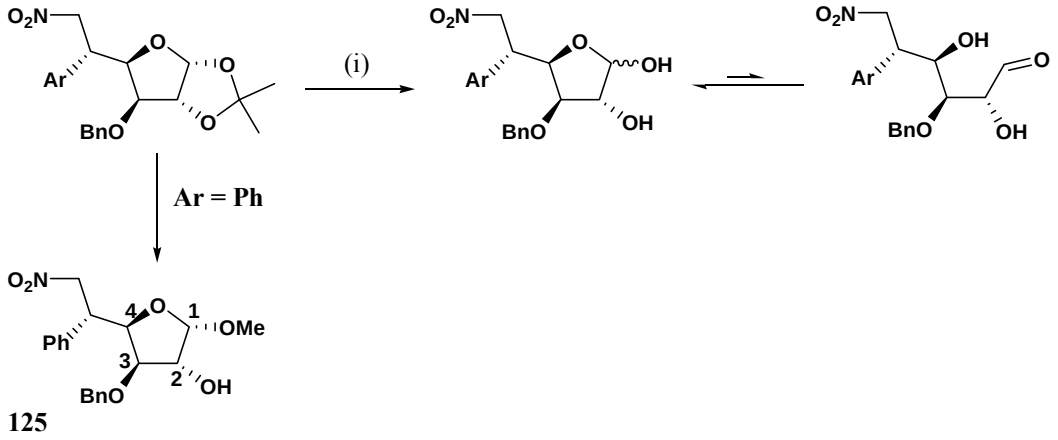

Scheme 37. *(i)* See *Table 4.2.* below for reagents and conditions.

A brief literature survey suggested various other deprotection possibilities, which were attempted in the hope of overcoming this problem (*Table 4.2)*. All the experimental syntheses attempted in *Table 4.2* were carried out on both the phenyl **117** and the dioxolylphenyl **118** adducts which were prepared previously in *Chapter 3*. No reaction was observed for reactions **2** and **5** as evident from the ^{1}H NMR spectra which indicated the presence of starting material as the only product. This led to the understanding that deprotection conditions were perhaps too mild and it was necessary to activate the system further. Unfortunately, reactions **6** and **7** seemed to have resulted only in decomposition of the starting material.

Table 4.2. Various reaction conditions for the attempted acetonide deprotection reaction of precursors **117** and **118**.

Reaction	Reagents and conditions	Reference
1	Dowex H^+ resin, MeOH, reflux–r.t., 18 h	37,38
2	5M HCl, dioxane, r.t., 96 h	76
3	CF_3CO_2H, H_2O, r.t., 48 h	77
4	75% CH_3CN/H_2O , conc. HCl, r.t., 96 h	
5	CF_3CO_2H, 4:1 THF/H_2O, r.t., 12 h	78
6	BCl_3, CH_2Cl_2, r.t., 30 min	79
7	80% AcOH, reflux-r.t., 1 h	80

The NMR spectra of the product from reactions **3** and **4** showed the loss of the acetonide CH_3 peaks and led to the hope of encouraging results. The TLC analysis for reaction **4** showed an increase in polarity, and the R_f value decreased remarkably to 0.14 from 0.64 for precursor **117**, and to 0.11 from 0.50 for precursor **118** (in 30% EtOAc/hexane). No hydroxyl or aldehyde peaks could be seen in the ^1H NMR spectra for reaction **3**; however, the middle region of the spectra underwent significant peak broadening resulting in a disordered appearance, which could attest to hydroxyl peaks being hidden within the spectra. Conversely, the ^1H NMR spectra of reaction **4** exhibited a broad singlet integrating for two protons at 3.26 ppm, and although the spectra were not entirely distinct, some signals and their couplings could be seen.

4.2.2. Attempted cyclization of ring *C* using deprotected nitro compounds

It was thus assumed that the various attempts at deprotection were successful and that the products were only complicated by the appearance of hydroxyl peaks causing additional peak broadening. Most of the attempts on ring closure *(Scheme 38)* were made with the expectation that the acetonide deprotection occurred in the presence of Dowex H^+ resin. The reaction progress was monitored by TLC (in eluent ranging from 50-100% AcOEt/hexane) which revealed highly polar products which did not migrate from the baseline. This suggested that a salt was being formed during the reaction. Further insight into the understanding of the possible mechanism was deduced and it was noted that potassium carbonate is a very weak base and probably not strong enough to perform the ring closure unaided. It is also rather likely that the potassium carbonate will undergo additional transformations in methanol. The emission of CO_2(g) from the system could also induce KOH formation, which is also a basic substance. Aqueous acid would be used in the work-up of the reaction to ensure that protonation of the products occurred.

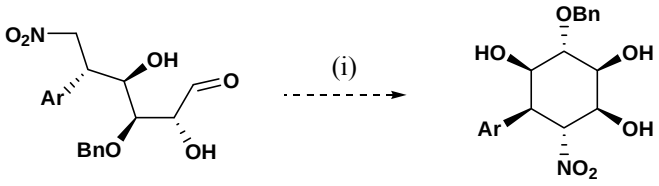

Scheme 38. *(i)* K_2CO_3, MeOH, r.t., 48 h. Ar = Ph, dioxolylphenyl.

The ^{1}H NMR spectra for these experiments showed a diversity of complex products. Only the skeletal frame of the compound could still be seen, suggesting that the product had not succumbed entirely to decomposition. Some interesting results were however observed with one of the dioxolylphenyl products in which the acetonide peaks disappeared from the ^{1}H NMR spectrum and two very broad peaks at 2.87 and 2.01 ppm and two sharp singlets at 3.51 and 3.44 ppm were subsequently observed. This could possibly suggest the presence of the hydroxyl groups in the compound; however, no other conclusions could be drawn. In an attempt to further clarify the spectral data, an acetyl protection was selected.

4.2.3. Acetyl protection of the presumed cyclized nitro product

The acetylation reaction *(Scheme 39)* was performed using the same methodology discussed in *section 4.1.3* above. The ^{1}H NMR spectrum suggested that there was a mixture of products, due to the complexity of the spectrum. Nonetheless, the two downfield peaks, most probably corresponding to H-3a, H-5 and H-6a appeared at 6.94 and 6.67 ppm, both giving singlets which were suggestive of the presence of the protons adjacent to acetyl groups. There was also evidence to suggest the presence of the acetyl peaks further upfield at 2.22, 1.99 and 1.97 ppm. Various other anomalies were observed at 4.99, 3.66, 3.39, 3.33 ppm; all these signals gave singlets, which suggest a possible side-reaction with the acetyl onto other potential OH sites. No further deductions could be made from this spectrum. Unfortunately, the in-house mass spectroscopy service was not available and could have possibly aided in the characterization of our desired product from within the crude mixture. However, owing to time constraints the route was suspended at this point.

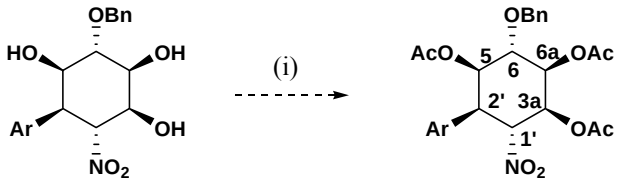

Scheme 39. *(i)* Ac_2O, pyridine, r.t., 96 h.

CHAPTER 5: CONCLUSIONS AND FUTURE PROSPECTS

5.1. Summary of results achieved

Through chemistry which was previously established, the syntheses of both the nitro olefin **105** and the enoate **106** were successfully reproduced. Further analysis into the stereochemistry of the products and their precursors was also accomplished in order to confirm the carbohydrate systems obtained.

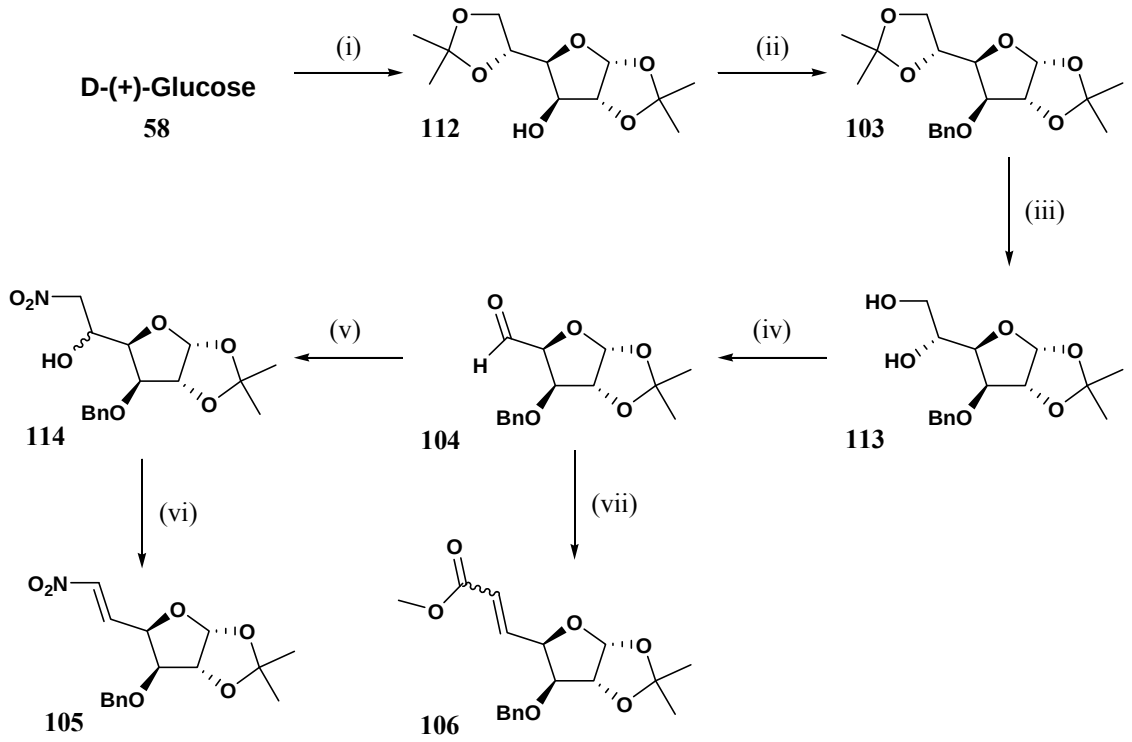

Scheme 40. *(i)* CH_3COCH_3, I_2, r.t., 20 h, 58%; *(ii)* NaH (65% in oil), Bu_4NI, BnBr, THF, r.t., 22 h, 72%;. *(iii)* 50% acetic acid/H_2O, r.t., 48 h, 76% or conc. HCl, MeOH, r.t., 96 h, 78%; *(iv)* $NaIO_4$, MeOH, H_2O, 0°C–r.t.; *(v)* CH_3NO_2, Et_3N, Et_2O, 95% mixture of isomers; *(vi)* $MeSO_2Cl$, Et_3N, Et_2O, 84%; *(vii)* methyl phosphonoacetate, NaH (60%), THF, 63% ***trans*-106**, 2% ***cis*-106.**

D-(+)-Glucose **58** was trapped in its furanose ring state **112** through a reaction with acetone, thus blocking the anomeric carbon from further reactivity *(Scheme 40)*. The acetone also protected four of the surrounding hydroxyl groups (as diol pairs) with acetonide protecting groups. The remaining hydroxyl group then underwent a protection with benzyl bromide (BnBr) to form the benzyl ether **103**. A selective deprotection of the acetonide group containing the primary alcohol was carried out under mildly acidic conditions to give **113** in a reasonable yield of 78%. An oxidation of the diol was induced with the aid of sodium periodate ($NaIO_4$) to give the aldehyde intermediate **104**. Finally, the aldehyde was used in two different syntheses. The first produced the nitroalkene **105** from the Henry reaction. The second route produced almost exclusively *(E)*-enoate **106** in 63% by the Horner-Wadsworth-Emmons reaction. The intermediate step prior to achieving the nitroalkene **105** produced nitroalcohols **114a** and **114b**. These isomers were analyzed in order to ascertain the stereochemistry of the major product. Despite the mixture of nitroalcohols the dehydration afforded the nitro olefin **105** in an 84% yield as a single geometric isomer.

The aim of performing the conjugate addition reactions utilizing two different approaches was to examine the stereochemical outcomes of the reaction. Accordingly, the previously recorded data reported by Paulsen and Stubbe[37,38] in 1983 were used as a basis of comparison and hence a foundation to improve upon.

The organocuprate approach required a transmetallation of copper with a Grignard reagent to produce the reagent that was essential to the conjugate addition process. The conjugate addition was only attempted using bromobenzene, thus producing the phenyl-containing products **115** and **117** (*Figure 15*). The resulting reactions were not highly efficient due to the preparation of the Grignard reagent being problematic and affording an insufficient amount of precursors necessary to attain the product. Consequently, the yields of the product were somewhat low and the conjugate addition by the cuprate reagents was abandoned.

The rhodium-catalyzed induction of conjugate addition was found to be a highly atom economical reaction when compared to the organocuprate method. The yields improved markedly, and because the aromatic precursor was a commercially available arylboronic acid, a variety of novel products could be produced.

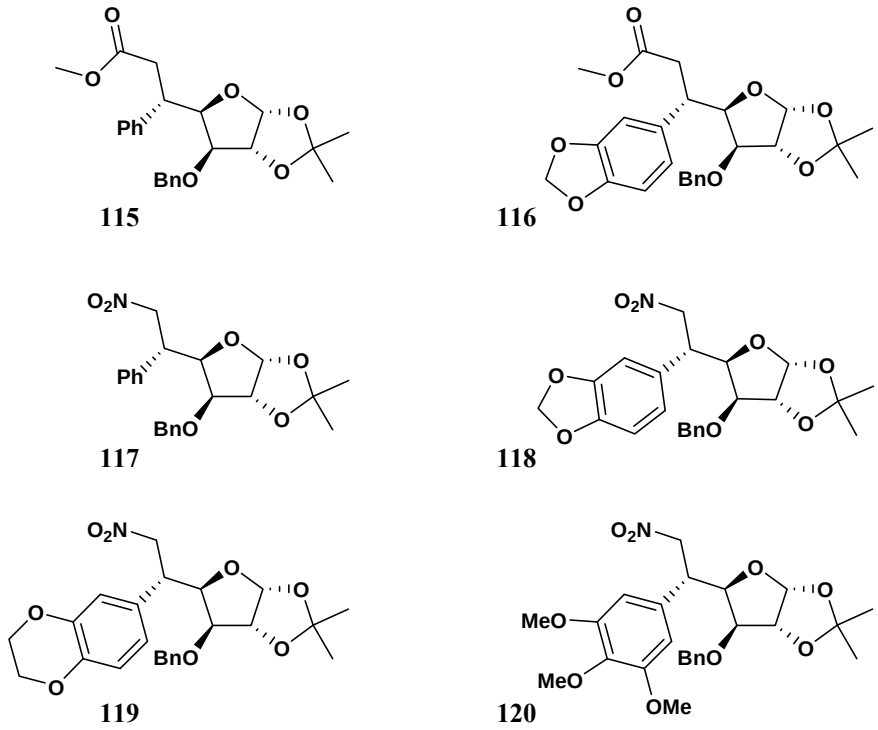

Figure 15. Aromatic analogues prepared by conjugate addition reactions.

However, in the future, it would be profitable to expose both the enoate **106** and the nitroalkene **106** to organocuprate reactions using the same aromatic substituents as used in the rhodium-catalyzed method for conjugate addition *(Figure 15)*. In doing so a comparison and thus enhanced understanding of the two methods could be drawn. Nonetheless, from the data obtained in our synthesis it was shown that the *anti* product was highly selected for in both methods. An approximate *anti:syn* ratio obtained for these aromatic additions was 14:1 for compounds **115** and **117** where the diastereomer could be isolated.

Despite an in-depth literature survey of numerous experimental methods for the deprotection of the acetonide group, all the attempts seemed to show that either no reaction had occurred, or that a complex mixture of products had formed, judging from the NMR spectra which were highly complex and difficult to analyse conclusively. Our primary method, utilising Dowex H^+ resin in methanol, showed the formation of product **125** (*Figure 16*), containing a methyl protected hydroxyl at the hemiacetal carbon, resulting in the method being discarded.

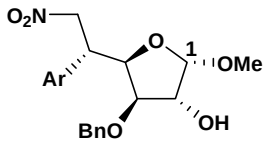

125

Figure 16. Compound **125**, showing methyl protected hydroxyl group.

The ring-closure was attempted using potassium carbonate and methanol under various experimental conditions. However, all attempts at ring closure were inconclusive, as judged from the NMR of the crude products. If the deprotection can be performed then the ring closure should occur quite readily for the nitro adducts due to acidity of the α-carbon.

5.2. Future prospects for the completion of the total synthesis

Aspirations to produce pancratistatin **4** require the formation of ring **B** in pancratistatin as the final goal towards the completion of the total synthesis. A brief literature survey has shown that a Bischler-Napieralski reaction has often been used for this purpose.[25,28,41,42,81]

The nitro-containing compounds (the dioxolylphenyl adduct **126** was used to illustrate the synthesis in *Scheme 41* as it directly generates deoxypancratistatin **5**) would need to undergo a reduction with H_2-Pd/C.[46] Alternatively an aluminium amalgam could form the amine **127**. In the process of that reduction the remaining benzyl-protected hydroxyl group will probably also undergo a deprotection. The amine will then be converted into the carbamate **128** which could be cyclized using a combination of

trifluoromethanesulfonic (triflic) anhydride (Tf_2O) and 4-dimethylaminopyridine (DMAP) to yield deoxypancratistatin **5**.[25]

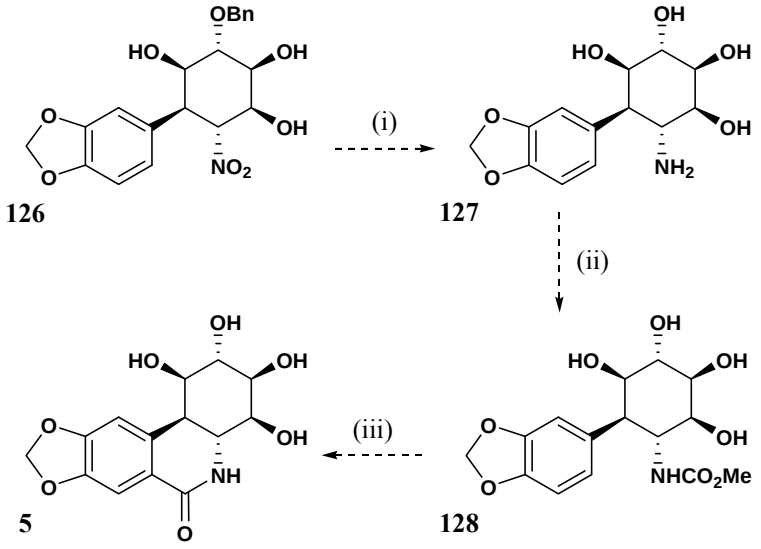

Scheme 41. *(i)* H_2/Pd/C or Al/Hg, EtOH/H_2O; *(ii)* $ClCO_2Me$, CH_2Cl_2, pyridine; *(iii)* Tf_2O, DMAP.

An alternative solution would be required when preparing the ester-containing compounds (*Scheme 42)*.[82] The ester **129** could be hydrolyzed to a carboxylic acid **130**, which could then undergo the Curtius rearrangement reaction by treatment with diphenylphosphoryl azide (DPPA) in the presence of triethylamine (Et_3N), to form an isocyanate **131**. This compound could be cyclized directly to deoxypancratistatin **5** using a Lewis Acid such as $AlCl_3$, followed by the deprotection of the benzyl ether with H_2-Pd/C (*Scheme 42*).

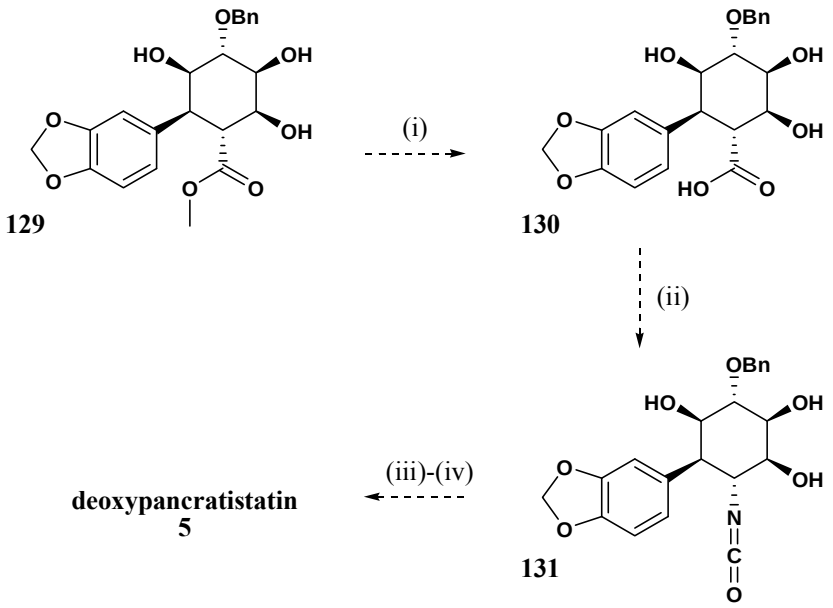

Scheme 42. *(i)* LiOH, THF; *(ii)* DPPA, Et_3N, $PhCH_3$ *(iii)* $AlCl_3$; (iv) H_2/Pd/C, EtOH/H_2O.

Although various aromatic substituents were prepared in order to produce a collection of pancratistatin analogues, the fundamental aim was to produce pancratistatin **4**. The only aromatic adduct resembling pancratistatin **4** at this juncture would be the dioxolylphenyl derivatives **116** and **118**. Therefore, it would be necessary to find a procedure to insert a hydroxyl into the C-7 position of the pancratistatin analogue (*Scheme 43*). This was reported in 1997 by Haseltine and coworkers.[40] Treatment of deoxypancratistatin with *n*-butyllithium (*n*-BuLi) and borane in tetrahydrofuran (BH_3.THF) would generate an intermediate arylborohydride, which could be oxidized with hydrogen peroxide (H_2O_2) to form the phenolic C-7 hydroxyl and finally pancratistatin **4**. Alternatively, the boronic acid **132** (*Figure 17*), could be prepared and used in the arylation reactions.[83]

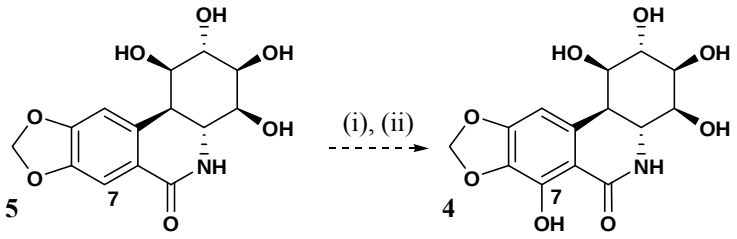

Scheme 43. *(i) n*-BuLi, BH_3.THF; *(ii)* H_2O_2, NaOH.

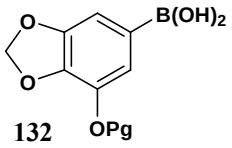

Figure 17. 7-hydroxybenzodioxolylboronic acid **132**.

In conclusion, the natural product D-(+)-glucose **58** was observed to be an efficient starting material for the stereochemical production of the α,β-unsaturated compounds **105** and **106**. These olefins were also successfully used in both organocuprate and rhodium(I)-catalyzed conjugate addition of a variety of commercially available aryl substituents. The desired *anti* stereochemistry was achieved in high ratios of 14:1. Despite the inconclusive evidence pertaining to the acetonide deprotection and ring closure for the prepared compounds, **115**, **116**, **117, 118, 119** and **120**, the correct stereochemistry is in place for future synthetic attempts at the synthesis of pancratistatin **4**.

CHAPTER 6: EXPERIMENTAL

6.1. General procedures

6.1.1. Purification of solvents

All solvents used for preparative chromatography were distilled before use. Unless otherwise stated, solvents used in reactions were pre-dried in their reagent bottles and then distilled over the appropriate drying mediums under a nitrogen atmosphere. Tetrahydrofuran (THF) and diethyl ether (Et_2O) were distilled from sodium wire using benzophenone as an indicator. Toluene (CH_3Ph) was distilled from sodium metal lumps. Acetonitrile (CH_3CN) and dichloromethane (CH_2Cl_2) were distilled from calcium hydride. Pyridine was distilled from potassium hydroxide.

6.1.2. Chromatography

Separation of compounds by column chromatography was performed using Merck silica-gel (particle size 0.063–0.200 mm) as an adsorbent. Separation of compounds by flash column chromatography was performed using Merck silica-gel (particle size 0.04–0.063 mm). The R_f values quoted are for thin layer chromatography (TLC) on aluminum-backed Merck silica-gel 60 F_{254} sheets. Compounds on the TLC plates were either viewed under UV lights, by dipping the plates into basic potassium permanganate ($KMnO_4$) or iodine absorbed onto silica.

6.1.3. Spectroscopic and physical data

Melting points were obtained on a Reichert hot-stage microscope, and are uncorrected.

Optical rotations were measured on a Jasco DIP 3-70 instrument at 22 °C at the sodium D line (589 nm), and $[\alpha]_D$ values are given in $deg.cm^2.g^{-1}$.

Infra-red spectra were recorded on Bruker Vector-22 Fourier Transform spectrometer or on a Bruker Tensor 27 Fourier Transform spectrometer.

^1H NMR and ^{13}C NMR spectra were recorded either on a Bruker AVANCE 300 (300.13 MHz) or on a Bruker DRX-400 (400.13 MHz) spectrometer. All spectra were recorded in deuterated chloroform ($CDCl_3$) and chemical shifts are reported in parts per million (ppm) relative to tetramethyl silane, the internal standard. *J* values are given in hertz (Hz).

High-resolution mass spectra were recorded either on a VG70 MS (Mass spectrum CC Pyramid data system) or on a VG70 SEQ (VG 11-205J or Marc 11 data system) or on a DFS High Resolution Magnetic Sector mass spectrometer.

Intensity data were collected on a Bruker APEX II CCD area detector diffractometer with graphite monochromated Mo K_α radiation (50kV, 30mA) using the APEX 2[84] data collection software. The collection method involved ω-scans of width 0.5° and 512x512 bit data frames. Data reduction was carried out using the program *SAINT+*.[85] The crystal structure was solved by direct methods using *SHELXTL*.[86] Non-hydrogen atoms were first refined isotropically followed by anisotropic refinement by full matrix least-squares calculations based on F^2 using *SHELXTL*. Hydrogen atoms were first located in the difference map then positioned geometrically and allowed to ride on their respective parent atoms. Diagrams and publication material were generated using SHELXTL, PLATON[87] and ORTEP-3.[88]

6.1.4. Other general procedures

All reactions were carried out under nitrogen using a standard manifold line connected to a vacuum pump. The reaction vessels used were dried either in an oven or flame-dried whilst under vacuum.

The term "*in vacuo*" refers to the removal of solvent under reduced pressure on a rotary evaporator followed by removal of trace amounts of solvent using a high vacuum (oil) pump.

6.2. Experimental work pertaining to chapter 2

6.2.1. (3a*S*,5*R*,6*S*,6a*S*)-5-[(4*R*)-2,2-Dimethyl-1,3-dioxolan-4-yl]-2,2-dimethyltetrahydrofuro[2,3-*d*][1,3]dioxol-6-ol 112

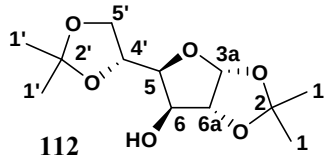

112

D-(+)-glucose **58** (10.04 g, 55.2 mmol, 1 equiv.) was stirred in distilled acetone (400 cm^3) to give a white suspension, this was then followed by the addition of iodine (2.84 g, 11.2 mmol, 0.2 equiv.), which immediately transformed the mixture to a brown colour. The suspension was stirred at room temperature, under an atmosphere of nitrogen, for 20 hours. The reaction mixture was quenched with a saturated solution of sodium thiosulfate ($Na_2S_2O_3$), which was added slowly while stirring, until the brown colour disappeared. The solvent was then evaporated and the product was extracted with ethyl acetate (AcOEt) (50 cm^3), washed with water (3 × 50 cm^3), then brine (50 cm^3) and dried over anhydrous $MgSO_4$. The solvent was then removed *in vacuo* to give a white solid, which could be recrystalized with benzene to give compound **112** (8.42 g, 32.4 mmol, 58%).

R_f: 0.83 (10% AcOEt/hexane); **$[\alpha]_D$:** –10.0 (*c* 2.0, $CHCl_3$, 22 °C)**; M.p.:** 112–114 °C, (literature[57] 109–110 °C); **^{1}H NMR** (300 MHz, $CDCl_3$, δ/ppm): 5.94 (d, *J* = 3.6 Hz, 1H, H-3a), 4.53 (d, *J* = 3.6 Hz, 1H, H-6a), 4.38-4.30 (m, 1H, H-6, H-4'), 4.17 (dd, *J* = 8.6, 6.2 Hz, 1H, H-5'), 4.07 (dd, *J* = 7.7, 2.7 Hz, 1H, H-5), 4.00 (dd, *J* = 8.6, 5.3 Hz, 1H, H-5'), 2.76 (d, *J* = 3.8 Hz, 1H, OH), 1.50 (s, 3H, H-1'), 1.45 (s, 3H, H-1'), 1.37 (s, 3H, H-1), 1.32 (s, 3H, H-1); **^{13}C NMR** (100 MHz, $CDCl_3$, δ/ppm): 111.8 (C-2), 109.7 (C-2'), 105.3 (C-3a), 85.1 (C-6a), 81.2 (C-5), 75.2 (C-6), 73.4 (C-4'), 67.7 (C-5'), 26.9 (C-1'), 26.8 (C-1'), 26.2 (C-1), 25.2 (C-1); **IR** (υ/cm^{-1}): 3424 (m, O-H stretch), 2984 (m, C-H stretch), 1458 (w, C-H stretch), 1373 (m, C-H stretch), 1215 (s, O-H bend), 1000 (s, C-O stretch), 845 (s, C-C stretch); **HRMS (EI) $[M–CH_3]^+$:** calculated for $C_{11}H_{17}O_6$ 245.1013 found 245.1014; **M/z (%):** 245.1014 (100),241.2067 (11).

6.2.2. (3a*R*,5*R*,6*S*,6a*R*)-6-(Benzyloxy)-5-(2,2-dimethyl-1,3-dioxolan-4-yl)-2,2-dimethyl-tetrahydrofuro[2,3-*d*][1,3]dioxole 103

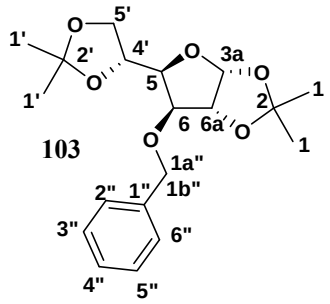

103

Compound **112** (3.21 g, 12.3 mmol, 1 equiv.) was dissolved in distilled THF (160 cm^3) and stirred at 0 °C under an atmosphere of nitrogen. Sodium hydride (NaH) (60% in paraffin oil, 1.52 g, 37.0 mmol, 3 equiv.) was slowly added to the mixture, which began to turn a deep yellow colour, once deprotonation was complete. Benzyl bromide (BnBr) (4.00 cm^3, 2.47 mmol, 2.6 equiv.) and tetrabutylammonium iodide (Bu_4NI) (0.910 g, 2.47 mmol, 0.2 equiv.) were then added and the stirring mixture was allowed to warm to room temperature for 22 hours, were it became a deep yellow-orange opaque mixture. The crude product was then quenched with acetic acid (AcOH) (2 cm^3) and the solvent was

evaporated. The organic layer was extracted with ethyl acetate (AcOEt) (50 cm^3) and washed with water (3 × 50 cm^3), then brine (50 cm^3) and dried with $MgSO_4$. The solvent was evaporated under vacuum to produce a crude oil. The oil was further purified by column chromatography (10% AcOEt/hexane) to afford a compound **103** as a pale yellow oil (3.10 g, 8.85 mmol, 72%).

R_f: 0.28 (10% AcOEt/hexane); **$[\alpha]_D$:** –22.5 (*c* 2.0, $CHCl_3$, 22 °C); **^{1}H NMR** (300 MHz, $CDCl_3$, δ/ppm): 7.36-7.30 (m, 5H, H-2”–H-6”), 5.89 (d, *J* = 3.6 Hz, 1H, H-3a), 4.68 (d, *J* = 11.8 Hz, 1H, H-1a”), 4.63 (d, *J* = 11.9 Hz, 1H, H-1b”), 4.58 (d, *J* = 3.7 Hz, 1H, H-6a), 4.37 (td, *J* = 7.7, 6.0 Hz, 1H, H-4’), 4.17-4.08 (m, 2H, H-5, H-5’), 4.03-3.97 (m, 2H, H-6, H-5’), 1.49 (s, 3H, H-1’), 1.43 (s, 3H, H-1’), 1.37 (s, 3H, H-1), 1.31 (s, 3H, H-1); **^{13}C NMR** (100 MHz, $CDCl_3$, δ/ppm): 137.6 (C-1”), 128.4 (C-2”, C-6”), 127.8 (C-4”), 127.6 (C-3”, C-5”), 111.8 (C-2), 109.0 (C-2’), 105.3 (C-3a), 82.7 (C-6), 81.7 (C-6a), 81.3 (C-5), 72.5 (C-1a”/b”), 72.4 (C-4’), 67.4 (C-5’), 26.8(C-1’), 26.8 (C-1’), 26.2(C-1), 25.4 (C-1); **IR** (υ/cm^{-1}): 2986 (w, C-H stretch), 1541 (w, C=C stretch), 1372 (m, C-H stretch), 1212 (m, C-O stretch), 1071 (s, C-O stretch); **HRMS (EI):** calculated for $C_{19}H_{23}O_6$ 350.1730 found 350.1726; **M/z (%):** 350.1726 (4), 341.0881 (1), 335.1488 (100, M–CH_3^+), 332.1112 (2), 321.1463 (2).

Assignments denoted by * are interchangeable

6.2.3. (1*R*)-1-{(3a*R*,5*R*,6*R*,6a*R*)-2,2-Dimethyl-6-[(phenylmethyl)oxy]tetrahydrofuro[2,3-*d*][1,3]dioxol-5-yl}ethane-1,2-diol 113

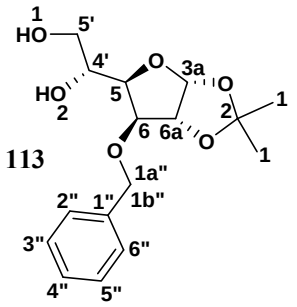

Procedure 1:

Compound **103** (4.8856 g, 13.94 mmol, 1 equiv.) was dissolved in a 50% acetic acid (AcOH) solution (100 cm^3) and allowed to stir in an atmosphere of nitrogen over 48 hours at room temperature. The reaction mixture was diluted further in water (50 cm^3) and treated with sodium hydrogen carbonate ($NaHCO_3$) until the effervescence subsided. The product was then extracted with ethyl acetate (AcOEt) (3 × 50 cm^3) and the organic extracts were combined and further washed with water (3 × 50 cm^3), then brine (50 cm^3). The organic extract was dried with $MgSO_4$ and the solvent was evaporated. The product was purified by column chromatography, initially with 10% AcOEt/hexane and then increasing the polarity by 5% every 100 cm^3 until 50% AcOEt/hexane. This afforded a pale yellow oil (3.2726 g, 10.5 mmol, 76%).

Procedure 2:

A solution of MeOH (470 cm^3), distilled water (45 cm^3) and concentrated HCl (2.5 cm^3) was added to compound **103** (51 g, 145.5 mmol, 1 equiv.) and allowed to stir under an atmosphere of nitrogen for 96 hours, at room temperature. The solution was neutralized with a NH_4OH and the organic layer was extracted with ethyl acetate (AcOEt) (3 × 50 cm^3) and washed with water (3 × 50 cm^3), followed by brine. The organic layer was then dried over $MgSO_4$ and the solvent was evaporated. Purification of the crude product was done by column chromatography in 50% AcOEt/hexane, to give compound **113** as a pale yellow oil (35.33 g, 113.8 mmol, 78%).

R_f: 0.26 (10% AcOEt/hexane); **$[\alpha]_D$:** –50.8 (*c* 2.0, $CHCl_3$, 22 °C); **^{1}H NMR** (300 MHz, $CDCl_3$, δ/ppm): 7.39-7.25 (m, 5H, H-2"–H-6"), 5.92 (d, *J* = 3.8 Hz, 1H, H-3a), 4.71 (d, *J* = 11.8 Hz, 1H, H-1a"*), 4.61 (d, *J* = 3.8 Hz, 1H, H-6a), 4.56 (d, *J* = 11.8 Hz, 1H, H-1b"*), 4.15-4.08 (m, 2H, H-5, H-6), 4.06-3.97 (m, 1H, H-4'), 3.84-3.74 (m, 1H, H-5'), 3.73-3.63 (m, 1H, H-5'), 2.75 (d, *J* = 6.1 Hz, 1H, OH-2), 2.54 (t, *J* = 5.9 Hz, 1H, OH-1), 1.48 (s, 3H, H-1), 1.31 (s, 3H, H-1); **^{13}C NMR** (100 MHz, $CDCl_3$, δ/ppm): 138.1 (C-1"), 129.5 (C-2",C-6"), 129.0 (C-4"), 128.7 (C-3", C-5"), 112.6 (C-2), 106.0 (C-3a), 83.0 (C-6), 82.8 (C-6a), 80.8 (C-5), 73.0 (C-1a"/b"), 70.0 (C-4'), 65.2 (C-5'), 27.6 (C-1), 27.1 (C-1); **IR** (υ/cm^{-1}): 3423 (m br, O-H stretch), 2935 (w, C-H stretch), 1213 (m, O-H bend), 1071 (s, C-O stretch), 885 (m, C-C stretch); **HRMS (EI):** calculated for $C_{16}H_{22}O_6$ 310.1416 found 309.8962; **M/z (%):** 309.8962 (8), 306.0315 (3), 301.8138 (2), 296.2617 (16), 295.1659 (100), 291.8672 (34).

Assignments denoted by * are interchangeable

6.2.4. (3a*R*,5*S*,6*R*,6a*R*)-2,2-Dimethyl-6-[(phenylmethyl)oxy]tetrahydrofuro[2,3-*d*][1,3]dioxole-5-carbaldehyde 104

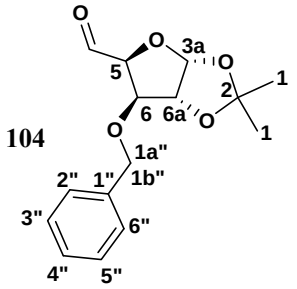

Compound **113** (5.04 g, 16.2 mmol, 1 equiv.) in MeOH (50 cm^3) was cooled to 0 °C. A solution of sodium periodate ($NaIO_4$) (6.23 g, 29.1 mmol, 1.8 equiv.) in water (35 cm^3) was then slowly added over 30 minutes. A white precipitate began to form making the solution a thick emulsion, which was left to stir at room temperature for 18 hours, under an atmosphere of nitrogen. The reaction was then diluted with water (200 cm^3) to dissolve all the inorganic salts and the organic product was extracted with ethyl acetate

(AcOEt) (3 × 50 cm^3). The organic extracts were then collected and washed with brine (2 × 50 cm^3), dried ($MgSO_4$) and the solvent was evaporated. Compound **104** (crude yield: 4.3384 g, 15.59 mmol, 96%) was used without further purification.

R_f: 0.72 (50% AcOEt/hexane); **$[\alpha]_D$:**–49.0 (*c* 2.0, $CHCl_3$, 22 °C); **^{1}H NMR** (300 MHz, $CDCl_3$, δ/ppm): 9.67 (s, 1H, H-1'), 7.44–7.18 (m, 5H, H-2"–H-6"), 6.12 (d, *J* = 3.3 Hz, 1H, H-3a), 4.93–4.00 (m, 4H), 3.51–3.40 (m, 1H), (s, 3H, H-1), 1.33 (s, 3H, H-1); **IR** (υ/cm^{-1}): 2936 (m, C-H stretch), 1738 (m, C=O stretch), 1072 (s, C-O stretch).

6.2.5. Methyl (2*E*)-3-{(3a*R*,5*R*,6*R*,6a*R*)-2,2-dimethyl-6-[(phenylmethyl)oxy]tetrahydrofuro[2,3-*d*][1,3]dioxol-5-yl}prop-2-enoate 106

Sodium hydride (NaH) in 60% paraffin oil (0.75 g, 18.7 mmol, 1.3 equiv.) in THF (50 cm^3) was cooled to –60 °C. Trimethyl phosphonoacetate (2.6 cm^3, 18.0 mmol, 1.25 equiv.) was slowly added, and the mixture was then left to warm to room temperature for 1 hour. The reaction vessel was then recooled to –60 °C and compound **104** (4.0 g, 14.4 mmol, 1 equiv.) in THF (20 cm^3) was added to stirring mixture. The reaction was again allowed to warm to room temperature and left to stir under an atmosphere of nitrogen for 20 hours. The reaction was quenched with solid ammonium chloride (NH_4Cl) (2.5 g, 4.67 mmol, 3.26 equiv.) and poured into water (100 cm^3). The product was extracted with ethyl acetate (AcOEt) (3 × 50 cm^3) and the combined organic extracts were washed with brine (2 × 50 cm^3), dried over $MgSO_4$ and the solvent was then removed *in vacuo* to give a crude product. Flash chromatography was prepared in 20% AcOEt/hexane, to give the major *E*-isomer, compound ***trans*-106** as a pale yellow oil (3.7603 g, 11.2 mmol, 78%) and the minor *Z*-isomer, compound ***cis*-106** (0.5359 g, 1.60 mmol, 11%).

R_f: *trans*-106: 0.33, ***cis*-106**: 0.42 (20% AcOEt/hexane); **$[\alpha]_D$: *trans*-106**: –92.5, ***cis*-106**: –58.5 (*c* 2.0, $CHCl_3$, 22 °C).

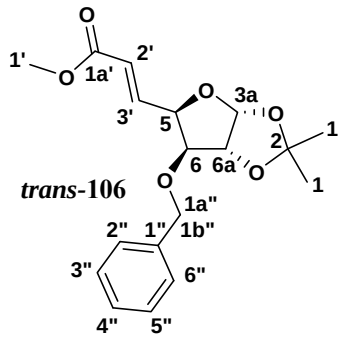

trans-106

^{1}H NMR (300 MHz, *CDCl$_3$*, δ/ppm) ***trans*-106**: 7.44–7.16 (m, 5H, H-2”–H-6”), 6.96 (dd, *J* = 15.8, 5.0 Hz, 1H, H-3’), 6.17 (dd, *J* = 15.8, 1.7 Hz, 1H, H-2’), 5.99 (d, *J* = 3.7 Hz, 1H, H-3a), 4.79 (ddd, *J* = 5.0, 3.3, 1.7 Hz, 1H, H-5), 4.63 (d, *J* = 3.3 Hz, 1H, H-6a), 4.61 (d, *J* = 12.5 Hz, 1H, H-1a”*), 4.49 (d, *J* = 12.2 Hz, 1H, H-1b”*), 3.97 (d, *J* = 3.01 Hz, 1H, H-6), 3.75 (s, 3H, H-1’), 1.48 (s, 3H, H-1), 1.32 (s, 3H, H-1); **^{13}C NMR** (100 MHz, *CDCl$_3$*, δ/ppm): 166.8 (C-1a’), 142.2 (C-3a’), 137.5 (C-1”), 128.9 (C-2”, C-6”), 128.5 (C-4”), 128.2 (C-3”, C-5”), 123.2 (C-2’), 112.3 (C-2), 105.4 (C-3a), 83.3 (C-6), 83.2 (C-6a), 79.8 (C-5), 72.6 (C-1a”/b”), 52.1 (C-1’), 27.2 (C-1), 26.6 (C-1); **IR** (υ/cm^{-1}): 2989 (w, C-H stretch), 1720 (s, C=O stretch), 1438, 1374 (m, C-H bend), 1201, 1072 (s, C-O stretch), 855 (m, C-C stretch); **HRMS (EI) [M–CH$_3$]$^+$:** calculated for $C_{17}H_{19}O_6$ 319.1169 found 319.1177; **M/z (%):** 319.1177 (100), 316.9829 (88), 309.9818 (20), 302.9857 (9).

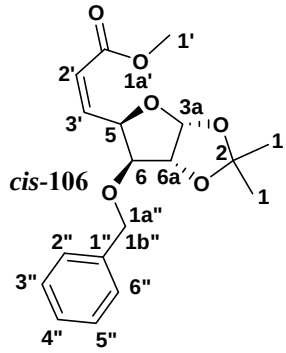

cis-106

^{1}H NMR (300 MHz, *CDCl$_3$*, δ/ppm) ***cis*-106**: 7.36–7.21 (m, 5H, H-2”–H-6”), 6.40 (dd, *J* = 11.7, 6.7 Hz, 1H, H-3’), 6.01 (d, *J* = 3.5 Hz, 1H, H-3a), 5.93 (dd, *J* = 11.8, 1.7 Hz, 1H, H-2’), 5.65 (ddd, *J* = 6.8, 3.3, 1.7 Hz, 1H, H-5), 4.64 (d, *J* = 3.5 Hz, 1H, H-6a), 4.61 (d, *J* = 11.8 Hz, 1H, H-1a”*), 4.45 (d, *J* = 12.0 Hz, 1H, H-1b”*), 4.29 (d, *J* = 3.3 Hz, 1H, H-6), 3.66 (s, 3H, H-1’), 1.52 (s, 3H, H-1), 1.33 (s, 3H, H-1).

Assignments denoted by * are interchangeable

6.2.6. (1*S*) and (1*R*)-1-{(3a*R*,5*R*,6*R*,6a*R*)-2,2-Dimethyl-6-[(phenylmethyl)oxy]tetrahydrofuro[2,3-*d*][1,3]dioxol-5-yl}-2-nitroethanol 114a and 114b

Triethylamine (Et_3N) (1.40 cm^3, 10.9 mmol, 1.2 equiv.) was added to a stirring mixture of aldehyde **104** (2.52 g, 9.20 mmol, 1 equiv.) in nitromethane ($MeNO_2$) (15 cm^3) and left to stir at room temperature for 24 hours under an atmosphere of nitrogen. The solvents were then evaporated under reduced pressure. The product was preabsorbed onto silica and purified by column chromatography by increasing the polarity from 5 to 20% AcOEt/hexane. The major *α*-D-*gluco* isomer **114a** was collected as a pale yellow oil (2.2702 g, 6.67 mmol, 73%) and the minor *β*-L-*ido* isomer **114b** was collected as an opaque white oil (0.2979 g, 0.875 mmol, 9.5%).

Isomeric ratio: 8: 1; **de:** 63% ; **R_f: 114a**: 0.44 , **114b**: 0.33 (30% AcOEt/hexane); **M.p.: 114b**: 90–92 °C; **$[\alpha]_D$: 114a**: –37.0, **114b:** –51.9 (*c* 2.0, $CHCl_3$, 22 °C); **IR** (υ/cm^{-1}): 3449 (m, O-H stretch), 1548 (s, N-O stretch), 1380 (m, C-H bend), 1210 (m, O-H bend), 1027 (s, C-O stretch), 850 (C-C stretch); **HRMS (EI) $[M–CH_3]^+$:** calculated for $C_{15}H_{18}O_7N$ 324.1071 found 324.1077; **M/z (%):** 324.1077 (100), 322.2507 (9), 316.9827 (30).

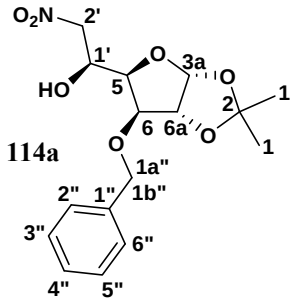

^{1}H NMR (300 MHz, $CDCl_3$, δ/ppm) **114a**: 7.42–7.30 (m, 5H, H-2”–H-6”), 5.91 (d, *J* = 3.6 Hz, 1H, H-3a), 4.74 (d, *J* = 11.7 Hz, 1H, H-1a”*), 4.63 (d, *J* = 3.7 Hz, 1H, H-6a), 4.79–4.59 (m, 2H, H-1’, H-2’), 4.53 (d, *J* = 11.8 Hz, 1H, H-1b”*), 4.46 (dd, *J* = 13.1, 8.9 Hz, 1H, H-2’), 4.12–4.06 (m, 1H, H-5), 4.07 (d, *J* = 3.38 Hz, 1H, H-6), 2.64 (d, *J* = 5.5 Hz, 1H, OH), 1.47 (s, 3H, H-1), 1.32 (s, 3H, H-1); **^{13}C NMR** (100 MHz, $CDCl_3$, δ/ppm): 136.9 (C-1”), 128.8 (C-2”, C-6”), 128.3 (C-4”), 127.9 (C-3”, C-5”), 112.1 (C-2), 105.2 (C-3a), 81.9 (C-6), 81.0 (C-6a), 80.0 (C-5), 78.6 (C-2’), 72.1 (C-1a”/b”), 66.3 (C-1’), 26.7 (C-1), 26.1 (C-1).

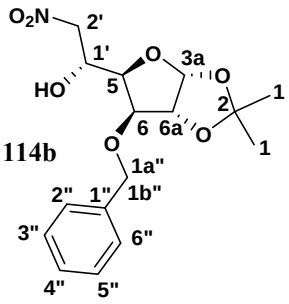

^{1}H NMR (300 MHz, *CDCl$_3$*, δ/ppm) **114b**: 7.42–7.29 (m, 5H, H-2"–H-6"), 6.00 (d, *J* = 3.7 Hz, 1H, H-3a), 4.75 (d, *J* = 11.8 Hz, 1H, H-1a"*), 4.67 (d, *J* = 3.8 Hz, 1H, H-6a), 4.78–4.62 (m, 1H, H-1'), 4.50 (d, *J* = 11.8 Hz, 1H, H-1b"*), 4.50 (dd, *J* = 11.8, 3.2 Hz, 1H, H-2'), 4.33 (dd, *J* = 12.8, 3.2 Hz, 1H, H-2'), 4.17 (t, *J* = 4.1 Hz, 1H, H-5), 4.09 (d, *J* = 3.9 Hz, 1H, H-6), 3.34 (s, 1H, OH), 1.47 (s, 3H, H-1), 1.34 (s, 3H, H-1); **^{13}C NMR** (100 MHz, *CDCl$_3$*, δ/ppm): 136.1 (C-1"), 128.8 (C-2", C-6"), 128.6 (C-4"), 128.1 (C-3", C-5"), 112.3 (C-2), 105.0 (C-3a), 82.6 (C-6), 82.2 (C-6a), 79.1 (C-5), 77.6 (C-2'), 72.0 (C-1a"/b"), 67.7 (C-1'), 26.8 (C-1), 26.3 (C-1).

6.2.7. (3a*R*,5*R*,6*R*,6a*R*)-2,2-Dimethyl-5-[(*E*)-2-nitroethenyl]-6-[(phenylmethyl)oxy]tetrahydrofuro[2,3-*d*][1,3]dioxole 105

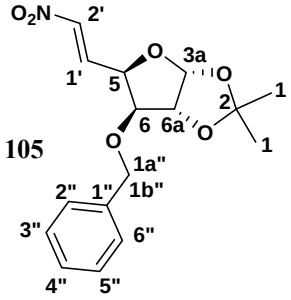

Compound **114a** (7.75 g, 22.79 mmol, 1 equiv.) was dissolved in diethyl ether (Et_2O) (70 cm^3) and stirred at 0 °C. Methylsulfonylchloride ($MeSO_2Cl$) (3 cm^3) and Et_2O (50 cm^3) were added to a dropping funnel and added to the stirring mixture over 45 minutes, the mixture was then left to stir for an additional 30 minutes. The reaction vessel was then allowed to warm to room temperature and left to stir under an atmosphere of nitrogen for 36 hours. The reaction was quenched with 5 % HCl (250 cm^3), extracted with ethyl acetate (AcOEt) (3 × 50 cm^3) and washed the organic layer with brine (3 × 50 cm^3), dried over $MgSO_4$ and then the solvents were evaporated under reduced pressure. The crude

product was purified by flash chromatography in 25% AcOEt/hexane to give a deep yellow oil as compound **105** (6.12 g, 19.1 mmol, 84%).

R_f: 0.47 (25% AcOEt/hexane); **$[\alpha]_D$:** –24.5 (*c* 2.0, $CHCl_3$, 22 °C); **^{1}H NMR** (300 MHz, $CDCl_3$, δ/ppm): 7.39–7.20 (m, 6H, H-2"–H-6", H-2' *), 7.16 (dd, *J* = 13.3, 3.5 Hz, 1H, H-1' *), 5.99 (d, *J* = 3.6 Hz, 1H, H-3a), 4.90 (dt, *J* = 3.5, 1.3 Hz, 1H, H-5), 4.66 (d, *J* = 11.7 Hz, 1H, H-1a" #), 4.67 (d, *J* = 3.9 Hz, 1H, H-6a), 4.46 (d, *J* = 12.1 Hz, 1H, H-1b" #), 4.05 (d, *J* = 3.4 Hz, 1H, H-6), 1.49 (s, 3H, H-1), 1.34 (s, 3H, H-1); **^{13}C NMR** (100 MHz, $CDCl_3$, δ/ppm): 140.9 (C-1'), 136.6 (C-2'), 135.8 (C-1"), 128.6 (C-2", C-6"), 128.3 (C-4"), 127.8 (C-3", C-5"), 112.3 (C-2), 105.1 (C-3a), 82.4 (C-6), 82.3 (C-6a), 72.2 (C-1a"/b"), 66.8 (C-5), 26.8 (C-1), 26.1 (C-1); **IR** (υ/cm^{-1}): 2938 (w, C-H stretch), 1662 (w, C=C stretch), 1526 (s, N-O stretch), 1354 (m, C-H bend), 1075 (s, C-O stretch); **HRMS (EI) $[M–CH_3]^+$:** calculated for $C_{15}H_{16}O_6N$ 306.0865 found 306.0983; **M/z (%):** 306.0983 (100), 304.1012 (9), 298.0362 (4), 291.0794 (9).

Assignments denoted by * and # are interchangeable

6.3. Experimental work pertaining to chapter 3

General procedure for cuprate mediated conjugate additions:

A three-necked round bottom flask equipped with a rubber septum, containing magnesium turnings, was flame dried under vacuum. THF (10 cm^3) was added followed by the slow addition of bromobenzene (PhBr) (10 equiv.) in THF (10 cm^3), which induced a highly exothermic reaction. The reaction was left to cool to room temperature once the reaction stopped, and was left to stir under an atmosphere of nitrogen for 1 hour until the mixture changed to a grey-yellow colour. In a second flame-dried three-necked flask, cuprous iodide (CuI) (5 equiv.) in THF (20 cm^3) was cooled to –78 °C. The previously prepared Grignard reagent was then cannulated to the cooled cuprate solution and allowed to warm to room temperature for 3 hours. The reaction vessel was again cooled to –78 °C and unsaturated alkene (1 equiv.) in THF (30 cm^3) was then cannulated

to the organocuprate mixture, which caused the mixture to turn opaque yellow in appearance. The reaction mixture was left to warm to room temperature and left to stir in an atmosphere of nitrogen for 20 hours. The reaction appeared to have changed a brown colour overnight. The reaction was quenched with 10% NH_4OH/NH_4Cl solution (in water). The organic phase was extracted with ethyl acetate (AcOEt) (3×50 cm^3), washed with water (2×50 cm^3) and brine (50 cm^3). The organic extract was dried over $MgSO_4$, filtered and evaporated under reduced pressure. The crude product was purified by column chromatography (20% AcOEt/hexane) to afford the product.

Trimethylsilyl chloride (TMSCl, 10.0 equiv.) was used to prepare the propanoate derivative **115**. TMSCl (10 equiv.) was cannulated along with the enoate (1 equiv.) and THF (30 cm^3).

General procedure for rhodium-catalyzed conjugate additions:

Phenylboronic acid (2 equiv.) and $\{[(cod)RhCl]_2\}$ catalyst (3% mol equiv.) were added to a stirring mixture of nitroalkene **105** or enoate **106** (1 equiv.), in a 10:1 dioxane/H_2O mixture (25 cm^3). After 5 minutes of stirring at room temperature, triethylamine (Et_3N) (1.2 equiv.) was added to the reaction, which changed in appearance from yellow-orange in colour to dark red-brown in colour. The system was left to stir at room temperature, under nitrogen, for 5 days. The solvents were removed *in vacuo*, the product was then preabsorbed onto silica and purified by flash column chromatography (20% AcOEt/hexane) to afford the product.

6.3.1. Methyl (3*S*)-3-{(3a*R*,5*R*,6*R*,6a*R*)-2,2-dimethyl-6-[(phenylmethyl)oxy]tetrahydrofuro[2,3-*d*][1,3]dioxol-5-yl}-3-phenylpropanoate 115

Major diasteriomer **115** afforded a clear yellow oil (0.271 g, 0.657 mmol, 55%) achieved for the cuprate conjugate addition reaction and (0.261 g, 0.632 mmol, 94%) achieved for the rhodium catalyzed conjugate addition. **R_f: 115:** 0.53, **115b:** 0.47 (30% AcOEt/hexane); **$[\alpha]_D$: 115** –29.5, **115b:** –43.0 (*c* 2.0, $CHCl_3$, 22 °C $_3$); **IR** (υ/cm^{-1}): 2990 (w, C-H stretch), 1738 (s, C=O stretch), 1498, 1375 (w, C-H bend), 1073, 1016 (s, C-O stretch);); **HRMS (EI):** calculated for $C_{24}H_{28}O_6$ 412.1886 found 412.1791; **M/z (%):** 412.1791 (7), 410.0845 (1), 402.9792 (1), 399.1676 (4), 398.1644 (26), 397.1654 (100, $M–CH_3^+$), 395.1725 (2).

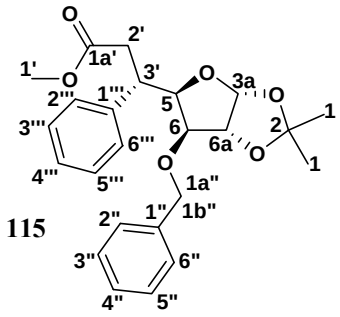

115

^{1}H NMR (300 MHz, $CDCl_3$, δ/ppm) **115**: 7.36-7.21 (m, 10H, H-2”–H-6”, H-2’’’–H-6’’’), 5.95 (d, *J* = 3.8 Hz, 1H, H-3a), 4.52 (d, *J* = 3.8 Hz, 1H, H-6a), 4.39 (d, *J* = 11.6 Hz, 1H, 1a”*), 4.38 (dd, *J* = 10.2, 3.5 Hz, 1H, H-5), 4.10 (d, *J* = 11.4 Hz, 1H, H-1b”*), 3.71 (dt, *J* = 10.5, 4.3 Hz, 1H, H-3’), 3.48 (s, 3H, H-1’), 3.44 (d, *J* = 3.0 Hz, 1H, H-6), 3.11 (dd, *J* = 15.6, 4.3 Hz, 1H, H-2’), 2.69 (dd, *J* = 15.6, 10.6 Hz, 1H, H-2’), 1.53 (s, 3H, H-1), 1.30 (s, 3H, H-1); **^{13}C NMR** (100 MHz, $CDCl_3$, δ/ppm): 172.3 (C-1a’), 140.2 (C-1’’’), 137.2 (C-1”), 128.3 (C-2”, C-6”), 128.2 (C-2’’’, C-6’’’), 128.1 (C-3”, C-5”), 127.6 (C-4’), 127.5 (C-3’’’, C-5’’’), 126.8 (C-4’’’), 111.2 (C-2), 104.9 (C-3a), 83.2 (C-5), 81.8 (C-6a), 81.5 (C-6), 71.8 (C-1a”/b”), 51.1 (C-1’), 40.7 (C-3’), 38.6 (C-2’), 26.6 (C-1), 26.0 (C-1).

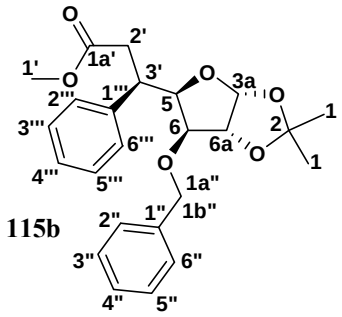

^{1}H NMR (300 MHz, *CDCl$_3$*, δ/ppm) **115b**: 7.42-7.16 (m, 10H, H-2"–H-6", H-2'''–H-6'''), 5.87 (d, *J* = 3.9 Hz, 1H, H-3a), 4.75 (d, *J* = 11.9 Hz, 1H, H-1a"*), 4.64 (d, *J* = 3.9 Hz, 1H, H-6a), 4.47 (d, *J* = 11.9 Hz, 1H, H-1b"*), 4.36 (dd, *J* = 9.7, 3.0 Hz, 1H, H-5), 3.89 (d, *J* = 3.0 Hz, 1H, H-6), 3.67 (dt, *J* = 9.7, 4.6 Hz, 1H, H-3'), 3.48 (s, 3H, H-1'), 2.54 (dd, *J* = 15.2, 9.9 Hz, 1H, H-2'), 2.45 (dd, *J* = 15.2, 4.6 Hz, 1H, H-2'), 1.47 (s, 3H, H-1), 1.29 (s, 3H, H-1).

Assignments denoted by * are interchangeable

6.3.2. Methyl (3*S*)-3-{(3a*R*,5*R*,6*R*,6a*R*)-2,2-dimethyl-6-[(phenylmethyl)oxy]tetrahydrofuro[2,3-*d*][1,3]dioxol-5-yl}-3-(1,3-benzodioxol-5-yl)propanoate 116

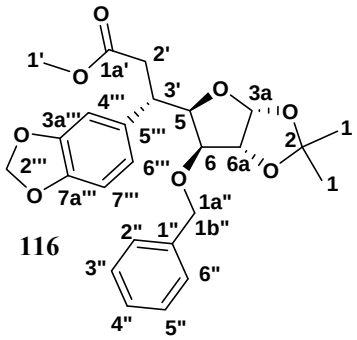

Clear yellow oil (0.10 g, 0.22 mmol, 26%) for the rhodium catalyzed conjugate addition. **R_f:** 0.47, (30% AcOEt/hexane); **$[\alpha]_D$:** –37.5 (*c* 2.0, *CHCl$_3$*, 22 °C); **^{1}H NMR** (300 MHz, *CDCl$_3$*, δ/ppm): 7.38-7.24 (m, 5H, H-2"–H-6"), 6.74-6.67 (m, 3H, H-4''', H-6''', H-7'''), 5.98-5.87 (m, 2H, H-2''', H-3a), 4.53 (d, *J* = 3.8 Hz, 1H, H-6a), 4.44 (d, *J* = 11.3 Hz, 1H, H-1a"*), 4.26 (dd, *J* = 10.4, 2.9 Hz, 1H, H-5), 4.16 (d, *J* = 11.3 Hz, 1H, H-1b"*), 3.60 (dt, *J* = 10.7, 4.2 Hz, 1H, H-3'), 3.52 (s, 3H, H-1'), 3.47 (d, *J* = 2.9 Hz, 1H, H-6), 3.06 (dd, *J* = 15.6, 4.2 Hz, 1H, H-2'), 2.61 (dd, *J* = 15.6, 10.8 Hz, 1H, H-2'), 1.51 (s, 3H, H-1), 1.30 (s, 3H, H-1); **^{13}C NMR** (100 MHz, *CDCl$_3$*, δ/ppm): 172.5 (C-1a'), 147.6 (C-

3a’’’[#]), 146.4 (C-7a’’’[#]), 137.3 (C-5’’’), 134.0 (C-1”), 128.4 (C-2”, C-6”, C-4”), 127.9 (C-3”, C-5”), 121.5 (C-4’’’), 111.5 (C-2), 108.5 (C-6’’’), 108.2 (C-7’’’), 105.0 (C-3a), 100.9 (C-2’’’), 83.4 (C-5), 81.9 (C-6a), 81.6 (C-6), 72.1 (C-1a”/b”), 51.4 (C-1’), 40.5 (C-3’), 38.8 (C-2’), 26.8 (C-1), 26.2 (C-1); **IR** (υ/cm^{-1}): 2988 (w, C-H stretch), 1734 (s, C=O stretch), 1504 (m, C=C stretch) 1440, 1373 (m, C-H bend), 1244 (s, C-C stretch), 1163 (m, C-C stretch), 1071, 1025 (s, C-O stretch); **HRMS (EI):** calculated for $C_{25}H_{28}O_8$ 456.1784 found 456.1762; **M/z (%):** 456.1762 (100), 452.9756 (1), 443.9760 (2), 441.1078 (6), 435.9735 (1), 431.9772 (1).

Assignments denoted by * and [#] are interchangeable

6.3.3. (3a*R*,5*R*,6*R*,6a*R*)-2,2-Dimethyl-5-[(1*R*)-2-nitro-1-phenylethyl]-6-[(phenylmethyl)oxy]tetrahydrofuro[2,3-*d*][1,3]dioxole 117

The major diasteriomer **117** was isolated as white crystals (1.29 g, 3.23 mmol, 55%) for cuprate conjugate addition and (0.210 g, 0.526 mmol, 68%) for the rhodium catalyzed conjugate addition. **R_f: 117:** 0.55, **117b:** 0.44 (30% AcOEt/hexane); **M.p.: 117**: 116 °C; **$[\alpha]_D$: 117** –26.8 (*c* 2.0, *$CHCl_3$*, 22 °C); **IR** (υ/cm^{-1}): 3033 (w, C-H stretch), 1554 (s, N-O stretch), 1383 (m, C-H bend), 1221, 1164 (m, C-C stretch), 1067 (s, C-O stretch); **HRMS (EI):** calculated for $C_{22}H_{25}NO_6$ 399.1682 found 400.9868; **M/z (%):** 400.9868 (100), 399.0050 (28), 397.9859 (8), 393.9712 (10), 391.9734 (2), 390.9791 (14), 388.9664 (4), 386.9540 (8), 385.9596 (15), 384.9556 (26), 382.9743 (16), 379.9894 (4).

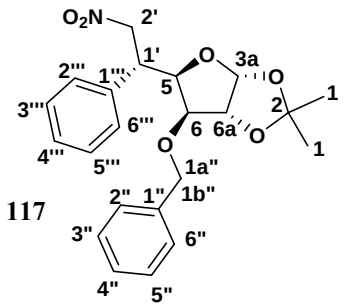

^{1}H NMR (300 MHz, *CDCl$_3$*, δ/ppm) **117**: 7.39-7.19 (m, 10H, H-2"–H-6", H-2'''–H-6'''), 5.95 (d, *J* = 3.7 Hz, 1H, H-3a), 5.00 (dd, *J* = 12.8, 4.4 Hz, 1H, H-2'), 4.72 (dd, *J* = 12.7, 10.8 Hz, 1H, H-2'), 4.54 (d, *J* = 3.8 Hz, 1H, H-6a), 4.44 (d, *J* = 11.5 Hz, 1H, H-1a"*), 4.40 (dd, *J* = 10.1, 3.2 Hz, 1H, H-5), 4.15 (d, *J* = 11.3 Hz, 1H, H-1b"*), 4.03 (dt, *J* = 10.4, 4.4 Hz, 1H, H-1'), 3.53 (d, *J* = 3.00 Hz, 1H, H-6), 1.50 (s, 3H, H-1), 1.30 (s, 3H, H-1); **^{13}C NMR** (100 MHz, *CDCl$_3$*, δ/ppm): 136.9 (C-1'''), 136.5 (C-1'), 128.8 (C-2''', C-6'''), 128.5 (C-2", C-6"), 128.1 (C-4", C-4'''), 128.0 (C-3''', C-5'''), 127.7 (C-3", C-5"), 111.7 (C-2), 105.1 (C-3a), 81.6 (C-6a), 81.5 (C-6), 81.2 (C-5), 78.7 (C-2'), 72.1 (C-1a"/b"), 43.0 (C-1'), 26.7 (C-1), 26.0 (C-1); **X-ray data**: $C_{22}H_{25}NO_6$; *M*=399.43; Orthorhombic; 0.71073 Å; a=8.90410(10) Å, b=10.2774(2) Å, c=22.5111(4) Å, *U*=2060.01(6) Å^3, 173(2) K, space group, $P2_12_12_1$, Z=4; μ(Mo-Kα)=0.094 mm^{-1} 46960 reflections measured. Final R indices [I>2σ(I)] R_1=0.0327, wR(F^2)=0.0846.

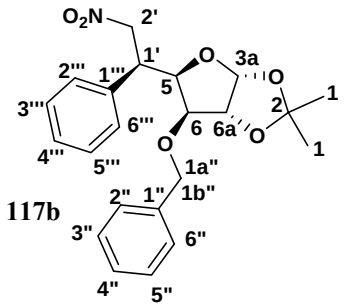

^{1}H NMR (300 MHz, *CDCl$_3$*, δ/ppm) **117b**: 7.45-7.17 (m, 10H, H-2"–H-6", H-2'''–H-6'''), 5.92 (d, *J* = 3.9 Hz, 1H, H-3a), 4.79 (dd, *J* = 13.2, 10.1 Hz, 1H, H-2'), 4.71 (d, *J* = 11.7 Hz, 1H, H-1a"*), 4.64 (dd, *J* = 13.2, 4.1 Hz, 1H, H-2'), 4.63 (d, *J* = 3.9 Hz, 1H, H-6a), 4.45 (d, *J* = 11.7 Hz, 1H, H-1b"*), 4.39 (dd, *J* = 7.7, 3.1 Hz, 1H, H-5), 4.09 (ddd, *J* = 10.0, 7.7, 4.1 Hz, 1H, H-1'), 3.81 (d, *J* = 3.1 Hz, 1H, H-6), 1.47 (s, 3H, H-1), 1.30 (s, 3H, H-1).

Assignments denoted by * are interchangeable

6.3.4. 5-((1*R*)-1-{(3a*R*,5*R*,6*R*,6a*R*)-2,2-Dimethyl-6-[(phenylmethyl)oxy]tetrahydrofuro[2,3-*d*][1,3]dioxol-5-yl}-2-nitroethyl)-1,3-benzodioxole 118

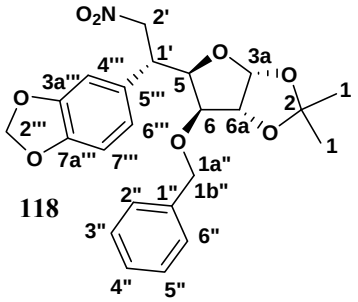

118

Clear yellow oil (0.496 g, 1.12 mmol, 84%) for the rhodium-catalyzed conjugate addition. **R_f:** 0.33, minor:(30% AcOEt/hexane); **$[\alpha]_D$:** –31.5 (*c* 2.0, $CHCl_3$, 22 °C); **^{1}H NMR** (300 MHz, $CDCl_3$, δ/ppm): 7.38-7.23 (m, 5H, H-2”–H-6”), 6.73-6.63 (m, 3H, H-4’’’, H-6’’’, H-7’’’), 5.92 (dd, *J* = 3.1, 1.4 Hz, 2H, H-2’’’), 5.94 (d, *J* = 3.8 Hz, 1H, H-3a), 4.95 (dd, *J* = 12.7, 4.4 Hz, 1H, H-2’), 4.64 (dd, *J* = 12.4, 11.1 Hz, 1H, H-2’), 4.55 (d, *J* = 3.8 Hz, 1H, H-6a), 4.48 (d, *J* = 11.3 Hz, 1H, H-1a”*), 4.32 (dd, *J* = 9.8, 2.9 Hz, 1H, H-5), 4.21 (d, *J* = 11.3 Hz, 1H, H-1b”*), 3.93 (dt, *J* = 10.3, 4.3 Hz, 1H, H-1’), 3.58 (d, *J* = 2.6 Hz, 1H, H-6), 1.49 (s, 3H, H-1), 1.29 (s, 3H, H-1); **^{13}C NMR** (100 MHz, $CDCl_3$, δ/ppm): 147.9 (C-3a’’’$^{\#}$), 147.2 (C-7a’’’$^{\#}$), 136.8 (C-1”), 129.9 (C-5’’’), 128.5 (C-2”, C-6”), 128.1 (C-4”), 127.9 (C-3”, C-5”), 121.6 (C-4’’’), 111.7 (C-2), 108.5 (C-6’’’), 108.2 (C-7’’’), 105.1 (C-2’’’), 101.2 (C-3a), 81.5 (C-6), 81.4 (C-6a), 81.2 (C-5), 78.9 (C-2’), 72.2 (C-1a”/b”), 42.8 (C-1’), 26.7 (C-1), 26.0 (C-1); **IR** (υ/cm^{-1}): 2988 (w, C-H stretch), 1551 (s, N-O stretch) 1490, 1376 (m, C-H bend), 1248 ((m, C-C stretch), 1163 (m, C-C stretch), 1071, 1024 (s, C-O stretch); **HRMS (EI):** calculated for $C_{23}H_{25}O_8N$ 443.1580 found 443.1559; **M/z (%):** 443.1559 (100), 440.9774 (30), 435.9738 (17), 428.9794 (60), 423.9732 (23), 417.9779 (10), 414.9768 (17).

Assignments denoted by * and $^{\#}$ are interchangeable

6.3.5. 6-((1*R*)-1-{(3a*R*,5*R*,6*R*,6a*R*)-2,2-Dimethyl-6-[(phenylmethyl)oxy]tetrahydrofuro[2,3-*d*][1,3]dioxol-5-yl}-2-nitroethyl)-2,3-dihydro-1,4-benzodioxine 119

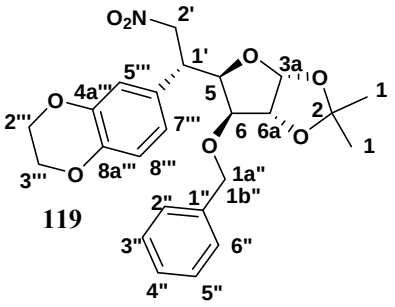

119

Clear oil (0.25 g, 0.55 mmol, 48%) for the rhodium-catalyzed conjugate addition. **Rf:** 0.33 (25% AcOEt/hexane); **$[\alpha]_D$:** –36.5 (*c* 2.0, $CHCl_3$, 22 °C); **^{1}H NMR** (300 MHz, $CDCl_3$, δ/ppm): 7.38-7.22 (m, 5H, H-2”–H-6”), 6.78-6.74 (m, 2H, H-2’’’, H-6’’’), 6.70-6.64 (m, 1H, H-5’’’), 5.93 (d, *J* = 3.7 Hz, 1H, H-3a), 4.93 (dd, *J* = 12.7, 4.4 Hz, 1H, H-2’), 4.65 (dd, *J* = 12.7, 10.9 Hz, 1H, H-2’), 4.55 (d, *J* = 3.8 Hz, 1H, H-6a), 4.46 (d, *J* = 11.2 Hz, 1H, H-1a”*****), 4.32 (dd, *J* = 10.1, 2.9 Hz, 1H, H-5), 4.20 (d, *J* = 11.3 Hz, 1H, H-1b”*****), 4.19 (s, 4H, H-7’’’, H-8’’’), 3.92 (dt, *J* = 10.5, 4.4 Hz, 1H, H-1’), 3.56 (d, *J* = 2.9 Hz, 1H, H-6), 1.49 (s, 3H, H-1), 1.29 (s, 3H, H-1); **^{13}C NMR** (100 MHz, $CDCl_3$, δ/ppm): 143.5 (C-4a’’’$^{\#}$), 143.2 (C-8a’’’$^{\#}$), 136.8 (C-1’’’), 129.4 (C-1”), 128.4 (C-2”, C-6”), 127.9 (C-4”), 127.8 (C-3”, C-5”), 121.2 (C-8’’’), 117.4 (C-5’’’), 116.5 (C-7’’’), 111.6 (C-2), 105.0 (C-3a), 81.4 (C-6), 81.3 (C-6a), 81.1 (C-5), 78.7 (C-2’), 72.0 (C-1a”/b”), 64.1 (C-2’’’, C-3’’’), 42.2 (C-1’), 26.6 (C-1), 25.9 (C-1); **IR** (υ/cm^{-1}): 2934 (w, C-H stretch), 1590 (C=C stretch), 1550 (s, N-O stretch), 1376 (m, C-H bend), 1287 (s, C-C stretch), 1067 (s, C-O stretch); **HRMS (EI):** calculated for $C_{24}H_{27}O_8N$ 457.1737 found 457.1715; **M/z (%):** 457.1715 (100), 452.9779 (7), 447.9720 (7), 441.0068 (6), 431.9767 (8).

Assignments denoted by * and $^{\#}$ are interchangeable

6.3.6. (3a*R*,5*R*,6*R*,6a*R*)-2,2-Dimethyl-5-{(1*R*)-2-nitro-1-[3,4,5-tris(methyloxy)phenyl]ethyl}-6-[(phenylmethyl)oxy]tetrahydrofuro[2,3-*d*][1,3]dioxole 120

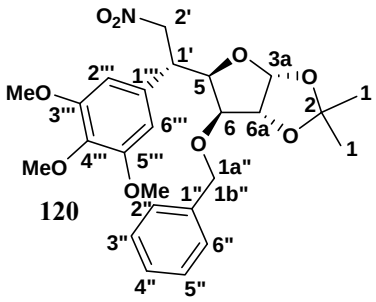

120

White oil (0.20 g, 0.41 mmol, 38%) for the rhodium-catalyzed conjugate addition. **R_f:** 0.47, (25% AcOEt/hexane); **$[\alpha]_D$:** –36.2 (*c* 1.9, $CHCl_3$, 22 °C); **^{1}H NMR** (300 MHz, $CDCl_3$, δ/ppm): 7.44-7.23 (m, 5H, H-2”–H-6”), 6.41 (s, 2H, H-2’’’, H-6’’’), 5.97 (d, *J* = 3.7 Hz, 1H, H-3a), 5.01 (dd, *J* = 12.9, 4.4 Hz, 1H, 2’), 4.72 (dd, *J* = 12.9, 10.7 Hz, 1H, H-2’), 4.58 (d, *J* = 3.9 Hz, 1H, H-6a), 4.58 (d, *J* = 11.6 Hz, 1H, H-1a”*), 4.37 (dd, *J* = 9.5, 2.6 Hz, 1H, H-5), 4.21 (d, *J* = 11.7 Hz, 1H, H-1b”*), 4.00 (dt, *J* = 10.4, 4.4 Hz, 1H, H-1’), 3.82 (s, 3H, OMe at C-4’’’), 3.69 (s, 6H, OMe at C-3’’’, C-5’’’), 3.62 (d, *J* = 2.6 Hz, 1H, H-6), 1.51 (s, 3H, H-1), 1.32 (s, 1H, H-1); **^{13}C NMR** (100 MHz, $CDCl_3$, δ/ppm): 153.4 (C-3’’’, C-5’’’), 137.7 (C-4’’’), 137.1 (C-1’’’), 132.2 (C-1”), 128.5 (C-2”, C-6”), 127.9 (C-4”), 126.9 (C-3”, C-5”), 111.7 (C-2), 105.2 (C-2’’’, C-6’’’), 105.1 (C-3a), 81.9 (C-6), 81.5 (C-6a), 81.2 (C-5), 78.7 (C-2’), 71.9 (C-1a”/b”), 60.8 (OMe at C-4’’’), 56.1 (OMe at C-3’’’, C-5’’’), 43.4 (C-1’), 26.7 (C-1), 26.0 (C-1); **IR** (υ/cm^{-1}): 2930 (w, C-H stretch), 1591 (s, N-O stretch), 1350 (m, C-H bend), 1243 (s, C-C stretch), 1164 (m, C-C stretch), 1072, 994 (s, C-O stretch); **HRMS (EI):** calculated for $C_{23}H_{25}O_8N$ 489.1998 found 489.1985; **M/z (%):** 489.1985 (100), 485.9654 (1), 478.9718 (4), 474.1570 (6), 472.0605 (1), 467.9872 (1).

Assignments denoted by * are interchangeable

6.4. Experimental work pertaining to chapter 4

6.4.1. (2*S*,3*R*,4*R*,5*R*)-4-(Benzyloxy)-2-methoxy-5-((*R*)-2-nitro-1-phenylethyl)-tetrahydrofuran-3-ol 125

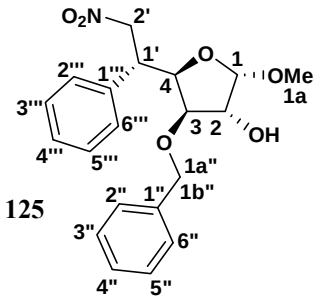

To a stirring mixture of compound **117** (0.49 g, 1.22 mmol, 1 equiv.) in MeOH (15 cm^3) was added Dowex H^+ resin (1.51 g, 3 × mass of starting material). Allowed reaction mixture to stir at room temperature under an atmosphere of nitrogen for 72 hours. Monitored reaction by TLC. Filtered off the resin with methanol and evaporated solvent. Prepared a column using neutral alumina with 30% AcOEt/hexane. Afforded a pale yellow oil (0.23 g, 0.62 mmol, 80%).

R_f: 0.25, (30% AcOEt/hexane); **^{1}H NMR** (300 MHz, *$CDCl_3$*, δ/ppm): 7.58-6.84 (m, 10H, H-2”–H-6”, H-2”’–H-6”’), 5.04 (d, *J* = 4.4 Hz, 1H, H-1), 4.91 (dd, *J* = 12.7, 5.1 Hz, 1H, H-2’), 4.61 (dd, *J* = 12.7, 9.8 Hz, 1H, H-2’), 4.41 (d, *J* = 11.7 Hz, 1H, H-1a”*), 4.36 (d, *J* = 4.0 Hz, 1H, H-2), 4.12 (d, *J* = 11.5 Hz, 1H, H-1b”*), 4.16-4.09 (m, 1H, H-4), 3.48 (dd, *J* = 4.0, 1.4 Hz, 1H, H-3), 3.44 (s, 3H, H-1a), 2.78 (d, *J* = 3.9 Hz, 1H, OH at C-2); **^{13}C NMR** (100 MHz, *$CDCl_3$*, δ/ppm): 137.2 (C-1’’’), 136.8 (C-1”), 128.7 (C-2’’’,C-6’’’), 128.3 (C-2”, C-6”), 128.1 (C-3’’’, C-5’’’), 127.8 (C-4’’’), 127.8 (C-4”), 127.7 (C-3”, C-5”), 102.5 (C-1), 83.4 (C-3), 80.1 (C-2), 78.8 (C-2’), 75.3 (C-4) , 71.8 (C-1a”/b”), 56.1 (C-1a), 43.4 (C-1’).

Assignments denoted by * are interchangeable

APPENDIX

X-Ray crystallographical data for (1*R*)-2-nitro-1-phenylethyl]-tetrahydrofuro-dioxole 117

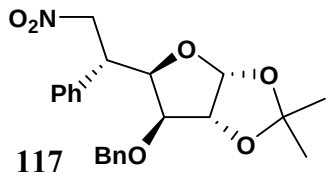

117

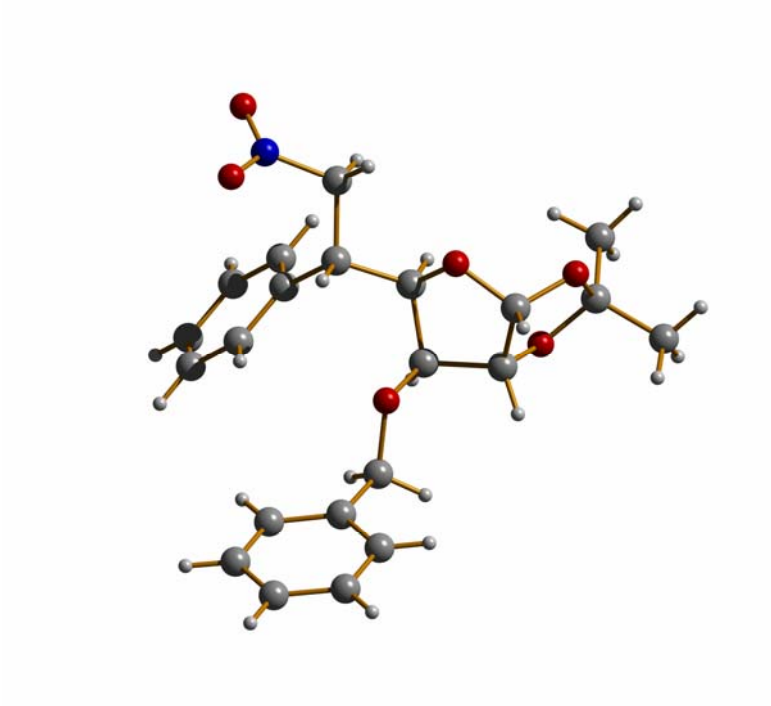

Table 1. Crystal data and structure refinement for 117.

Identification code	**117**
Empirical formula	C22 H25 N O6
Formula weight	399.43
Temperature	173(2) K
Wavelength	0.71073 Å
Crystal system	Orthorhombic
Space group	$P2_12_12_1$

Unit cell dimensions	a = 8.90410(10) Å	α= 90°.
	b = 10.2774(2) Å	β= 90°.
	c = 22.5111(4) Å	γ = 90°.
Volume	2060.01(6) $Å^3$	
Z	4	
Density (calculated)	1.288 Mg/m^3	
Absorption coefficient	0.094 mm^{-1}	
F(000)	848	
Crystal size	0.45 x 0.39 x 0.14 mm^3	
Theta range for data collection	1.81 to 28.00°.	
Index ranges	-11<=h<=11, -13<=k<=13, -29<=l<=29	
Reflections collected	46960	
Independent reflections	2824 [R(int) = 0.0367]	
Completeness to theta = 28.00°	100.0 %	
Absorption correction	None	
Refinement method	Full-matrix least-squares on F^2	
Data / restraints / parameters	2824 / 0 / 264	
Goodness-of-fit on F^2	1.062	
Final R indices [I>2sigma(I)]	R1 = 0.0327, wR2 = 0.0846	
R indices (all data)	R1 = 0.0378, wR2 = 0.0876	
Absolute structure parameter	-10(10)	
Largest diff. peak and hole	0.199 and -0.165 $e.Å^{-3}$	

Table 2. Atomic coordinates (x 10^4) and equivalent isotropic displacement parameters ($Å^2$x 10^3) for 117. U(eq) is defined as one third of the trace of the orthogonalized U^{ij} tensor.

	x	y	z	U(eq)
C(1)	3425(2)	1309(2)	-124(1)	33(1)
C(2)	4638(2)	1226(2)	355(1)	31(1)
C(3)	3775(2)	1348(2)	935(1)	29(1)
C(4)	2296(2)	700(2)	765(1)	28(1)
C(5)	4922(2)	-480(2)	-303(1)	38(1)
C(6)	4384(5)	-1863(2)	-289(1)	87(1)
C(7)	6302(3)	-283(3)	-677(1)	65(1)
C(8)	4757(2)	3207(2)	1409(1)	55(1)
C(9)	4523(2)	4630(2)	1527(1)	38(1)
C(10)	3814(3)	5035(2)	2038(1)	47(1)
C(11)	3665(3)	6346(2)	2160(1)	57(1)
C(12)	4243(3)	7257(2)	1778(1)	55(1)
C(13)	4958(2)	6871(2)	1270(1)	51(1)
C(14)	5093(2)	5563(2)	1140(1)	45(1)
C(15)	913(2)	1051(2)	1130(1)	28(1)
C(16)	-408(2)	281(2)	875(1)	34(1)
C(17)	1162(2)	779(2)	1787(1)	30(1)
C(18)	1202(2)	-470(2)	2012(1)	41(1)
C(19)	1442(2)	-680(2)	2616(1)	52(1)
C(20)	1644(2)	358(3)	2991(1)	56(1)
C(21)	1612(3)	1598(3)	2772(1)	58(1)
C(22)	1372(2)	1820(2)	2172(1)	43(1)
N(1)	-1796(2)	491(2)	1232(1)	37(1)
O(1)	2029(1)	1103(1)	161(1)	32(1)
O(2)	3758(2)	327(2)	-524(1)	56(1)
O(3)	5197(1)	-66(1)	293(1)	35(1)
O(4)	3531(1)	2683(1)	1068(1)	33(1)
O(5)	-2470(2)	-454(2)	1419(1)	61(1)
O(6)	-2179(2)	1614(2)	1319(1)	55(1)

Table 3. Bond lengths [Å] and angles [°] for 117.

C(1)-O(2)	1.384(2)
C(1)-O(1)	1.415(2)
C(1)-C(2)	1.529(2)
C(1)-H(1)	1.0000
C(2)-O(3)	1.426(2)
C(2)-C(3)	1.521(2)
C(2)-H(2)	1.0000
C(3)-O(4)	1.421(2)
C(3)-C(4)	1.526(2)
C(3)-H(3)	1.0000
C(4)-O(1)	1.4413(19)
C(4)-C(15)	1.524(2)
C(4)-H(4)	1.0000
C(5)-O(2)	1.417(2)
C(5)-O(3)	1.427(2)
C(5)-C(6)	1.500(3)
C(5)-C(7)	1.504(3)
C(6)-H(6A)	0.9800
C(6)-H(6B)	0.9800
C(6)-H(6C)	0.9800
C(7)-H(7A)	0.9800
C(7)-H(7B)	0.9800
C(7)-H(7C)	0.9800
C(8)-O(4)	1.439(2)
C(8)-C(9)	1.501(3)
C(8)-H(8A)	0.9900
C(8)-H(8B)	0.9900
C(9)-C(10)	1.377(3)
C(9)-C(14)	1.391(3)
C(10)-C(11)	1.382(3)
C(10)-H(10)	0.9500
C(11)-C(12)	1.371(3)
C(11)-H(11)	0.9500
C(12)-C(13)	1.368(3)

C(12)-H(12)	0.9500
C(13)-C(14)	1.380(3)
C(13)-H(13)	0.9500
C(14)-H(14)	0.9500
C(15)-C(17)	1.521(2)
C(15)-C(16)	1.529(2)
C(15)-H(15)	1.0000
C(16)-N(1)	1.489(2)
C(16)-H(16A)	0.9900
C(16)-H(16B)	0.9900
C(17)-C(18)	1.380(3)
C(17)-C(22)	1.390(2)
C(18)-C(19)	1.392(3)
C(18)-H(18)	0.9500
C(19)-C(20)	1.372(3)
C(19)-H(19)	0.9500
C(20)-C(21)	1.367(4)
C(20)-H(20)	0.9500
C(21)-C(22)	1.386(3)
C(21)-H(21)	0.9500
C(22)-H(22)	0.9500
N(1)-O(5)	1.217(2)
N(1)-O(6)	1.219(2)

O(2)-C(1)-O(1)	111.93(15)
O(2)-C(1)-C(2)	105.46(14)
O(1)-C(1)-C(2)	106.97(12)
O(2)-C(1)-H(1)	110.8
O(1)-C(1)-H(1)	110.8
C(2)-C(1)-H(1)	110.8
O(3)-C(2)-C(3)	109.72(13)
O(3)-C(2)-C(1)	103.27(13)
C(3)-C(2)-C(1)	104.21(13)
O(3)-C(2)-H(2)	113.0
C(3)-C(2)-H(2)	113.0
C(1)-C(2)-H(2)	113.0

O(4)-C(3)-C(2)	109.75(14)
O(4)-C(3)-C(4)	110.01(13)
C(2)-C(3)-C(4)	100.57(12)
O(4)-C(3)-H(3)	112.0
C(2)-C(3)-H(3)	112.0
C(4)-C(3)-H(3)	112.0
O(1)-C(4)-C(15)	107.95(12)
O(1)-C(4)-C(3)	104.73(13)
C(15)-C(4)-C(3)	117.29(13)
O(1)-C(4)-H(4)	108.9
C(15)-C(4)-H(4)	108.9
C(3)-C(4)-H(4)	108.9
O(2)-C(5)-O(3)	106.35(13)
O(2)-C(5)-C(6)	109.1(2)
O(3)-C(5)-C(6)	108.54(17)
O(2)-C(5)-C(7)	108.80(17)
O(3)-C(5)-C(7)	110.23(18)
C(6)-C(5)-C(7)	113.5(2)
C(5)-C(6)-H(6A)	109.5
C(5)-C(6)-H(6B)	109.5
H(6A)-C(6)-H(6B)	109.5
C(5)-C(6)-H(6C)	109.5
H(6A)-C(6)-H(6C)	109.5
H(6B)-C(6)-H(6C)	109.5
C(5)-C(7)-H(7A)	109.5
C(5)-C(7)-H(7B)	109.5
H(7A)-C(7)-H(7B)	109.5
C(5)-C(7)-H(7C)	109.5
H(7A)-C(7)-H(7C)	109.5
H(7B)-C(7)-H(7C)	109.5
O(4)-C(8)-C(9)	110.67(15)
O(4)-C(8)-H(8A)	109.5
C(9)-C(8)-H(8A)	109.5
O(4)-C(8)-H(8B)	109.5
C(9)-C(8)-H(8B)	109.5
H(8A)-C(8)-H(8B)	108.1

C(10)-C(9)-C(14)	118.79(19)
C(10)-C(9)-C(8)	120.4(2)
C(14)-C(9)-C(8)	120.7(2)
C(9)-C(10)-C(11)	120.3(2)
C(9)-C(10)-H(10)	119.8
C(11)-C(10)-H(10)	119.8
C(12)-C(11)-C(10)	120.4(2)
C(12)-C(11)-H(11)	119.8
C(10)-C(11)-H(11)	119.8
C(13)-C(12)-C(11)	120.0(2)
C(13)-C(12)-H(12)	120.0
C(11)-C(12)-H(12)	120.0
C(12)-C(13)-C(14)	120.0(2)
C(12)-C(13)-H(13)	120.0
C(14)-C(13)-H(13)	120.0
C(13)-C(14)-C(9)	120.46(19)
C(13)-C(14)-H(14)	119.8
C(9)-C(14)-H(14)	119.8
C(17)-C(15)-C(4)	111.33(13)
C(17)-C(15)-C(16)	112.45(14)
C(4)-C(15)-C(16)	107.23(12)
C(17)-C(15)-H(15)	108.6
C(4)-C(15)-H(15)	108.6
C(16)-C(15)-H(15)	108.6
N(1)-C(16)-C(15)	111.12(13)
N(1)-C(16)-H(16A)	109.4
C(15)-C(16)-H(16A)	109.4
N(1)-C(16)-H(16B)	109.4
C(15)-C(16)-H(16B)	109.4
H(16A)-C(16)-H(16B)	108.0
C(18)-C(17)-C(22)	118.89(16)
C(18)-C(17)-C(15)	122.14(15)
C(22)-C(17)-C(15)	118.96(16)
C(17)-C(18)-C(19)	120.43(19)
C(17)-C(18)-H(18)	119.8
C(19)-C(18)-H(18)	119.8

C(20)-C(19)-C(18)	120.0(2)
C(20)-C(19)-H(19)	120.0
C(18)-C(19)-H(19)	120.0
C(21)-C(20)-C(19)	119.97(18)
C(21)-C(20)-H(20)	120.0
C(19)-C(20)-H(20)	120.0
C(20)-C(21)-C(22)	120.6(2)
C(20)-C(21)-H(21)	119.7
C(22)-C(21)-H(21)	119.7
C(21)-C(22)-C(17)	120.1(2)
C(21)-C(22)-H(22)	120.0
C(17)-C(22)-H(22)	120.0
O(5)-N(1)-O(6)	124.21(17)
O(5)-N(1)-C(16)	118.66(17)
O(6)-N(1)-C(16)	117.13(15)
C(1)-O(1)-C(4)	109.05(12)
C(1)-O(2)-C(5)	110.78(13)
C(2)-O(3)-C(5)	108.04(13)
C(3)-O(4)-C(8)	110.91(13)

Symmetry transformations used to generate equivalent atoms:

Table 4. Anisotropic displacement parameters ($Å^2 x 10^3$)for 117. The anisotropic displacement factor exponent takes the form: $-2\pi^2[h^2 a^{*2} U^{11} + ... + 2 h k a^* b^* U^{12}]$

	U^{11}	U^{22}	U^{33}	U^{23}	U^{13}	U^{12}
C(1)	30(1)	39(1)	28(1)	6(1)	4(1)	4(1)
C(2)	26(1)	31(1)	35(1)	-1(1)	2(1)	2(1)
C(3)	27(1)	32(1)	27(1)	-2(1)	-2(1)	6(1)
C(4)	28(1)	32(1)	24(1)	-3(1)	1(1)	3(1)
C(5)	42(1)	41(1)	30(1)	-3(1)	10(1)	5(1)
C(6)	156(3)	52(1)	54(1)	-12(1)	4(2)	-31(2)
C(7)	44(1)	102(2)	50(1)	3(1)	19(1)	16(1)
C(8)	41(1)	48(1)	75(1)	-23(1)	-30(1)	12(1)
C(9)	27(1)	42(1)	44(1)	-14(1)	-13(1)	3(1)
C(10)	48(1)	51(1)	41(1)	-6(1)	0(1)	-8(1)
C(11)	58(1)	63(1)	49(1)	-25(1)	6(1)	2(1)
C(12)	51(1)	45(1)	68(1)	-18(1)	-13(1)	2(1)
C(13)	42(1)	55(1)	56(1)	4(1)	-10(1)	-11(1)
C(14)	30(1)	67(1)	37(1)	-10(1)	-3(1)	-2(1)
C(15)	26(1)	29(1)	28(1)	-2(1)	2(1)	3(1)
C(16)	28(1)	41(1)	34(1)	-5(1)	1(1)	2(1)
C(17)	23(1)	40(1)	27(1)	-3(1)	4(1)	3(1)
C(18)	42(1)	44(1)	38(1)	3(1)	1(1)	7(1)
C(19)	42(1)	67(1)	46(1)	20(1)	2(1)	11(1)
C(20)	39(1)	99(2)	28(1)	5(1)	1(1)	8(1)
C(21)	60(1)	79(2)	34(1)	-17(1)	0(1)	-2(1)
C(22)	47(1)	48(1)	34(1)	-8(1)	4(1)	1(1)
N(1)	27(1)	50(1)	35(1)	8(1)	-1(1)	3(1)
O(1)	26(1)	47(1)	24(1)	-1(1)	-1(1)	2(1)
O(2)	46(1)	89(1)	33(1)	-21(1)	-6(1)	25(1)
O(3)	36(1)	38(1)	32(1)	-4(1)	1(1)	12(1)
O(4)	27(1)	34(1)	37(1)	-9(1)	-7(1)	5(1)
O(5)	46(1)	70(1)	65(1)	22(1)	5(1)	-14(1)
O(6)	44(1)	60(1)	60(1)	10(1)	15(1)	21(1)

Table 5. Hydrogen coordinates (x 10^4) and isotropic displacement parameters ($Å^2$x 10^3) for 117.

	x	y	z	U(eq)
H(1)	3446	2178	-324	39
H(2)	5436	1903	309	37
H(3)	4288	883	1269	35
H(4)	2433	-266	773	33
H(6A)	3492	-1926	-36	131
H(6B)	5179	-2423	-130	131
H(6C)	4131	-2143	-693	131
H(7A)	6085	-530	-1088	98
H(7B)	7120	-826	-523	98
H(7C)	6602	634	-663	98
H(8A)	5709	3081	1189	65
H(8B)	4836	2735	1791	65
H(10)	3425	4410	2308	56
H(11)	3158	6618	2510	68
H(12)	4147	8157	1867	66
H(13)	5362	7502	1006	61
H(14)	5579	5299	784	54
H(15)	705	2000	1079	33
H(16A)	-589	556	460	41
H(16B)	-157	-657	872	41
H(18)	1066	-1191	1754	50
H(19)	1464	-1542	2768	62
H(20)	1807	215	3403	67
H(21)	1756	2314	3033	69
H(22)	1352	2685	2024	52

Table 6. Torsion angles [°] for 117.

O(2)-C(1)-C(2)-O(3)	-20.37(17)
O(1)-C(1)-C(2)-O(3)	98.95(15)
O(2)-C(1)-C(2)-C(3)	-135.03(15)
O(1)-C(1)-C(2)-C(3)	-15.72(17)
O(3)-C(2)-C(3)-O(4)	166.07(13)
C(1)-C(2)-C(3)-O(4)	-83.92(16)
O(3)-C(2)-C(3)-C(4)	-78.03(15)
C(1)-C(2)-C(3)-C(4)	31.99(16)
O(4)-C(3)-C(4)-O(1)	77.85(15)
C(2)-C(3)-C(4)-O(1)	-37.86(15)
O(4)-C(3)-C(4)-C(15)	-41.77(19)
C(2)-C(3)-C(4)-C(15)	-157.48(14)
O(4)-C(8)-C(9)-C(10)	92.3(2)
O(4)-C(8)-C(9)-C(14)	-91.5(2)
C(14)-C(9)-C(10)-C(11)	0.5(3)
C(8)-C(9)-C(10)-C(11)	176.8(2)
C(9)-C(10)-C(11)-C(12)	-1.1(4)
C(10)-C(11)-C(12)-C(13)	0.7(4)
C(11)-C(12)-C(13)-C(14)	0.2(3)
C(12)-C(13)-C(14)-C(9)	-0.8(3)
C(10)-C(9)-C(14)-C(13)	0.5(3)
C(8)-C(9)-C(14)-C(13)	-175.82(18)
O(1)-C(4)-C(15)-C(17)	-174.41(13)
C(3)-C(4)-C(15)-C(17)	-56.51(19)
O(1)-C(4)-C(15)-C(16)	62.20(17)
C(3)-C(4)-C(15)-C(16)	-179.90(14)
C(17)-C(15)-C(16)-N(1)	53.37(19)
C(4)-C(15)-C(16)-N(1)	176.06(13)
C(4)-C(15)-C(17)-C(18)	-72.6(2)
C(16)-C(15)-C(17)-C(18)	47.8(2)
C(4)-C(15)-C(17)-C(22)	106.65(18)
C(16)-C(15)-C(17)-C(22)	-133.00(17)
C(22)-C(17)-C(18)-C(19)	0.4(3)
C(15)-C(17)-C(18)-C(19)	179.61(17)

C(17)-C(18)-C(19)-C(20)	-0.2(3)
C(18)-C(19)-C(20)-C(21)	-0.1(3)
C(19)-C(20)-C(21)-C(22)	0.2(4)
C(20)-C(21)-C(22)-C(17)	0.0(4)
C(18)-C(17)-C(22)-C(21)	-0.3(3)
C(15)-C(17)-C(22)-C(21)	-179.51(19)
C(15)-C(16)-N(1)-O(5)	-126.75(18)
C(15)-C(16)-N(1)-O(6)	53.1(2)
O(2)-C(1)-O(1)-C(4)	106.30(15)
C(2)-C(1)-O(1)-C(4)	-8.74(18)
C(15)-C(4)-O(1)-C(1)	155.55(14)
C(3)-C(4)-O(1)-C(1)	29.85(17)
O(1)-C(1)-O(2)-C(5)	-107.63(17)
C(2)-C(1)-O(2)-C(5)	8.3(2)
O(3)-C(5)-O(2)-C(1)	7.1(2)
C(6)-C(5)-O(2)-C(1)	123.97(19)
C(7)-C(5)-O(2)-C(1)	-111.7(2)
C(3)-C(2)-O(3)-C(5)	135.69(14)
C(1)-C(2)-O(3)-C(5)	25.05(16)
O(2)-C(5)-O(3)-C(2)	-20.80(18)
C(6)-C(5)-O(3)-C(2)	-138.1(2)
C(7)-C(5)-O(3)-C(2)	96.97(19)
C(2)-C(3)-O(4)-C(8)	-89.05(18)
C(4)-C(3)-O(4)-C(8)	161.19(16)
C(9)-C(8)-O(4)-C(3)	177.68(17)

Symmetry transformations used to generate equivalent atoms:

REFERENCES

1. A. Padwa and H. J. Zhang, *J. Org. Chem.*, 2007, **72**, 2570-2582.
2. T. Hudlicky, X. R. Tian, K. Konigsberger, R. Maurya, J. Rouden and B. Fan, *J. Am. Chem. Soc.*, 1996, **118**, 10752-10765.
3. T. Hudlicky, U. Rinner, D. Gonzalez, H. Akgun, S. Schilling, P. Siengalewicz, T. A. Martinot and G. R. Pettit, *J. Org. Chem.*, 2002, **67**, 8726-8743.
4. M. Manpadi and A. Kornienko, *Tetrahedron Lett.*, 2005, **46**, 4433-4437.
5. J. McNulty, J. J. Nair, C. Codina, J. Bastida, S. Pandey, J. Gerasimoff and C. Griffin, *Phytochemistry*, 2007, **68**, 1068-1074.
6. M. Matveenko, O. J. Kokas, M. G. Banwell and A. C. Willis, *Org. Lett.*, 2007, **9**, 3683-3685.
7. K. Afarinkia and A. Ndibwami, *Synlett*, 2007, 1940-1944.
8. A. Kazi, R. Hill, T. E. Long, D. J. Kuhn, E. Turos and Q. P. Dou, *Biochem. Pharmacol.*, 2004, **67**, 365-374.
9. N. Kekre, C. Griffin, J. McNulty and S. Pandey, *Cancer Chemother. Pharmacol.*, 2005, **56**, 29-38.
10. A. McLachlan, N. Kekre, J. McNulty and S. Pandey, *Apoptosis*, 2005, **10**, 619-630.
11. H. Yuan, M. Mutomba, I. Prinz and R. A. Gottlieb, *Mitochondrion*, 2001, **1**, 61-69.
12. T. Hudlicky and J. W. Reed, *The Way of Synthesis*, Wiley-VCH, Weinheim, 2007.
13. M. Matveenko, M. G. Banwell and A. C. Willis, *Tetrahedron*, 2008, **64**, 4817-4826.
14. G. R. Pettit, V. Gaddamidi, G. M. Cragg, D. L. Herald and Y. Sagawa, *J. Chem. Soc., Chem. Commun.*, 1984, 1693-1694.
15. A. E. Hakansson, A. Palmelund, H. Holm and R. Madsen, *Chem. Eur.J.*, 2006, **12**, 3243-3253.
16. M. Manpadi and A. Kornienko, *Org. Prep. Proced. Int.*, 2008, **40**, 109-161.
17. S. K. Rastogi and A. Kornienko, *Tetrahedron: Asymmetry*, 2006, **17**, 3170-3178.
18. S. Kim, H. Ko, E. Kim and D. Kim, *Org. Lett.*, 2002, **4**, 1343-1345.

19. S. Danishefsky and J. Y. Lee, *J. Am. Chem. Soc.*, 1989, **111**, 4829-4837.
20. M. Li, A. M. Wu and P. J. Zhou, *Tetrahedron Lett.*, 2006, **47**, 3707-3710.
21. G. R. Pettit, N. Melody and D. L. Herald, *J. Org. Chem.*, 2001, **66**, 2583-2587.
22. J. Collins, M. Drouin, X. T. Sun, U. Rinner and T. Hudlicky, *Org. Lett.*, 2008, **10**, 361-364.
23. T. Hudlicky, *ARKIVOC*, 2006, **vii**, 276-291.
24. T. Hudlicky, U. Rinner, K. J. Finn and I. Ghiviriga, *J. Org. Chem.*, 2005, **70**, 3490-3499.
25. J. McNulty, V. Larichev and S. Pandey, *Bioorg. Med. Chem. Lett.*, 2005, **15**, 5315-5318.
26. J. McNulty, J. J. Nair, C. Griffin and S. Pandey, *J. Nat. Prod.*, 2008, **71**, 357-363.
27. M. Moser, X. T. Sun and T. Hudlicky, *Org. Lett.*, 2005, **7**, 5669-5672.
28. U. Rinner, H. L. Hillebrenner, D. R. Adams, T. Hudlicky and G. R. Pettit, *Bioorg. Med. Chem. Lett.*, 2004, **14**, 2911-2915.
29. T. Hudlicky, M. Moser, S. C. Banfield, U. Rinner, J. C. Chapuis and G. R. Pettit, *Can. J. Chem.*, 2006, **84**, 1313-1337.
30. A. S. Kireev, O. N. Nadein, V. J. Agustin, N. E. Bush, A. Evidente, M. Manpadi, M. A. Ogasawara, S. K. Rastogi, S. Rogelj, S. T. Shors and A. Kornienko, *J. Org. Chem.*, 2006, **71**, 5694-5707.
31. S. Pandey, B. Smith, P. R. Walker and M. Sikorska, *Apoptosis*, 2000, **5**, 265-275.
32. G. B. Corcoran, L. Fix, D. P. Jones, M. T. Moslen, P. Nicotera, F. A. Oberhammer and R. Buttyan, *Toxicol. Appl. Pharmacol.*, 1994, **128**, 169-181.
33. U. Rinner, P. Siengalewicz and T. Hudlicky, *Org. Lett.*, 2002, **4**, 115-117.
34. M. Ouarzane-Amara, J. F. Franetich, G. R. Pettit, L. Meijer, C. Doerig and I. Desportes-Livage, *Antimicrob. Agents Chemother.*, 2001, **45**, 3409-3415.
35. J. C. Mottram, *Parasitology Today*, 1994, **10**, 253-257.
36. X. R. Tian, T. Hudlicky and K. Konigsberger, *J. Am. Chem. Soc.*, 1995, **117**, 3643-3644.
37. H. Paulsen and M. Stubbe, *Tetrahedron Lett.*, 1982, **23**, 3171-3174.
38. H. Paulsen and M. Stubbe, *Liebigs Ann. Chem.*, 1983, 535-556.
39. B. M. Trost and S. R. Pulley, *J. Am. Chem. Soc.*, 1995, **117**, 10143-10144.

40. T. J. Doyle, M. Hendrix, D. VanDerveer, S. Javanmard and J. Haseltine, *Tetrahedron*, 1997, **53**, 11153-11170.
41. P. Magnus, J. M. Bailey and M. J. Porter, *Tetrahedron*, 1999, **55**, 13927-13936.
42. P. Magnus and I. K. Sebhat, *J. Am. Chem. Soc.*, 1998, **120**, 5341-5342.
43. J. H. Rigby, U. S. M. Maharoof and M. E. Mateo, *J. Am. Chem. Soc.*, 2000, **122**, 6624-6628.
44. H. J. Ko, E. Kim, J. E. Park, D. Kim and S. Kim, *J. Org. Chem.*, 2004, **69**, 112-121.
45. M. Bols, *Carbohydrate Building Blocks*, John Wiley & Sons, Inc., New York, 1996.
46. J. Clayden, N. Greeves, S. Warren and P. Wothers, *Organic Chemistry*, Oxford University Press, Oxford, 2001.
47. H. M. I. Osborn, *Carbohydrates*, Elsevier Science Ltd, Kidlington, 2003.
48. J. McMurry, *Organic Chemistry*, 3rd edn., Brooks/Cole Publishing Company, California, 1992.
49. B. Christenson, G. Hallnemo and C. Ullenius, *Tetrahedron*, 1991, **47**, 4739-4752.
50. S. Woodward, *Chem. Soc. Rev.*, 2000, **29**, 393-401.
51. M. Muller, A. Schoenfelder, B. Didier, A. Mann and C. G. Wermuth, *Chem. Commun.*, 1999, 683-684.
52. A. S. Vellekoop and R. A. J. Smith, *Tetrahedron*, 1998, **54**, 11971-11994.
53. S. H. Bertz, S. Cope, M. Murphy, C. A. Ogle and B. J. Taylor, *J. Am. Chem. Soc.*, 2007, **129**, 7208-7209.
54. H. P. Hu and J. P. Snyder, *J. Am. Chem. Soc.*, 2007, **129**, 7210-7211.
55. A. S. Vellekoop and R. A. J. Smith, *J. Am. Chem. Soc.*, 1994, **116**, 2902-2913.
56. A. Segura and A. G. Csaky, *Org. Lett.*, 2007, **9**, 3667-3670.
57. E. A. Davidson, *Carbohydrate Chemistry*, Holt, Rinehart and Winston, Inc., New York, 1967.
58. C. J. F. Bichard, J. R. Wheatley and G. W. J. Fleet, *Tetrahedron: Asymmetry*, 1994, **5**, 431-440.
59. S. M. Roberts and K. A. Shoberu, *J. Chem. Soc., Perkin Trans. 1*, 1992, 2625-2632.

60. J. Frigell and I. Cumpstey, *Tetrahedron Lett.*, 2007, **48**, 9073-9076.
61. A. H. Ingall, P. R. Moore and S. M. Roberts, *Tetrahedron: Asymmetry*, 1994, **5**, 2155-2162.
62. C. Chakraborty and D. D. Dhavale, *Carbohydr. Res.*, 2006, **341**, 912-917.
63. C. Willis, Willis, M., *Organic Synthesis*, Oxford University Press, Oxford, 1995.
64. M. Funabashi, Kobayashi, K., Yoshimura, J., *J. Org. Chem.*, 1979, **44**, 1618-1621.
65. T. Hanaya, H. Yamamoto and H. Yamamoto, *Bull. Chem. Soc. Jpn.*, 1992, **65**, 1154-1156.
66. J. Kovar, Baer, H.H., *Carbohydr. Res.*, 1975, **39**, 19-32.
67. M. Funabashi, Yoshimura, J., *J. Chem. Soc., Perkin Trans. 1*, 1979, 1425-1429.
68. S. Torii, T. Inokuchi, R. Oi, K. Kondo and T. Kobayashi, *J. Org. Chem.*, 1986, **51**, 254-256.
69. A. S. Kireev, M. Manpadi and A. Kornienko, *J. Org. Chem.*, 2006, **71**, 2630-2640.
70. S. Hanessian, E. Demont and W. A. L. van Otterlo, *Tetrahedron Lett.*, 2000, **41**, 4999-5003.
71. S. Hanessian, W. A. L. van Otterlo, I. Nilsson and U. Bauer, *Tetrahedron Lett.*, 2002, **43**, 1995-1998.
72. M. Sakai, H. Hayashi and N. Miyaura, *Organometallics*, 1997, **16**, 4229-4231.
73. H. Hayashi and K. Yamasaki, *Chem. Rev.*, 2003, **103**, 2829-2844.
74. H. Freibolin, *Basic One- and Two-Dimensional NMR Spectroscopy*, 2nd edn., VCH Publishers, Weinheim, 1993.
75. *Spectral Database of Organic Compounds (SBDS),* National Institute for Advanced Industrial Science and Technology. http://riodb.ibase.aist.go.jp.
76. M. P. Maguire, P. L. Feldman and H. Rapoport, *J. Org. Chem.*, 1990, **55**, 948-955.
77. H. S. Elkhadem and J. Kawai, *Carbohydr. Res.*, 1983, **115**, 131-138.
78. Y. Leblanc, B. J. Fitzsimmons, J. Adams, F. Perez and J. Rokach, *J. Org. Chem.*, 1986, **51**, 789-793.
79. T. J. Tewson and M. J. Welch, *J. Org. Chem.*, 1978, **43**, 1090-1092.

80. M. L. Lewbart and J. J. Schneider, *J. Org. Chem.*, 1969, **34**, 3505-3512.

81. M. G. Banwell, B. D. Bissett, S. Busato, C. J. Cowden, D. C. R. Hockless, J. W. Holman, R. W. Read and A. W. Wu, *J. Chem. Soc., Chem. Commun.*, 1995, 2551-2553.

82. Y. S. Cho and C. G. Cho, *Tetrahedron*, 2008, **64**, 2172-2177.

83. R. S. Coleman and S. R. Gurrala, *Org. Lett.*, 2005, **7**, 1849-1852.

84. Bruker, *APEX2. Version 2.0-1*, Madison, Wisconsin, USA, 2005.

85. Bruker, *SAINT+. Version 6.0. (includes XPREP and SADABS)*, Madison, Wisconsin, USA, 2005.

86. Bruker, *SHELXTL. Version 5.1. (includes XS, XL, XP, XSHELL)*, Madison, Wisconsin, USA, 1999.

87. A. L. Spek, *J. Appl. Crystallogr.* 2003, **36**, 7-13.

88. L. J. Farrugia, *J. Appl. Crystallogr.*, 1997, **30**, 565.